Design and Testing of a 6 inch Control Valve with a Multi-stage Anti-cavitation trim

N.A. Wedzinga
Student Engineering Fluid Dynamics
University of Twente

March 8, 2015

Contents

I General 4

1 General 5
- 1.1 Foreword 5
- 1.2 Summary 5
- 1.3 Introduction 6
- 1.4 General valve Terminology 7
- 1.5 Used symbol and abbreviations 10

II Design 11

2 Design Conditions 12
- 2.1 Preliminary Calculations 12
- 2.2 Preliminairy Results 13

3 Design of the Trim 16
- 3.1 Cavitation and the number of stages 16
- 3.2 Determination of the flow area 17
- 3.3 Design Process 19
- 3.4 Design Concept I 21

III Design verification 23

4 Orifce Testing 24
- 4.1 Orifice plate Design 24
  - 4.1.1 Summary design 25
  - 4.1.2 Pressure tappings 25
  - 4.1.3 Configuration combinations 27
  - 4.1.4 Configurations 28
  - 4.1.5 Drawings 28
- 4.2 Orifice calculation method 29
- 4.3 Preliminary calculations 30
- 4.4 CFD Simulations set-up 31

4.4.1 Single orifice plates set-up 31
4.4.2 Boundary Conditions 32
4.4.3 Multiple orifice plate configurations set-up 33
4.5 CFD Results 34
4.5.1 Single orifice plates results 2D Axisymmetric 34
4.5.2 Single Orifice plates results 3D Quater-Model 39
4.5.3 Comparison 2D Axisymmetric and 3D 41
4.5.4 Pressure recovery coefficient single stage orifices . . . 41
4.5.5 Multiple orifice plates results 42
4.5.6 Normal versus Alternating offset 46
4.6 Full-scale testing setup 48
4.7 Pressure gage calibration 50
4.7.1 Method 51
4.7.2 Outlier Removal 54
4.7.3 Correctionfactor 55
4.8 Full scale test Data 56
4.8.1 Single orifice plates 56
4.8.2 Multiple orifice plates 57
4.9 Full scale test Results 59
4.9.1 Single orifice plates 59
4.9.2 Multiple orifice plates 60
4.10 Comparison between staggered (normal) and alternating offset 64
4.11 Measurement report orifice plates 65
4.12 Conclusion and Discussion 66

5 Full Scale tests 68
5.1 Testing Setup 68
5.1.1 Specifications of the used instrumentation 71
5.2 Calculation Method 71
5.2.1 Density 72
5.2.2 Dynamic Visosity 72
5.3 Testing programme 73
5.4 Data 74
5.4.1 Undertype 74
5.4.2 Overtype 75
5.5 Results 76
5.5.1 Undertype 76
5.5.2 Overtype 81
5.6 Summary Results 85
5.7 Measurement report Concept I 85
5.8 Preliminairy conclusions 85
5.9 Orifice coefficients parts 86
5.10 Orifice coefficients stages 86
5.11 Conclusion and Discussion 86

IV Conclusion and Discussion **89**

V Recommendations **91**

VI List of Figures **93**

VII List of Tables **97**

VIII Appendix **101**

6 Flow equations for sizing of Control Valves **102**
6.1 Liquid flow service 102
6.2 Gas flow service 104

7 Valve Design and Design considerations **107**
7.1 Cavitaition factor sigma σ 107
7.2 Inherent Valve Characteristics 109
7.2.1 Quick opening 110
7.2.2 Linear 110
7.2.3 Equal percentage 110
7.3 Multi-stage trim 111
7.4 Number of stages and the pressure drop relation 113
7.5 C_v value and resistance coefficient K 118
7.6 K and C_v values in series 119

8 Orifice Theory **121**
8.1 Derrivation of the orifice equation 121
8.1.1 Orifice Theory for compressible flows 122
8.2 Derivation of the relation between C_d and C_v 123
8.2.1 Compressible flow 123
8.2.2 Incompressible flow 125
8.2.3 Alternative derrivation 127
8.3 Orifice in series and parallel 128
8.3.1 Series 128
8.3.2 Improved correction factor Concept I 131
8.3.3 Parallel 132
8.4 Derrivation of the pressure ratio 133

Part I

General

Chapter 1

General

1.1 Foreword

In front of you is the intership report of N.A.Wedzinga. I performed my internship at Key Valve Technology LTD in Siheung-si, South Korea. During my internship i did some research on the theory behind the multi-stage trim controlvalve. Key valve Technologies has been making valves for a long time in many different shapes and size. The control valve is a relatively new product for this company. The goal of the internship was to give some theoretical background to the already known data and to get hands on experience with controlvalve sizing, calculations, assembly and testing.

Key valve technology is a subsidairy company of H.P. Valves Oldenzaal B.V. Through H.P. Valves i was able to perform this assignment, for which i am very thankfull. I would like to thanks Mr. Hinsenveld for the oppurtunity he gave me to exploit myself in the world of the control valves and bringing me into contact with Key Valve Technologies.

I would like to thank Mr. Key Min for his support, knowlegde and open discussions during my intership. Furthermore i would like to thank my daily supervisors Mr.J.S. Woo, Mr. J.T. Kim for their support and introduction to the control valve world and technology. A special thanks i would like to give to mr. G.Kim for his support in CFD related issues and in general for being a good friend to me. And offcourse many thanks to the other staff of Key Valve Technologies who made my stay very pleasant.

I hope you enjoy reading this report.

1.2 Summary

In this internship report the performance aspects of a anti-cavitation multi-stage control valve trim are discussed. The internship was at Key Valve Technologies LTD, based in Siheung-si, South Korea.

From a given case a custom control valve trim is designed for operation

in cavatiting conditions. To gain more insight in the working of the multi-stage trim an additional prototype was designed to represent only one hole of the multi-stage trim hole pattern.

The general working of a multi-stage control valve trim is based on orifice technology. From the designdata available a single hole from a control valve trim was build with 5 single orifice plates. The orifice plates were tested each seperately and then in a combination. The combination varied from 2 until the maximum of 5 plates.

The holes in a multi-stage control valve trim are placed one after another with a certain offset. In a normal configuration the offset increases from the first plate to the next. An alternative offset is also evaluated where the offset alternates around zero.

The performance of the orifice plates and the and the combinations of orifice plates in different settings is evaluted with Computational Fluid Dynamics as well as full-scale test and algebraic calculations.

The full scale test have been performed at the testing laboratiorium of Key Valve Technologies LTD in Siheung-si, South Korea.

Additionally some background information of control valves and orifices is given in the appendix and the calibration of the pressure gages is discussed.

1.3 Introduction

Control valves are fluid control devices that are generally used in the industry. The controlvalve is different from a normal valve in the way that it does not only have an on-off function like a normal e.g. gate valve has, but also a throttling function.

The throtlling function of a control valve can be used to alter certain property values of fluid to a desires value. Controlvalve can be used to relieve pressure, control volume flow or initiate a phase transition from gas to liquid.

The controlvalve in this report discussed extensively is a multi-stage anti-cavitation type control valve. The valve itself is very similair to a standard globe valve, but with the addition of a cage surrounding the plug. The cage is built up out of multiple cylinders in eachother. The fluid travels from on cylinder to the next and is relieved in pressure gradually over the total number of stages.

The number of stages is determined by the likelyhood of the flow to cavitate. When the pressure is relieved gradually there is less overshoot in pressure drop and cavitation is less likely to occur.

1.4 General valve Terminology

In figure 1.2 a drawing of general globe valve is seen, in table 1.4 the names for the general parts are given. The drawing can be used for a reference. More information on valve terminoloy can be found in VIII.

Number	Part Name
1	Body
2	Seatring
3	Plug
4	Backseat
5	Gland Packing
6	Spindle
7	Gland
8	Bonnet
9	Yoke & Yoke bushing
10	Hand Wheel
11	Nut

Table 1.1: Part names of a general Globe Valve

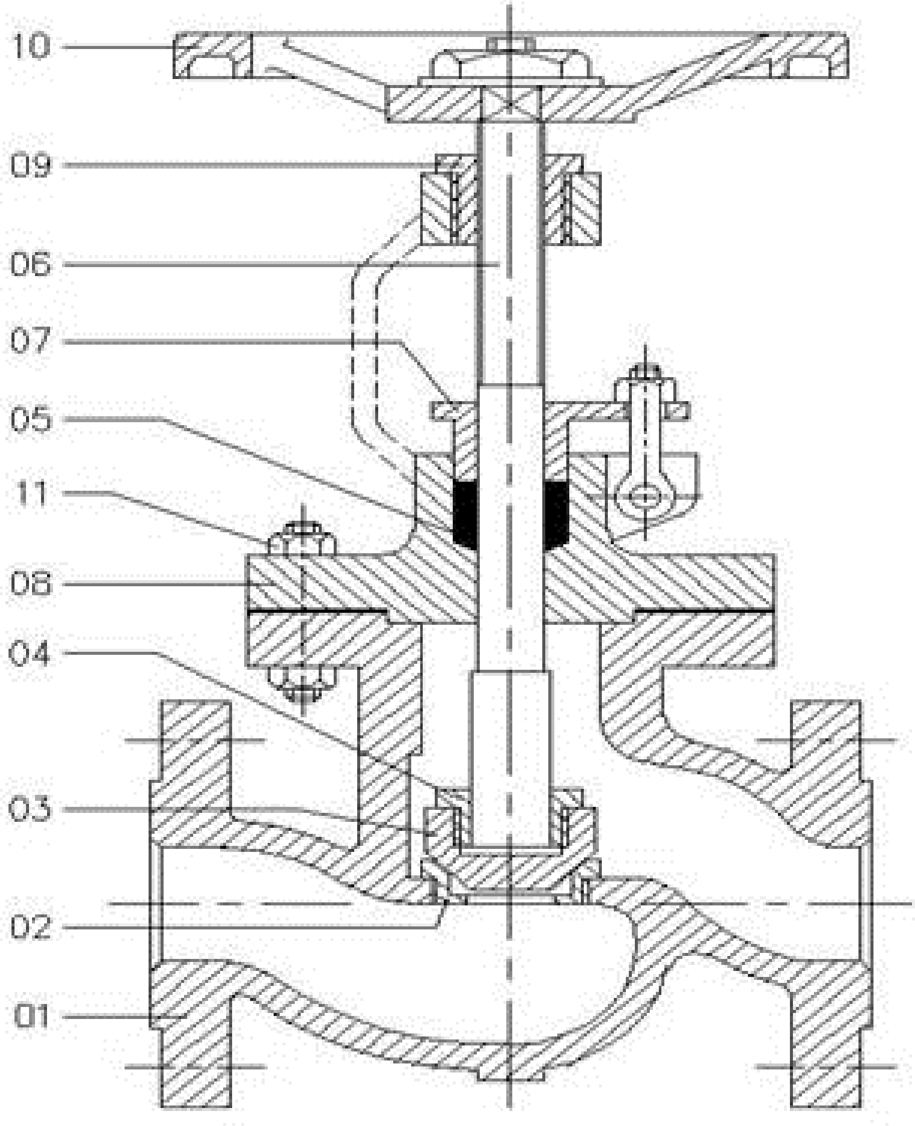
10
09
06
07
05
11
08
04
03
02
01

Figure 1.1: Drawing of a standard Globe valve

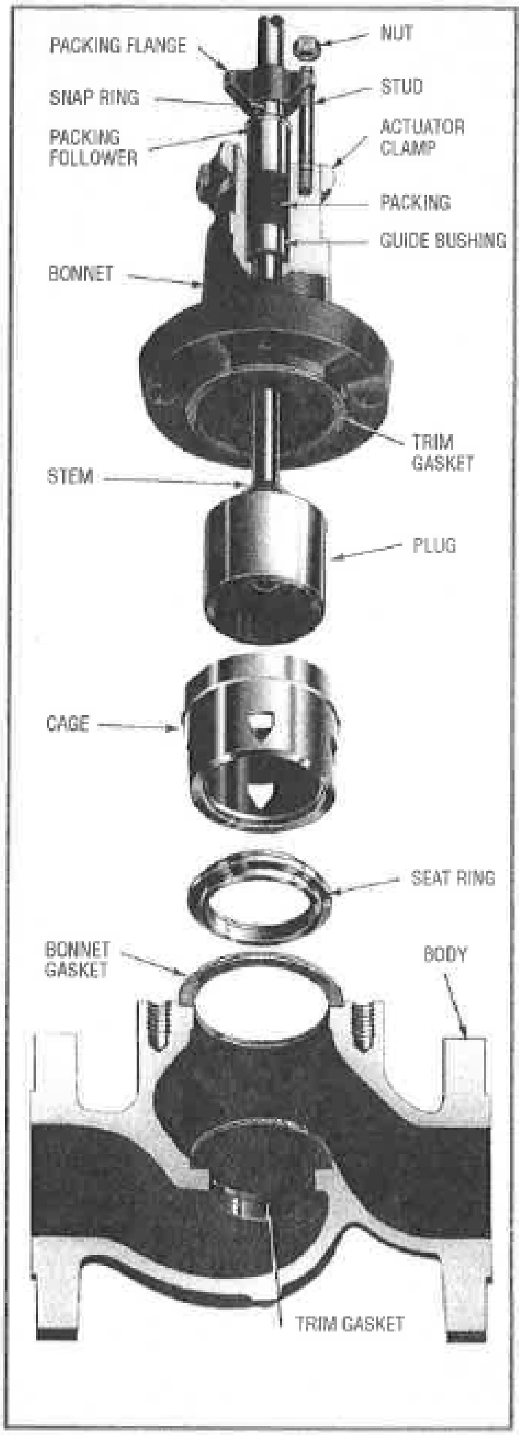
PACKING FLANGE
NUT
SNAP RING
STUD
PACKING FOLLOWER
ACTUATOR CLAMP
PACKING
GUIDE BUSHING
BONNET
TRIM GASKET
STEM
PLUG
CAGE
SEAT RING
BONNET GASKET
BODY
TRIM GASKET

Figure 1.2: Exploded view of a Cage style Globe Control valve

1.5 Used symbol and abbreviations

Symbol	Description	Physical Meaning
p	bar	Pressure
p_1	bar	Inlet pressure
p_2	bar	Outlet pressure
p_v	bar	Vapor pressure
p_c	bar	Critical thermodynamic pressure
p_{vc}	bar	Pressure at the vena contracta
ρ	kg/m^3	Density
ρ_1	kg/m^3	Density inlet
ρ_2	kg/m^3	Density outlet
ρ_0	kg/m^3	Density water at $15.5^{\cdot}C$
Q	m^3/h	Volume flow rate
C_v	$Gpm/\sqrt{psi}$	Valve coefficient Imperial
K_v	$m^3/h/\sqrt{bar}$	Valce coefficient Metric
C_d	$[-]$	Orifice coefficient
β	$[-]$	Contraction coefficient of an orifice
N_1	$[-]$	Numerical constant
N_6	$[-]$	Numerical constant
SG	$[-]$	Specific gravity
F_L	$[-]$	Liquid pressure recovery factor
F_F	$[-]$	Liquid critical pressure ratio factor
F_γ	$[-]$	Specific heat ratio factor
x	$[-]$	Ratio of pressure differential and absolute inlet pressure
x_t	$[-]$	Pressure differential factor at chocked flow
σ	$[-]$	Cavitation index
σ_c	$[-]$	Cavitation index at chocked flow
R	$[-]$	Rangeability
T	$[-]$	Turndownratio
N	$[-]$	Number of holes in a multi-stage trim
T	$[-]$	Number of starts of a multi-stage trim

Table 1.2: List of used symbols and abbreviations

Part II

Design

Chapter 2

Design Conditions

The calculation for the multi-stage trim always begins with a given load case, or in this instance load cases. The load cases are prescibed by the process and are essential to calculate the right size and type of control valve to be installed.The data for the loadcases is given in table 2.1. From the design conditions we can already conclude that we need to be able to have some throtlling range since the desired fluid properties differ reasonable. If this was not the case another device could be more suitable e.g. orifice. Since this is not the case, the control valve seems to be a good choice to start from.

Condition	Case 1 Maximum flow	Case 2 Normal flow	Case 3 Minimal flow	Case 4 Startup	Symbol	Unit
Inlet pressure	110	70	80	90	p_1	bar
Outlet pressure	10	10	7.0	50	p_2	bar
Inlet Temperature	110	110	40	110	T_1	°C
Mass flow rate	800.000	500.000	35.000	700.000	$\dot{m}$	kg/h
Medium	Water	Water	Water	Water	$[-]$	$[-]$

Table 2.1: Design Condtions

2.1 Preliminary Calculations

From the given flow data in table 2.1 of the different load cases the first calculations can be done. These are used to determine the valve style and to see if there are any implications concerning cavitation of flashing control. In order to compute these calculations we need a little more information about the properties of the fluid. These can be found in tables or estimate using emperical formulae. Furthermore to check whether we have to deal with a chocked flow or not, we will make some general assumptions. Note that the absolute thermodynamic critical pressure is a constant, only dependent on the type medium.

Condition	Case 1 Maximum flow	Case 2 Normal flow	Case 3 Minimal flow	Case 4 Startup	Symbol	Unit
Density at Inlet	9536.12	954.23	995.65	955.17	ρ	kg/m^3
Vapor Pressure	1.43	1.43	0.07	1.43	p_v	bar
Absolute Thermodynamic critical pressure	220.64	220.64	220.64	220.64	p_c	bar

Table 2.2: Preliminary Calculations

For the valve will make some first assumptions. We have to do this because some properties of in the sizing calculation are dependent on the valve style. We have not yet determined the valve style, this is part of the sizing. For the first calculations we will use a liquid pressure recovery factor equal to that of a general globe type valve. These valves can also be used as control valves and have the lowest pressure recovery factor. Other more advanced designs have better a better pressure recovery factor, so this a conservative assumption. We will use this to check for a chocked flow and the presence of a cavitating flow.

Property	Case 1 Maximum flow	Case 2 Normal flow	Case 3 Minimal flow	Case 4 Startup	Symbol	Unit
Liquid pressure recovery factor	0.85	0.85	0.85	0.85	F_L	$[-]$
Liquid critical pressure ratio factor	0.94	0.94	0.94	0.94	F_f	$[-]$

Table 2.3: Fluid properties used for the preliminary Calculations

2.2 Preliminairy Results

The results of the calculation are seen in table 2.4. This gives the valve coefficient in SI and imperial units next to the flow regime and cavitation index. The calculations have been made with the sizing method given in ISA 75.01 [1].

Property	Case 1 Maximum flow	Case 2 Normal flow	Case 3 Minimal flow	Case 4 Startup
Chocked flow	Yes	Yes	No	No
C_v	112	84	5.3	131
K_v	97	73	4.6	113
σ	1.10	1.14	1.09	2.21

Table 2.4: Calculation results for a $F_L = 0.85$

From the results we can see that there is a large change in pressure and that there will be cavitation would a normal valve be selected.The sigma value is smaller than 1.4 for some cases, this is treated as the onset of cavitation for a globe valve. From the pressure drop which is required and the cavitation index we can conclude that we need to select an anti-cavitation trim. One of the virtues of an anti-cavitation trim is that the pressure recovery is much better than with a standard type valve such as an globe valve. The pressure recovery factor for a cage-type control valve is about 0.9 (conservative) . Changing this factor we can obtain more accurate resulsts.The resuslts of these calculations are seen in table 2.5.

Property	Case 1 Maximum flow	Case 2 Normal flow	Case 3 Minimal flow	Case 4 Startup
Chocked flow	Yes	Yes	No	No
C_v	106	79.4	5.1	131
K_v	91.6	68.7	4.4	113
σ	1.10	1.14	1.09	2.21

Table 2.5: Calculation results for a $F_L = 0.9$

The values for Case 4 the startup dont change since there is no chocked flow. The pressure recovery factor is only used for the calculation of the chocked flow conditions. Also the sigma factor has not changed since this only a function of the inlet-, outlet- and vapor pressure.The condition of a chocked flow is not desireable, so to prevent this we need a higher pressure recovery factor than the 0.9 we assumed. This already indicates that we need a multi-stage trim which has beter pressure recovery. With the required Cv know for all load cases the maximum Cv can be estimated from which the design can be made. The choice has been made to design the trim for a maximum Cv of 150. The type of valve will be a multi-stage trim type. The design of a multi-stage trim is normally a linear or equal percentage

Property	Case 1 Maximum flow	Case 2 Normal flow	Case 3 Minimal flow	Case 4 Startup
C_v	106	79.4	5.1	131
% of rated C_v	70.7	52.9	3.4	87.3
% of Stroke linear	70.7	52.9	3.4	87.3
% of Stroke equal percentage	91.1	89.7	13.5	96.5

Table 2.6: Used percentage of stroke for different inherent valve characteristics

type. When the valve has a linear type cage then each increment in travel corresponds to an equal increment in Cv. When an equal percentage type of cage is installed then each equal increment in travel correspond to an equal gain in percentage of Cv. The increment in Cv thus less at lower openings and increasing at larger opening rates.

$$\text{\% of Rated } C_v = \frac{C_{v_{required}}}{C_{v_{maximum}}}$$

The Rangeability of the valve is the ratio between the smallest and the largest requested Cv value. For the given flow data this ratio is 29.4. For further calculation a Rangeability of 50 will be used. The Rangeability always has to be set to a higher value so the stroke for the smallest opening will be larger than zero.

$$\text{\% of flow} = \frac{opening\%}{100}(\text{linear})$$

$$\text{\% of flow} = R^{\frac{opening\%}{100}-1}(\text{equal percentage})$$

As a general rule the valve has to be operated between 15%-85% of its stroke. Using this rule of thumb it is easy to see why the equal percentage is more favorable.

Chapter 3

Design of the Trim

3.1 Cavitation and the number of stages

As stated before these flow conditions pose a significant risk of cavitation. The solution for this problem is to decrease the pressure gradually over multiple steps. The number of steps will be determined form the cavitation number threshold. The process is an iterative process. From the sigma number for a single stage pressure drop an initial guess is done for the number stages. These stages, with an initial guess for the pressure ratio is then used to perform some calculations. When the sigma number not high enough the number of stages will be increased. The inverse applies for when the sigma number is very high. Although a high sigma number is favorable a sigma number that is too high might signal that too many steps are used. When more steps are used the complexity of the design increases and it could pose problems when the hole diameter is calculated. Also there is an economical consideration, simpler designs are often cheaper. When the sigma number is high enough at a number of stages, but there is high variety in the sigma number the value of the pressure drop ratio can be altered. Changing the pressure drop ratio can result in a more consistent sigma number of the different stages. The aim is to have an increasing sigma number when the pressure is reduced. The risk of cavitation becomes larger when more pressure is relieved and the pressure becomes closer to the vapor pressure. The increased sigma at later stages will give extra protection against cavitation. The flow cases that determine the number of stages are case 1 and case 3. Case 4 has a high enough sigma number that even when only one stage is used there is no risk of cavitation. The sigma number of case 1 and case 3 a very close to each other sol both have to be examined since it is not immediately clear which one is worse. After finishing this iterative process the results for this design are; a three stage, 3 ring design. With an pressure drop ratio of 2.5 between each stage. The result graphs as seen on the next pages. Important also is to notice the chocked flow sigma condition, when the flow is chocked the pressure drop becomes independent of the mass flow and sonic velocities occur in the valve. These conditions are undesirable and should be avoided. The increase in sound level is also significant.

3.2 Determination of the flow area

With the determination of the number of stages and the pressure drop over each stage the rough calculations are completed and more detailed calculation of the trim design can be made. The parameters which need to be set are the number of holes, the hole diameter in the various rings and the hole overlap. For further design the hole pattern will need to be made to accommodate the request inherent valve characteristic.

The general formula which will be used to determine the flow area is given in 3.1

$$C_v = 38C_dA = 38C_d * 0.25\pi d^2 \tag{3.1}$$

The area and diameter are both given in inches since the relation is derived from the imperial relation between Cv (given in imperial units) and the orifice equation (also given in imperial units). The discharge coefficient is a dimensionless number and is the same for imperial and SI units. The conversion form inches to mm for the diameter however will be done. From the pressure drop ratio and the number of stages the equivalent area and orifice coefficient can be calculated. This will be used to calculate the equivalent area, wherefrom the areas of each stage can be calculated. The last factor which is not yet set in the number of holes. The number of holes determines the individual flow area and vice versa. An iterative process is used to determine a number of holes that is easily fitted to the cage. The factor which influence this will be discussed further on. The orifice coefficient for the final stage will be estimated at 0.83, the orifice coefficient of the intermediate stages will be estimated at 0.62. Together with the pressure drop ratio of 2.5 this gives an correction factor of 0.27.

The equivalent area needed for a C_v of 150 is thus; $6.23in^2$ or $4021.88mm^2$.

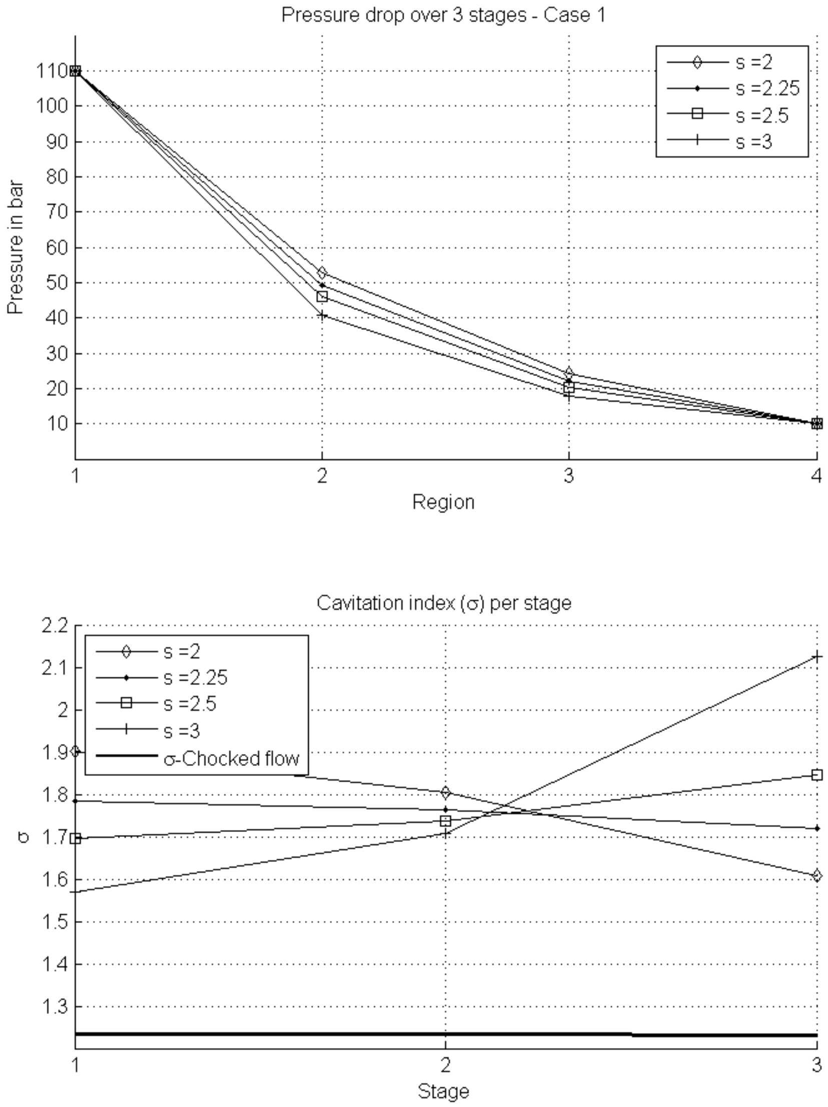

Figure 3.1: Pressure drop and sigma value at each stage for Case 1 - Maximum Flow

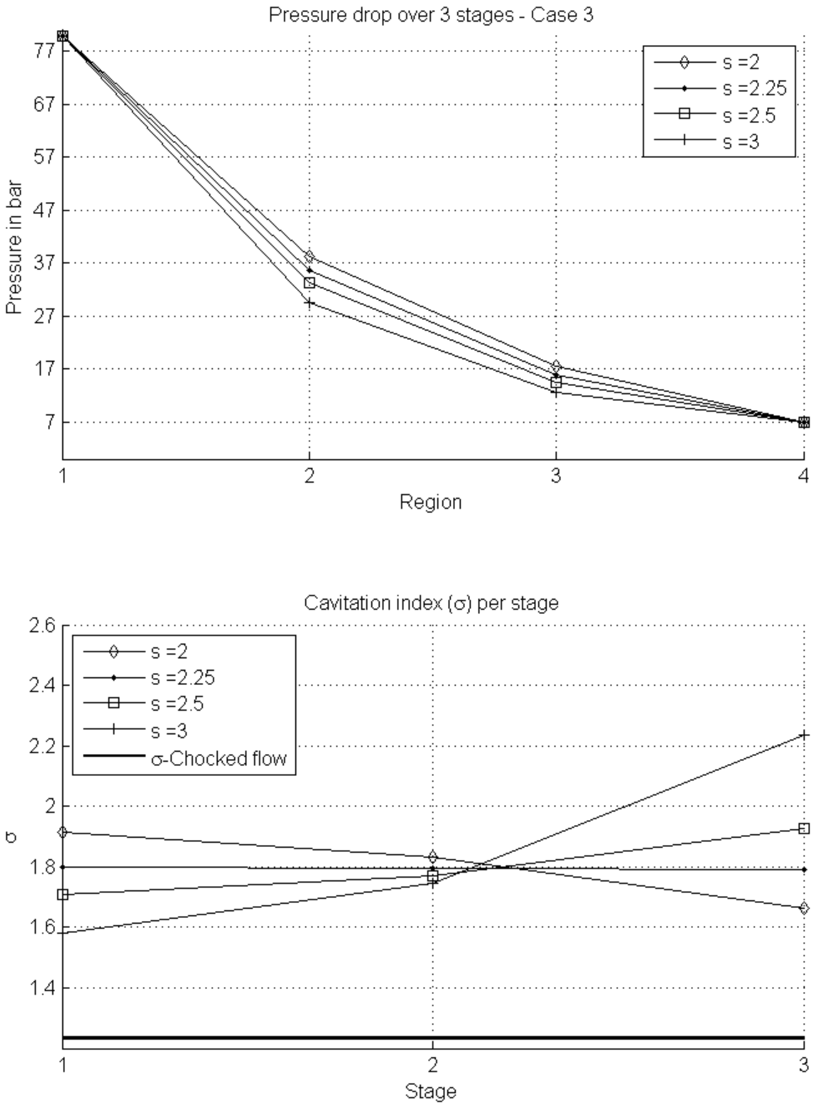

Figure 3.2: Pressure drop and sigma value at each stage for Case 3 - Minimal Flow

3.3 Design Process

For the first design a linear cage will be designed. There are obvious advantages to a equal percentage cage, but the linear type is simpler to design and produce. This is why this type is chosen for the first design.

The next step in de the design process the determination of the number of holes, the spacing, the overlap and the diameter itself. For this a relation is needed between the different attributes.

First of all, there are three orifice areas, the ratio between the size of these orifices is already set. The area ratio between two stages with the same discharge coefficient(one and two) is the square root of the pressure drop ratio or area ratio. The ratio between the last orifice and the second to last is different since they are assumed to have different discharge coefficients. The ratio between the orifice area and the expansion area directly after the orifice is set at the same ratio as the ratio between the orifices. For the final stage the total area is already known. With these factors the ratio between each area in completely determined. The overlap area will be calculated accordingly to ensure the cylinders have the right amount of overlap.

The last undetermined factor in the number of holes. For this we need to consider the hole pattern on the cage itself. The pattern will form and helix on the circumferential area of the cylinder, this helix can have a single start, or multiple starts. This is a design parameter.

The number of starts of the helix has to comply with the number of holes, the total number of holes dived by the number of starts must be a integer number. It is possible to have less holes, but this will sacrifice the linear character.

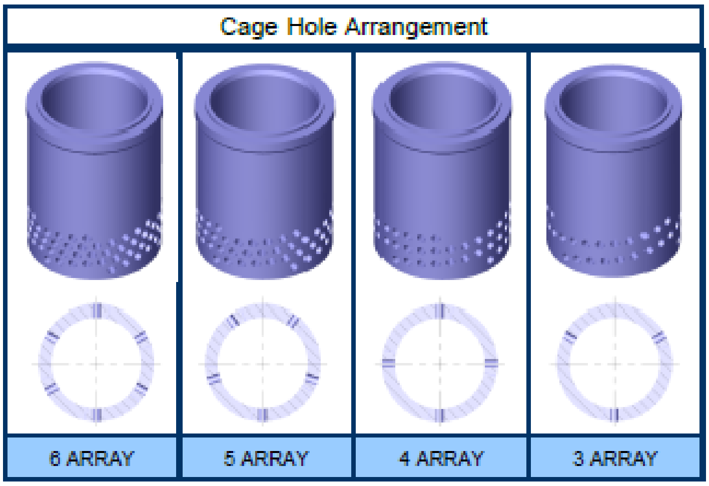

Figure 3.3: Different number of starts possible for the hole pattern of the cage. Picture courtesy of KVT Valves LTD.

Finally the type of cage needs to be determined. When the number of stages is limited, like in this design, then overtype as well as under type cages are well suited. The overtype is preferred in general. When the fluid flows from the outside to the inside it will collide with itself in the middle.

This continuous collision of the fluid particles in the middle will increase the pressure and will thus decrease the chance of cavitation. When many stages are needed to obtain the desired pressure drop then under types are generally used. When the fluid travels from on stage to the next the area increases, if an overtype would be used this would mean that the largest holes would be present in the inner and smallest cylinder, this is sometimes physically not possible, so under types are used, despite their inherent advantage. In close correlation with the number of holes and the number and of starts of the helix is; the number of columns.

The number of columns is the number of holes placed in overlap over the height of the cylinder. The number of columns needed is determined by the diameter of the hole in the most inner cage. The holes in the inner cage have to be placed in half overlap in order to accomplish the desired linear character when the plug moves past its. The maximum column height is the stroke of the plug.

The total process is an iterative process, first the total number is guessed. From this value the diameter of the holes and the overlap is calculated. With this the column height is checked, and the number of holes needed for one column. From this the number of starts can be determined. If the number of starts does not give and integer number or too much of the stroke is left unused then the number of holes has tol be adjusted. Starting with a initial hole number guess of 60,48 or 30 is recommended since these numbers can give integer number of starts of multiple column heights.

3.4 Design Concept I

The result of the iterative process is seen in figure 3.4. The hole pattern including the offset for the three cylinders is given. The data of the complete design in given in tabel 3.1

Property	Quantity	Symbol	Unit
Number of holes	60	N	-
Number of columns	15	C	-
Number of Starts	4	S	-
Stroke used	75.2	$[-]$	mm
Diameter of hole 1	9.2	d_1	mm
Diameter of hole 2	10.7	d_2	mm
Diameter of hole 3	10.7	d_3	mm
Offset cage 1-2	2.4	o_{12}	mm
Offset cage 2-3	5.3	o_{23}	mm

Table 3.1: Summary of the Design of Concept I

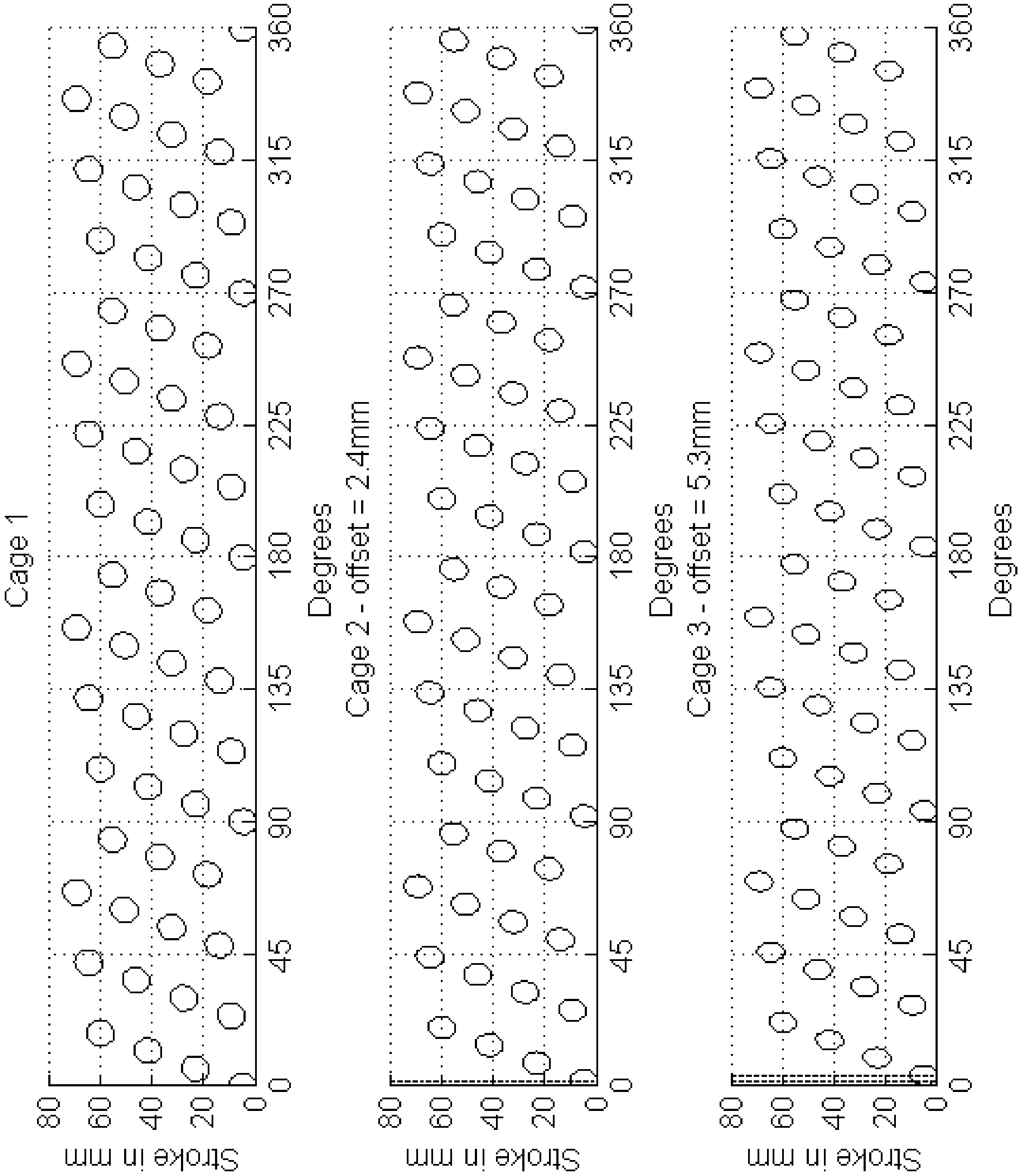

Figure 3.4: Hole Pattern of Design I

Part III

Design verification

Chapter 4

Orifce Testing

The calculations on Design on are done with assumed orifice discharge coefficients. The final stage of the orifice is assumed to be a tube type orifice which discharges into the valve body as the fluid exits the trim. The intermediate stages are assumed to be a square edged orifice. From the calculations it was already clear that the discharge coefficient had a significant impact on the final dimensions and performance of the trim. The orifice coefficient of the final stage has the most significant impact. The hole dimensions of all other holes are based on the final stage. The last stage is also a very odd orifice since it has strange dimensions to be a regular orifice but is it also not a nozzle since it is has no rounding on the edges. The best way to determine whether the orifice coefficient assumption is valid or not is to perform some more indepth research. The choice is made to investigate the flow thru some individual orifices and series of orifices. The calculation by hand will be compared to CFD calculations and full-scale tests.

4.1 Orifice plate Design

The design to test will be a 5 stage orifice with the same design considerations used as for a multi-stage trim. Essentially it is a single hole of a multi-stage trim of a control valve. The pressure drop ratio used is 2.25. The ratio implies that the area ratio between the subsequent orifice areas is 1.5, the orifice coefficient is set to be equal for each stage. Although this assumption is not valid for this instance it does not matter since the purpose of the test is to determine the orifice coefficient. The total assembly will be designed to fit in a 1.5 inch pipe. The small diameter pipe has some inherent benefits. The velocities in the pipe can be changed of a larger region than when e.g. a 6 inch pipe would be used. The limiting factor in the test facility is the capacity of the pump. Also will the design be smaller and thus faster, easier and cheaper to produce. The number of stages is limited to 5. Each stage has an offset from the previous stage. The total offset from the first stage increases as more and more as more stages are added. In the case of a trim in a control valve there is no real limit concerning the total offset since it is circular. In a straight tube where the offset is in the longitudinal direction this can pose a problem. When the number of stages is too large the total offset will physically not fit in the pipe, also when the exit stage is too close to the pipe wall backpressure effects can cause for undesired effects.

With the consideration as above in mind a design has been mode. The hole diameter of the first hole is chosen such stat the complete assemlby of 5 stages will fit into the pipe and does not come too close to the pipe wall. A summary of the design can be seen in table 4.1.1

4.1.1 Summary design

Stage	Diameter	Offset	Orifice Area
1	15	0	176.71
2	15	4	117.81
3	12.2	5.3	78.54
4	10	4.3	52.36
5	8.16	3.6	34.91

Table 4.1: Summary of the testing orifice Design

4.1.2 Pressure tappings

The design of an orifice itself is fairly simple. In any regular application an orifice in a circular hole made in a plate called the orifice plate. The orifice plate itself is mounted in an carrier which allows it to be mounted in the pipe. Depending on the application the carrier itself can be equipped with pressure tappings to allow the pressure upstream and downstream to be measured. The pressure tappings can be installed at various points. Conventional installation point are; Corner taps, D and D/2 taps, Flange taps. Other less regular types are; 2,5D and 8D taps and Vena contracta taps.

- Corner taps are placed immediately upstream and downstream of the orifice. This method is most commonly used when the orifice plate is mounted in a carrier.

- D and D/2 taps are placed 0.5 times the pipe diameter upstream and one times the diameter downstream of the orifice plate.

- Flange taps are placed 1 inch or 25.4mm upstream and downstream of the orifice plate. Often thiese are drilled holes in specially designed pipe flanges mounted on either side of the orifice plate.

- 2.5D and 8D taps are placed 2.5 times the diameter of the pipe upstream and 8 times the pipe diameter downstream. This point downstream is where the unrecoverable pressure loss is measured.
- Vena contracta tappings is are combination of one pressure tapping placed upstream and on 0.3 to 0.9mm downstream at the actual vena contracta of the flow. The actual vena contracta is behind the geometrical vena contracta. The distance between the geometrical and the real vena contracta is dependent on the diameter of the orifice. This means that for each orifice there is a different measuring point.

The pressure tapping that will be used in the measuring plates are flange tappings. On either side of the orifice plate will be a specially mounted orifice flange on which the orifice will mount and the pressure tappings will be installed. The testing facility already has pressure tappings installed in the pipe at 2 times the diameter upstream and 6 times the diameter downstream. Although the lengths upstream and downstream are not completely consistent with standard pressure tappings they are assumed to be far enough from the orifice plate to measure the unrecoverable pressure difference. The distance of the tappings is 2D and 6D measured from the mounting flanges of the tube. The orifice plate is mounted in between to measuring flanges of a thickness of 35mm. So it is fairly safe to say that the assumption is valid since the distance will be even larger than 2 and 6D. On the measuring flanges there will be four pressure tappings placed at equal distance radially. The pressure tappings will be connected as a pair with the opposite pair. So 1 and 2 will be connected, as well as 3 and 4. Finally the combination of 1-2 and 3-4 will be connected to eachother. The schematic of this is seen in figure 4.1 . The pair-wise connection and the multiple pressure tappings make sure that the static pressure measured by the measuring device is less dependent on local turbulence effects in the pipe The position, diameter and length of the pressure tappings according to ISO 5167-2 [6]. The distance upstream and downstream is 25.4mm +- 0.5mm. The diameter is 0.13 times die inside diameter of the pipe and the length is at least 2.5 times the diameter of the tappings themselves. The dimensions of the orifice will not be according to ISO 5167-2 [6] since the orifice themselves are odd-shaped. Not only the final stage which a tube type, but also the intermediate stages which are non-symmetrical ellipses.

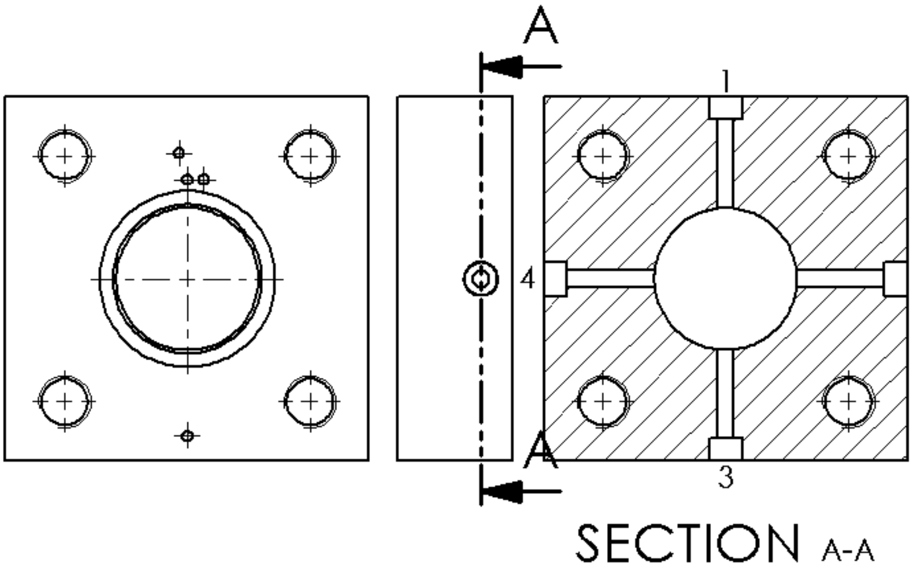

Figure 4.1: Drawing of the location of the pressure tappings in the orifice plate carrier.

4.1.3 Configuration combinations

With the orifice test plates and the orifice themselves are multiple configurations possible. The orifices can be mounted individually and in series. The orifice will firstly be tested in a single configuration. The only parameter that will change in these tests is the diameter of the hole. The different hole diameters will have cause for different area ratios so the influence of the ratio between the upstream diameter and the diameter of the geometrical vena contracta will be investigated.

The second parameter that can be changed the number of stages. The orifice is designed to be a 5 stage orifice with the same design considerations as a normal control valve trim. Variations can be made with the number of stages.

The third parameter that can be changed is the offset. The total offset can be set the same as in a regular control valve trim, so in an increasing offset with each stage seen from the first stage. As an extra design parameter the offset can also be set at an alternating sequence. This means for example that the first stage in aligned in the middle the tube, the second stage at positive offset. The third stage at a negative offset, so in the opposite direction of the second one. This will result in an entrance and exit stage which are closer to the longitudinal axis of the pipe.

4.1.4 Configurations

Single Stage orifice configurations

Stage plate	Diameter [mm]	Orifice Area [mm^2]
1	15	176.71
2	15	176.71
3	12.2	117.81
4	10	78.53
5	8.2	52.36

Table 4.2: Configuration and typical values for the single stage orifice configuration

Stage plates	Area 1 [mm^2]	Area 2 [mm^2]	Area 3 [mm^2]	Area 4 [mm^2]	Area 5 [mm^2]
1-2	176.71	117.81	n/a	n/a	n/a
1-2-3	176.71	117.81	78.54	n/a	n/a
1-2-3-4	176.71	117.81	78.54	52.35	n/a
1-2-3-4-5	176.71	117.81	78.54	52.35	34.91

Table 4.3: Configuration and typical values for the multiple stage orifice configurations

Stage plates	Area 1 [mm^2]	Area 2 [mm^2]	Area 3 [mm^2]	Area 4 [mm^2]	Area 5 [mm^2]
1-2-3	176.71	117.81	78.54	n/a	n/a
1-2-3-4	176.71	117.81	78.54	52.35	n/a
1-2-3-4-5	176.71	117.81	78.54	52.35	34.91

Table 4.4: Configuration and typical values for the multiple stage orifice configurations with alternating offset

The total number of configurations and test that can be done with this orifice plate is 11 since the single configuration of stage 1 and 2 is the same this does not give extra information. Also the alternating offset configuration for two plates is not a suitable test. Whether the offset is to the left or the right, when there are just two plates it is essentially the same.

4.1.5 Drawings

Drawings of the orifice plate assembly are seen in the annex.

4.2 Orifice calculation method

The orifice coefficient can be calculated via different methods. The most straightforward is from the definition of the coefficient. The coefficient is the ratio between the actual mass flow and the theoretical mass flow. When the density is the same in both cases, thus theoretical and actual then the ratio of the volume flow will also suffice.

$$C_d = \frac{\dot{m}_{actual}}{\dot{m}_{theory}} \tag{4.1}$$

$$C_d = \frac{Q_{actual}}{Q_{theory}} \tag{4.2}$$

$$C_d = \frac{\dot{m}\sqrt{1-\beta^4}}{A \cdot \sqrt{2\Delta p \cdot \rho}} \tag{4.3}$$

Determining the mass flow or the volume flow is not always straightforward. Measuring of mass flow requires the installation of a flow meter and a pressure and temperature meter in the loop. Another issue which arises is when multiple orifices are placed in series. The actual volume flow can be measured with a flow meter. Determining the theoretical mass flow is less straightforward since the equation of orifices in series requires a known C_d for each stage. When this C_d is set at one or ideal circumstances then there it will be possible to calculate the theoretical maximum mass flow. The orifice coefficient which will be calculated with this value is the orifice coefficient of the two orifices combined.

Another measuring method is proposed by ISO 5167-2 [6]. The norm gives a relationship between the pressure difference directly over the plate and the non-recoverable pressure drop. The pressure difference over the plate will be measured by the pressure taps installed at the flanges. The pressure which is not recovered is the pressure difference between the pressure tap installed upstream and downstream of the plate. For this the installed pressure tappings in the loop will be used which are placed 2D upstream and 6D downstream. These distances are according to ISO 5167-2 [6]

The relation between the pressure ratios, the meter coefficient and the beta ratio is given by equation 8.76

$$\frac{\Delta\omega}{\Delta p} = \frac{\sqrt{1-\beta^4(1-C_d^2)} - C_d\beta^2}{\sqrt{1-\beta^4(1-C_d^2)} + C_d\beta^2} \tag{4.4}$$

$$C = \frac{C_d}{\sqrt{1-\beta^4}} \tag{4.5}$$

The non-recoverable pressure loss data allows us to determine another property of the orifice. The resistance factor or K. The resistance factor is defined in equation 4.6.

$$K = \frac{\Delta \omega}{\frac{1}{2}\rho_1 V^2} \tag{4.6}$$

The velocity term in this equation poses some difficulties since this changes significantly when the fluid travels thru the vena contracta. Also it is not very easy to determine the velocity in the vena contracta. Following the convention the average velocity downstream will be used. Using equation 8.76 and equation 4.6 we can obtain another relation for the K factor of an orifice.

$$K = \left(\frac{\sqrt{1 - \beta^4 (1 - C_d^2))}}{C_d \beta^2} - 1 \right)^2 \tag{4.7}$$

Although above relations are very usefull, some difficulties will arise when multiple orifices are measured. The relation between the recoverable pressure and the pressure drop over plates utilizes the beta ratio. For a single orifice plate the beta ratio is very straightforward, however for multiple orifices this poses a problem. Therefore this method can only be applied so single stage orifices.

After retrieving the data it was decided not to use the methode decribed above because the measurements showed too much uncertainty.

The multi stage orifices consist of multiple orifices from which the orifice coeffient will be known from experiments and simulations. With this data it is possible to calculate the equivalent orifice diameter and discharge coeffient. There is one major implication. When a single orifice is examined, the flow will have enough time or distance downstream to recover to the pressure. When the orifice are mounted in close distance to eachother like in the test-assemlby, this pressure recovery mightl not take place between the stages. Therefore the actual orifice coeffient of the combination wil differ from the calculated equivalent.

The ratio between the calculated orifice coeffient of the assembly and the actual value from the test will be the correction factor c. The value of this correction factor will be dependent on the geometry, and will be specific of this geometry. Parameters which influence this factor are the area increase after the orifice and the distance between the orifices.

4.3 Preliminary calculations

With the given pipe diameters and orifice diameters some preliminairy calculations can be done. The contraction ratio β can be calculated as wel as the theoretical mass flow thru the orifice when a pressuredrop of 1 bar . The goal is to compare the CFD simulations and the field test results with the theoretical values. The results will enable us to enhance the calculation model for the multi-stage trim. Since the performance value of the trim is measured in the valve coeffiient, it will also be done for the orifices.

Orifice Diameter $[mm]$	Beta (β) ratio	Massflow [kg/s]
15	0.3488	2.517
12.2	0.2837	1.658
10	0.2326	1.111
8.2	0.1907	0.747

Table 4.5: Theoretical mass flow for the different orifice sizes with C_d =1 and Δ p = 1 bar.

4.4 CFD Simulations set-up

The different configurations will be also be examined via CFD calculation. The data from the calculations together with the field data will give a clear insight in the interaction between the different stages and the behaviour of the individual stages. The simulations can be split into two main parts. The single orifices will be examined as well as the combination of orifce plates.

4.4.1 Single orifice plates set-up

The single orifice plates are modelled using in 3D utilizing SolidWorks. From the full modell some alterations will be done to improve the simulations time. The model of the single orifice consist of an entrance tube with a diameter of 43mm, an orifice with on of the four different diameters and an exit tube with the same diameter as the entrance tube. The complete assemlby is Axi-symmetric over the longitudinal axis. The axi-symmetry has some inherent benefits. The simulation can be done in 2D, so just a slice of the model is used. The results of the slice will be multiplicated the full results can be obtained. The simpler geometry uses much less elements than the full 3D model. Since less elements are needed we can set a very fine mesh distribution without getting very large calculation times. The fine mesh enable use to get a very preciese result of the pressure and velocity distribution. There are also drawbacks to the 2D simulation. Since the flow assumed to only flow in 2D, the turbulence,mixing effects and losses in 3D will not be taking into account. In general this would lead to an over estimation of the performance of the orifice.

Next to the 2D simulation of the single orifices there will also be some 3d simulation. The latter willl be done using a reduced model. The model is cut twice over a symmetry plane. This gives a model that is one quarter of the full size model. Since the model is axi-symmeteric the model could have been reduced more. The quater model gives a compromise between calculation time and the inlcuding of 3D effects of the flow.

The simulations will be done with Autodesk Simulation CFD. The choice to perform the 2D calculations with Autodesk CFD is made since Ansys CFX is not albe to handle 2D models. The calculation for the 2D model could also have been done with Ansys Fluent, but Autodesk CFD is favored since I am more experienced with it. The comparison between two different programs is not madel. The main settings will be same for the boundary conditions, turbulence model and solver model for the different geometries.

The orifice coeffient is in general dependent on the Reynolds number, the contraction ratio β, sometimes called the velocity approach factor $\frac{1}{\sqrt{1-\beta^4}}$. The effect of the Reynolds number on the different orifices will be evaluated by changing the mass flow rate thru the orifices. The Reynolds number is given by;

$$Re = \frac{\rho \cdot V \cdot D}{\mu} \tag{4.8}$$

We can write the massflow as;

$$\begin{aligned} \dot{m} &= \rho \cdot Q = \rho \cdot V \cdot A \\ \dot{m} &= \rho \cdot V \cdot 0.25\pi D^2 \\ \rho \cdot V \cdot D &= \frac{\dot{m}}{0.25 \cdot \pi \cdot D} \end{aligned}$$

Combing gives an expression of the Reynolds number as a function of the mass flow.

$$Re = \frac{\rho \cdot V \cdot D}{\mu} = \frac{\dot{m}}{\mu \cdot 0.25 \cdot \pi \cdot D} \tag{4.9}$$

Equation 4.9 will be used to calculate the Reynolds number in the upstream part of the pipe of the orifice for different mass flows.

4.4.2 Boundary Conditions

For the simulations of the single and multiple orifices there will be different boundary conditions used. In general two different analysis will be performed. The first analysis is the simulation of a valve coefficient measurement. Over the inlet and outlet will be a pressure difference of one bar, the fluid will be water at 60 degrees Fahrenheit or 15.5 degrees Celcius. The result of the simlation will be a mass flow thru the complete assembly. With the mass flow can then the valve coeffient be calculated, as well as the orifice coeffient. A summary of all applied boundary conditions is given in table 4.6.

The other simulation will be different in their setup. The aim of the second series of simulations is to investigate the dependance of the orifice coeffient on the Reynolds number. The different Reynolds numbers will be achieved by running multiple simulations with different mass flows for each of the geometries. In order to reduce the simulation time these simulations will be performed in 2D general. The aim of the simulations is to investigate the relationship between the Orifice coeffient and Reynolds number. Therefore a quantative approach is valid, since the aim is not the kwalitative answers. A summary of the boundary conditions used for different Reynolds numbers is given in table 4.7.

Location	Boundary condition	Value
Inlet	Pressure	10 $[bar]$
Outlet	Pressure	9 $[bar]$
Wall	No slip	$[-]$
Symmetry plane (if applicable)	Symmetry	$[-]$
Fluid	Type	Water
Fluid	State	Incompressible
Fluid	Temperature	60 $^\circ F$
Fluid	Turbulence Model	$K-\epsilon$

Table 4.6: Boundary Conditions for C_v Analysis

Location	Boundary condition	Value
Inlet	Mass flow	Variable
Outlet	Pressure	0 $[Pa]$
Wall	No slip	$[-]$
Symmetry plane (if applicable)	Symmetry	$[-]$
Fluid	Type	Water
Fluid	State	Incompressible
Fluid	Temperature	60 $^\circ F$
Fluid	Turbulence Model	$K-\epsilon$

Table 4.7: Boundary Conditions for different Reynolds number Analysis

4.4.3 Multiple orifice plate configurations set-up

The multiple orifice configurations are analysed in a same manner as the single stage orifices. Using the geometry which was modelled in SolidWorks an assembly is made of the different orifice plates. The simulations are only run for one mass flowrate and thus Reynolds number. Ideally more results would be obtained but since simulation times for the 3D model are signifi-canlty longer then for the 2D simulations. Also much more configurations are available. The used boundary conditions are given in table 4.7.

4.5 CFD Results

4.5.1 Single orifice plates results 2D Axisymmetric

Orifice Diameter $[mm]$	Beta (β) ratio $[-]$	Mass flow simulation $[kg/s]$	Calculated C_d $[-]$	Reynolds Number $[-]$
15	0.3488	2.024	0.804	59.796
12.2	0.2837	1.284	0.774	37.925
10	0.2326	0.846	0.761	24.997
8.2	0.1907	0.554	0.741	16.335

Table 4.8: Results of the 2D Axi-symmetrical CV simulation for different orifice sizes

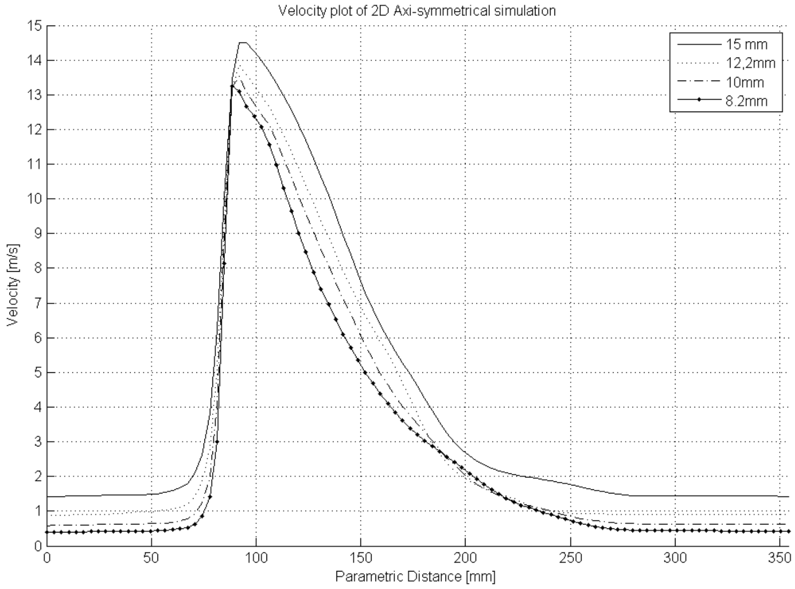

Figure 4.2: Velocity plot of the 2D Axi-symmetrical simulations for different orifice sizes

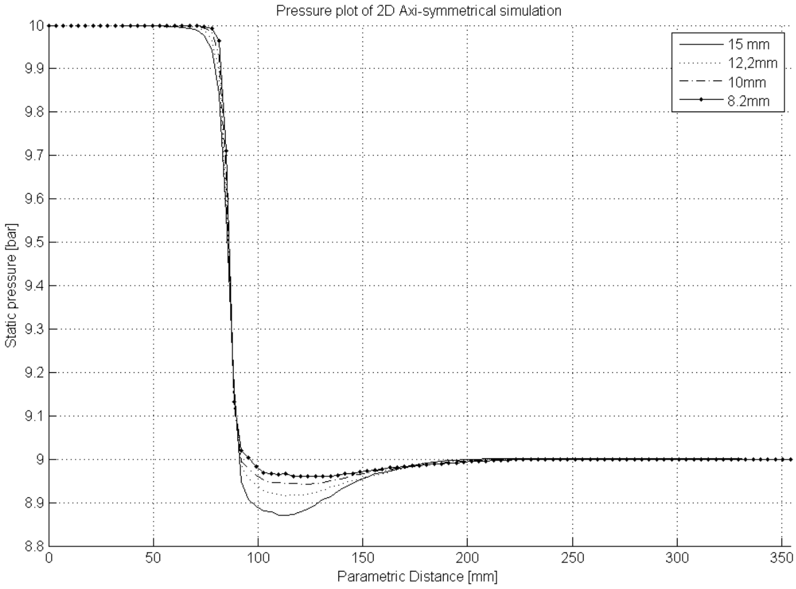

Figure 4.3: Pressure plot of the 2D Axi-symmetrical simulations for different orifice sizes

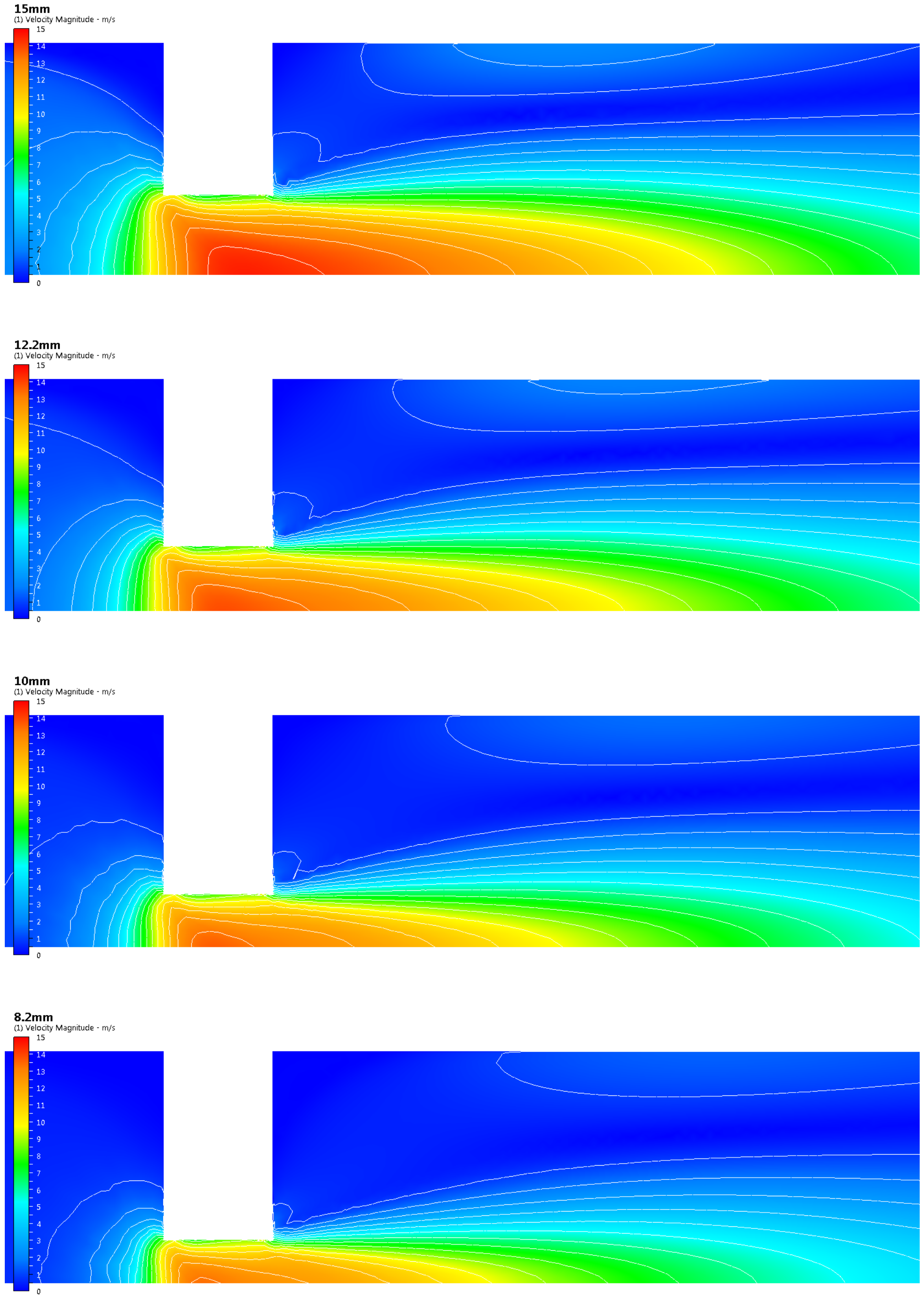

Figure 4.4: Velocity Contours plot from the Axi-symmetrical simulation for the different orifice sizes.

Mass flow rate [kg/s]	Reynolds Number [-]	15mm p_1 [Pa]	12.2mm p_1 [Pa]	10mm p_1 [Pa]	8.2mm p_1 [Pa]
0,25	7380.4	1466.59	3570.47	8503.52	19981,6
0,50	14760,8	5833,23	14238,8	34174,9	80722,5
1,00	29521,7	23654,2	58404	137409	327193
2,00	59043,3	94864	236436	558715	1317500
4,00	118087	378680	923990	2231010	5271870
6,00	177130	843823	2024570	4928990	11820520
8,00	236173	1466940	3590250	8733730	20988800

Table 4.9: Results of the 2D Axi-symmetrical Orifice simulation for different orifice sizes

Mass flow rate $[kg/s]$	15mm C_d $[-]$	12.2mm C_d $[-]$	10mm C_d $[-]$	8.2mm C_d $[-]$
0.25	0,820	0,798	0,771	0,748
0.50	0,822	0,799	0,769	0,745
1.00	0,817	0,789	0,767	0,740
2.00	0,816	0,784	0,761	0,737
4.00	0,816	0,793	0,761	0,737
6.00	0,820	0,804	0,768	0,738
8.00	0,830	0,805	0,770	0,739

Table 4.10: C_d values of the 2D Axi-symmetrical Orifice simulation for different orifice sizes

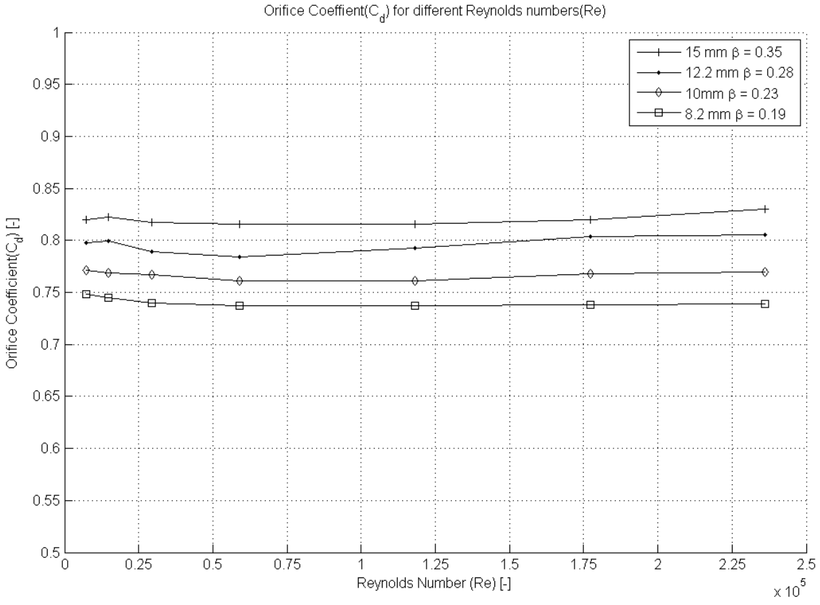

Figure 4.5: Plot of the orifice coeffients for different Reynolds values

The results of the different simulations are seen in table 4.8, 4.9 and 4.10, as well as figures 4.2, 4.3 and 4.4.

The graphs in figure 4.2 and 4.3 show that the overall behaviour of the different orifice sizes is similair in terms of pressure drop, pressure drop overshoot and velocity increase at the vena contactra. A clear relation can be seen between the beta ratio and the maximum velocity. The velocity increase for each stage is about the same, the difference lies in the intial velocity upstream. When the beta ratio is bigger then the contaction is smaller, this also means that the resistance is smaller. For this simulation series where the pressuredrop over the complete assembly is the same for all cases that a larger beta ratio means a larger mass flow and thus a larger velocity upstream. This is what one would expect since orifice is bigger.

The second aparent relation to see is between the pressure overshoot. The pressure locally at the vena contracta is lower then at the exit. The pressure will recover after the vena contracta to the exit pressure. The difference is the overshoot. From figure 4.3 it can be seen that the larger orifices, with the larger beta ratios have larger overshoots. The larger overshoot is becease the absolute velocity increase is also larger for the larger beta ratios. From bernouli's law we know that an velocity increase will result in a pressure drop and vice versa.

The velocity contour plots in figure 4.4 show the same overall result as the graphs. Here is can be clearly seen that the velocity profile at the orifice is the same for all for orifices. The size of the orifice directly determines the mass flow and thus also the size of the area with an velocity increase. The color scale for all contourplots is set equal. The absolute velocity is the highest for the first orifice and the lowest for the smallest orifice. The area which is need to dissipate the velocity increase when the flow area increases after the orifice is also proportional to the orifice area.

In figure 4.5 can be the results be seen for the simulation of the different orifices at different Reynolds numbers. Although there a small fluctution in the number we can see a an almost constant orifice coefficient for the different Reynolds numbers. The orifice coefficient seems the be slightly increasing near the laminair region. If this is the case cannot be said for sure since the aim was to do all simulations in the turbulent region, also a turbulent flow entering the assembly. This means that no near laminair or laminair situation could have been simulated. The orifice coeffient in the laminair region however is not of importance since the multi-stage orifice trim will only operate in the turbulent region in general.

We would expect that the orifice coefficient would be the same for all orifices. In the calculation of the orifice coefficient is a term that corrects for the β ratio. The difference lies in the ration between the diameter of the orifice and the thickness of the orifice plates. This ratio differs much for the different plates.This is what causes the orifice ratio to be different for each plate.

4.5.2 Single Orifice plates results 3D Quater-Model

The results of the 3D quater model simulation can be seen in table 4.11 and figures 4.6 and 4.7. The velocity contour plots have been omitted since they were very similair to the 2D simulations.

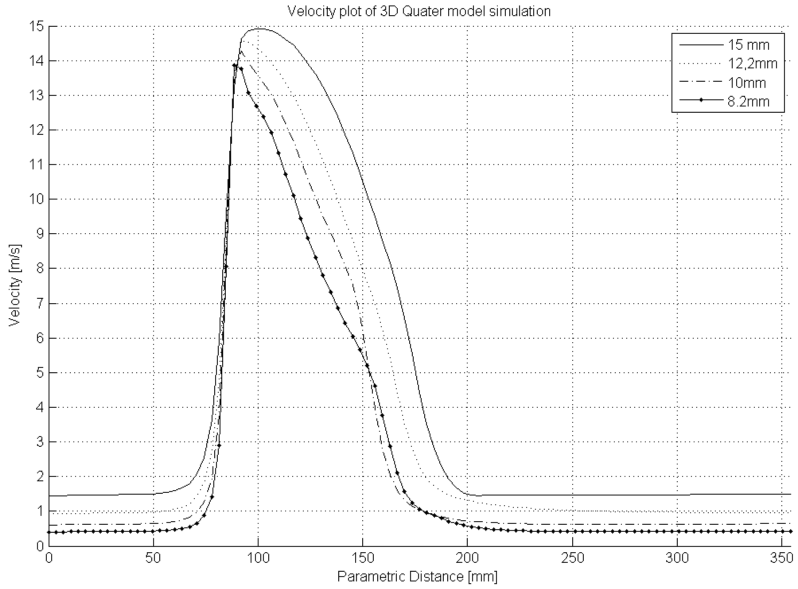

Figure 4.6: Velocity plot of the 3D simulations for different orifice sizes

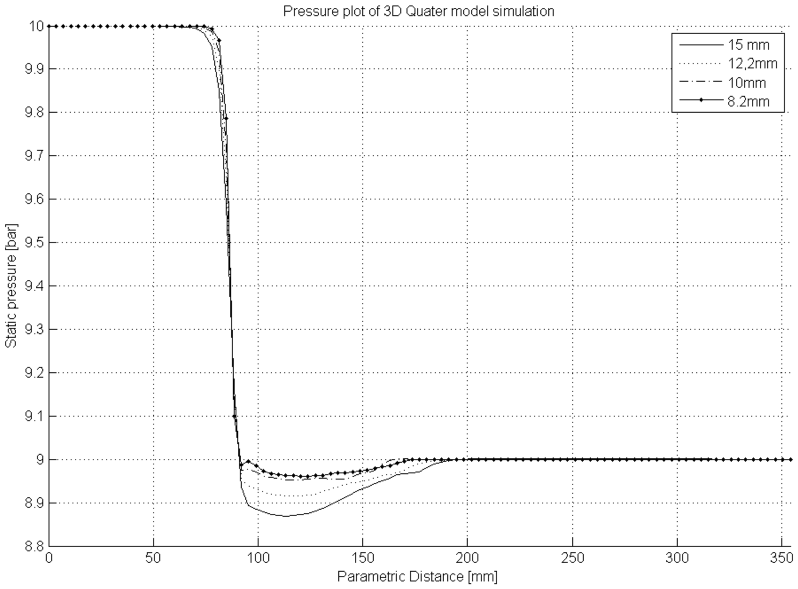

Figure 4.7: Pressure plot of the 3D simulations for different orifice sizes

Orifice Diameter $[mm]$	Beta (β) ratio $[-]$	Mass flow simulation $[kg/s]$	Calculated C_d $[-]$	Reynolds Number $[-]$
15	0.3488	2.028	0.806	59.796
12.2	0.2837	1.297	0.782	37.925
10	0.2326	0.849	0.764	24.997
8.2	0.1907	0.556	0.744	16.335

Table 4.11: Results of the 3D CV simulation for different orifice sizes

4.5.3 Comparison 2D Axisymmetric and 3D

The results for the 2D Axisymmetrical and 3D quater model simulation are given in table 4.12. From the results and the velocity and pressure contours plot the results are very similair. This is what we would expect since the geometry, boundary conditions and other settings of the different simulations are the same. In the 2D simulations the 3D swirl effects and pressure losses or normal friction components will not be accounted for. The program does offer an option to include this, but this has been omitted in the 2D simulations since the input for this was not available . With more extensive 3D simulations this could be investigated and be used as input to obtain more precise 2D results. The overall results of the 3D simulations are slightly better than the 2D simulations but the difference is marginal. Overall can be concluded that 2D simulations are a good alternative to obtain fast and accurate orifice coefficient results.

Orifice Diameter $[mm]$	Beta (β) ratio $[-]$	Mass flow 2D $[kg/s]$	Mass flow 3D $[kg/s]$	Calculated C_d 2D $[-]$	Calculated C_d 3D $[-]$
15	0.3488	2.024	2.028	0.804	0.806
12.2	0.2837	1.284	1.297	0.774	0.782
10	0.2326	0.846	0.849	0.761	0.764
8.2	0.1907	0.554	0.556	0.741	0.744

Table 4.12: Results of the 3D CV simulation for different orifice sizes

4.5.4 Pressure recovery coefficient single stage orifices

The pressure recovery coeffient for the different orifice calculations is given in table 4.13. The pressure recovery coefficient is the ratio between the recoverable and the non-recoverable pressure drop. It provides a measure for the overshoot in pressure drop when the fluid goes from the inlet pressure to the oulet pressure over the orifice. In the case of a controlvalve the excessive pressuredrop should be as low as possible since any additional pressuredrop, altough recoverable, can cause cavitation. The equation for the pressure recovery coefficient is;

$$F_L{}^2 = \frac{p_1 - p_2}{p_1 - p_{vc}} \tag{4.10}$$

Orifice Diameter $[mm]$	Beta (β) ratio $[-]$	F_L 2D $[-]$	F_L 3D $[-]$
15	0.3488	0.940	0.940
12.2	0.2837	0.960	0.961
10	0.2326	0.972	0.972
8.2	0.1907	0.980	0.981

Table 4.13: Pressure recovery coefficient for the 2D and 3D simulations for different orifice sizes

The pressure recovery factors for the 2D and 2D simulations are very similair. This is what we would expect since the velocity contours and pressure contours are also very similair. What is remarkable is the dependance on the geometry. When the beta ratio becomes smaller the pressure recovery factor becomes larger and thus better for our purpose. The decrease in beta ratio also marks a decrease in orifice coefficient in this case since the thickness ratio is also changes with different Beta ratios. The thickess of all orifice plates is the same but the orifice diameter differs.

Wheter the increase is pressure recovery factor is because of the difference in beta ratio of thickness ratio cannot be determined from this data. Additional simulations need to be used to conclude this.

Overall are the found values for the pressure recovery factor very optimistic. These values are not realistic for a controlvalve since the beta ratio which was used here is no where near the beta ratio in a control valve were many holes are and the ratio between the orifice area and the inlet area is much larger.

4.5.5 Multiple orifice plates results

In tables 4.14 and 4.15 the results of the CFD calculation for the multiple orifice configuration is given. There have been done significantly less results since the time was limited and the needed time for the simulations was much more then the 2D and quater model simulations. The choice has been made to only perform the simulations with one massflow. The construction of the mesh and the preperation of the model has been done in the same manner as the earlier simulations.

The model that has been used is a half model. In the single orifice has an infinite number of symmetry planes since it is a single hole installed in a tube, this made the use of 2D axial symmetric model possible. The combination of orifice plates is too wide to be able to be fitted in the center of the tube. The complete assembly was therefore mounted excentric. This means that the first used orifice plate is also mounted excentric so this simulation was also done. The excentric mounted hole however only has one symmetry plane so a half model was used. The combination also has one symmetry plane so this was also modelled and evaluated with a half model.

In figure 4.8 the velocity contours for the different configurations can be seen. The scales in all figures are the same for convenience. It is clear to see than when the number of stages increases, and the smallest crosssectional area decreases the peak velocity increases. This is what one would expect, if the mass of volume flow is constant and the flow passage becomes smaller then via the law of mass conservation the velocity must increase. In the figures is also clear to see the increase in velocity near the inlet, the regions of increases velocity radiate out from the center of the entrance. At the exit the increased velocity is smeared out over outlet portion in an elipse form or a jet. Interesting to see in the creation of an vortex like velocity region in the lower side of the outlet. The size of this affected area differs with the number of stages used and thus the peak velocity. The highspeed jet in the top portion of the outlet tries to carry fluid with it towards the outlet, this creates the wake region. When the velocity of the jet increases with an increase in stages we would expect the wake region also to increase. From the velocity contours we can see that this is not the case. There are two possible reasons for this. One reason is that the position of the jet changes with an increase in the number of stages and the second is that the walls of the tube are relatively close to the jet and the wake area. Both possible causes limit the size of the wake region

The influence of the orifice being placed excentric in the tube is investigated by running an additional simulation. The obtained results in axial-symmetric and quater model orifice of 15mm placed cocentric in the tube are seen in table 4.12. The average orifice coefficient for the cocentric mounted orifice is 0.805, for the not concentric mounting the obtained result is 0.801. The orifice coeffient is thus slightly smaller in a non concentric mounting. In the velocity contourplot the jet at the oulet is very close to the wall, but the influence seems negiable. An important differnce can be seen with the wake formation. In the concentric configuration a wake is formed all around the jet, however in the non-concentric mounting this is only seen in the lower part of the outlet tube. The influence of this concentric mounting seems negiable, however this is only for this situation. The roughness of the wall is not explicitly modelled, the no-slip boundary condition was applied, but the wall is still assumed to be smooth. The second remark is that the reynolds number for this flow is relatively small, maybe at higher reynolds number the influence of the wall will become a bigger contributing factor, as well as the formation of the wake.

The influence of the wall in this simulations is not very large, but is does have some significant influence on the results. For the calculation of the orifice coefficients of the stage combinations this is not ideal since the performance is obviously affected by the pipe wall. However the aim is still to find the performance characteristics of the multi-stage trim of a control valve. In a control valve the wall is not as near to the stage exit as in this simulation but other holes might be. The presence of a wall can mimic the influence that another jet in the near area has on the performance of one multi-stage hole. When we keep this in mind the presence of the wall is somewhat less inconvenient then one would think initially.

Configuration plates installed	Mass flowrate [kg/s]	Reynolds Number [-]	Inlet pressure [Pa]
5	0.135	2499	448.082
4-5	0.135	2499	729.954
3-4-5	0.135	2313	2151.24
2-3-4-5	0.125	2313	4229.63
1-2-3-4-5	0.125	2313	1,0002.8

Table 4.14: Data of the 3D Multiple orifice simulations with Normal offset

Configuration plates installed	Mass flowrate [kg/s]	C_d [-]	C_v [-]
5	0.135	0.801	8.41
4-5	0.135	0.943	6.58
3-4-5	0.135	0.874	3.83
2-3-4-5	0.125	0.861	2.53
1-2-3-4-5	0.125	0.847	1.64

Table 4.15: Results of the 3D Multiple orifice simulations with Normal offset

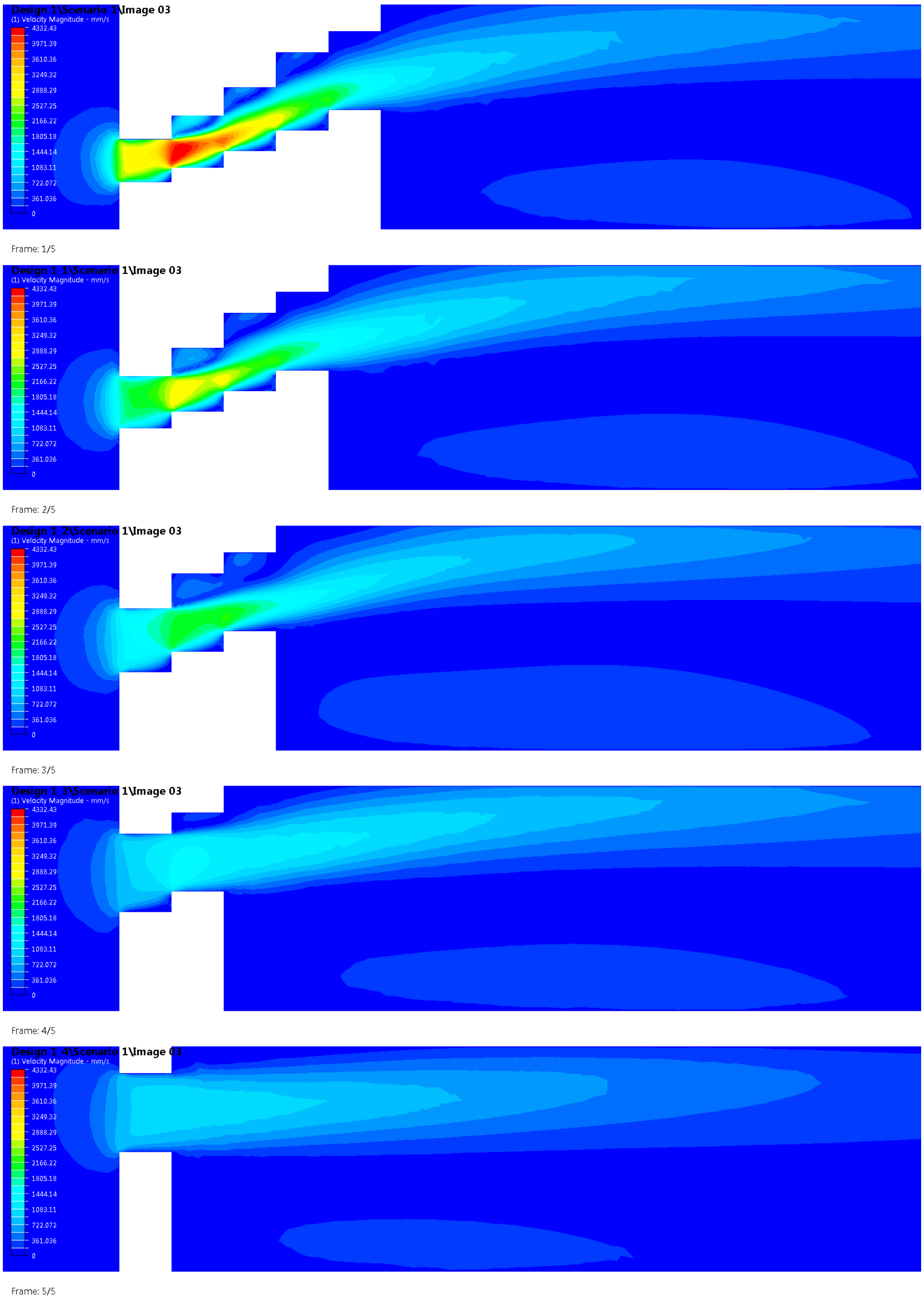

Figure 4.8: Velocity Contours plot of the different configurations with normal offset

4.5.6 Normal versus Alternating offset

In the design the orifice plates testing setup there is an option to configure the plates in two different ways. The offset from one plate to another can be done in a staggered configuration, in which the total offset, measured from the first plate, increases with each plate. Alternatively the can be chosen for an alternating offset in which the plates have the offset in opposite direction of the previous plate and the total offset is close to zero. The standard in the controlvalve is the staggered offset. To better understand this choiche the simulation between a conventional staggered offset and an alternating offset is compared.

The results from the normal offset are from the earlier performed simulation for the full configuration compared to the other configuration can be seen in tabel 4.16.

Configuration	Mass flowrate [kg/s]	Reynolds Number [-]	Inlet pressure [Pa]
Normal	0.125	2313	1.002.8
Alternating	0.125	2313	8594.69

Table 4.16: Data of the 3D Multiple orifice simulations with Normal and Alternating offset for configuration 1-2-3-4-5

Without any further calculations, we can already see a clear difference between the two configurations. With the same massflowrate applied the alternating configuration has a smaller pressure drop then the normal offset configuration. The boundary condition for the oulet is 0 Pa, so the inlet pressure is in this case equal to the pressure drop. When the pressuredrop is smaller this automically means that the valve coefficient C_v and the orifice coefficient C_d are higher for this configuration. After some calculations we obtain the following results as seen in table 4.17 and in figure 4.9. The orifice coeffient and the valve coefficient for the alternating offset is better than with the normal offset. This means that when the same pressuredrop is desired, the size of an alternating offset configuration can be smaller.

Configuration	Mass flowrate [kg/s]	C_d [-]	C_v [-]
Normal	0.125	0.847	1.64
Alternating	0.125	0.914	1.77

Table 4.17: Results of the 3D Multiple orifice simulations with Normal and Alternating offset for configuration 1-2-3-4-5

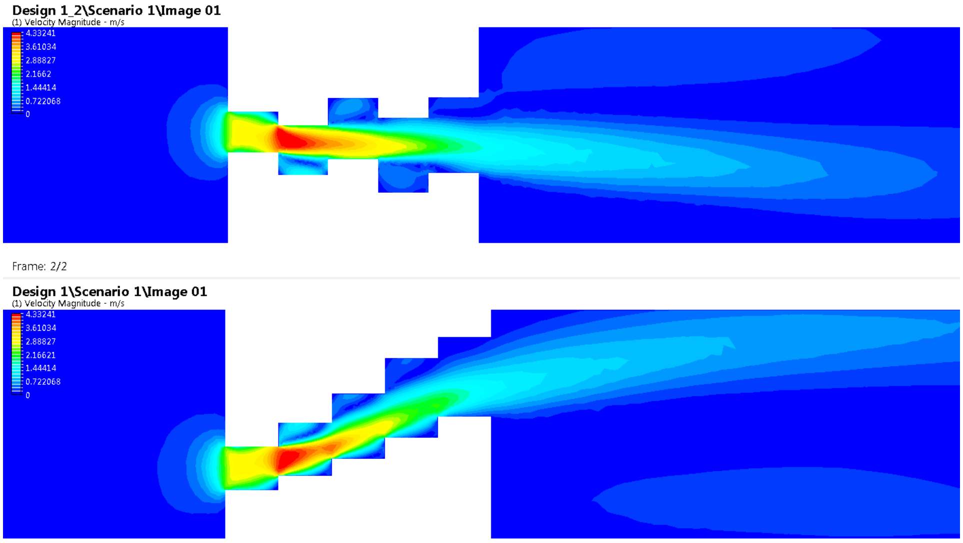

Figure 4.9: Velocity Contours plot of the different configurations with normal and alternating offset

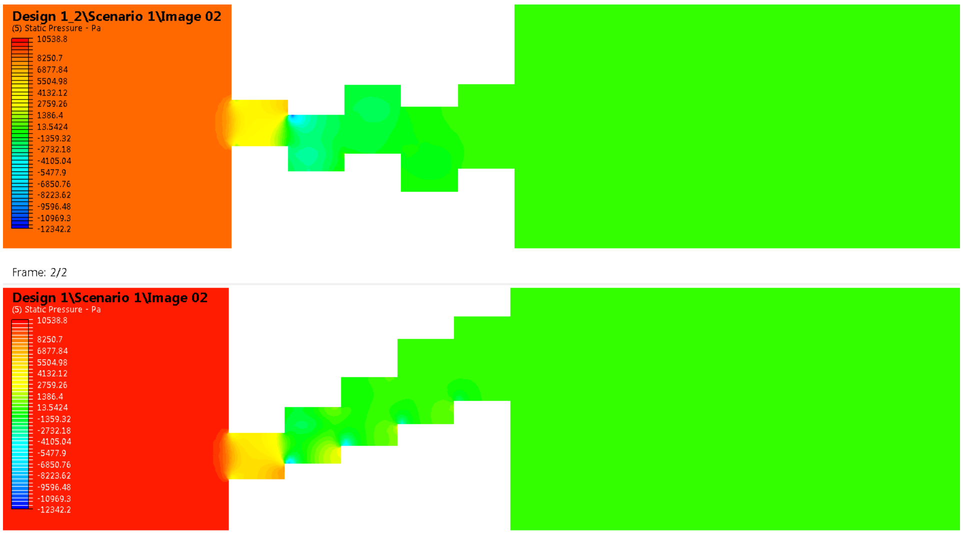

Figure 4.10: Pressure Contours plot of the different configurations with normal and alternating offset

Pressure recovery coefficient

In figure 4.11 the pressure plot of the two different configurations can be seen along a streamline. The pressure is made dimensionless by dividing it with the inlet pressure. The dimensionless pressure is in this case more convenient since the inlet pressure of the two analysis is different. For convenience the length is also made dimensionless. In the pressure plot there is a clear difference to be seen between the normal and alternating offset. The normal offset has an overshoot in pressuredrop which is much smaller then the overshoot of the alternating offset. Also the pressure is reduced in steps in the normal offset configuration, whereas the alternating offset has one large pressuredrop. With this data available the pressure recovery coefficient of the complete stages can be calculated. The calculated values are seen in table 4.18. From the graph and the data we can conclude that the normal offset is favorable since the pressure recovery is better, which reduces the chance that cavitation will occur.

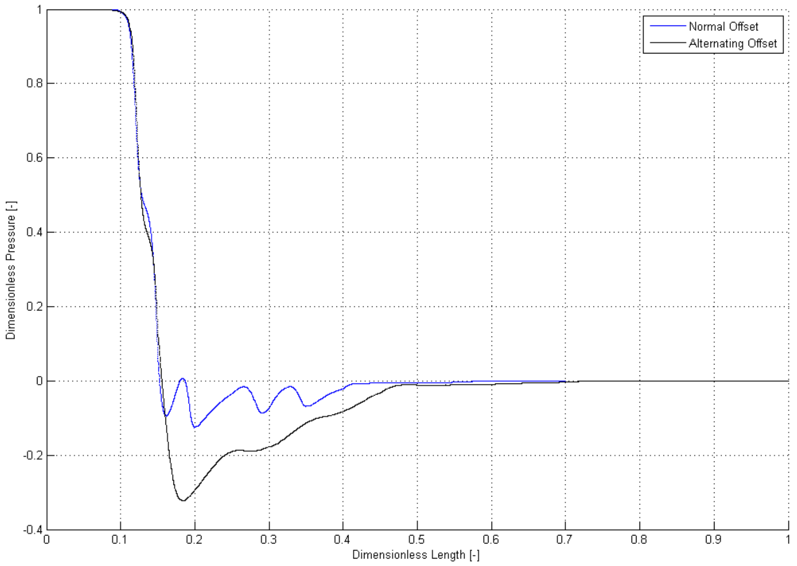

Figure 4.11: Pressure plot of the different configurations with normal and alternating offset

Configuration	F_L [-]
Normal	0.941
Alternating	0.868

Table 4.18: Pressure recovery coefficients for normal and alternating offset

4.6 Full-scale testing setup

An overview of the layout and the used instrumentation can be found in chapter 5.1 and chapter 5.1.1

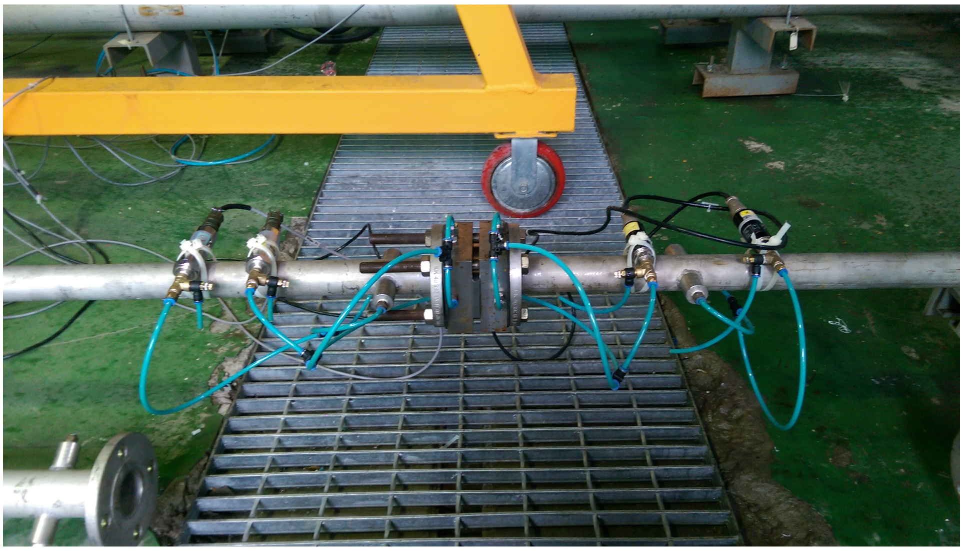

Figure 4.12: Picture of the orifice carrier plates and one plate installed in the flow-loop

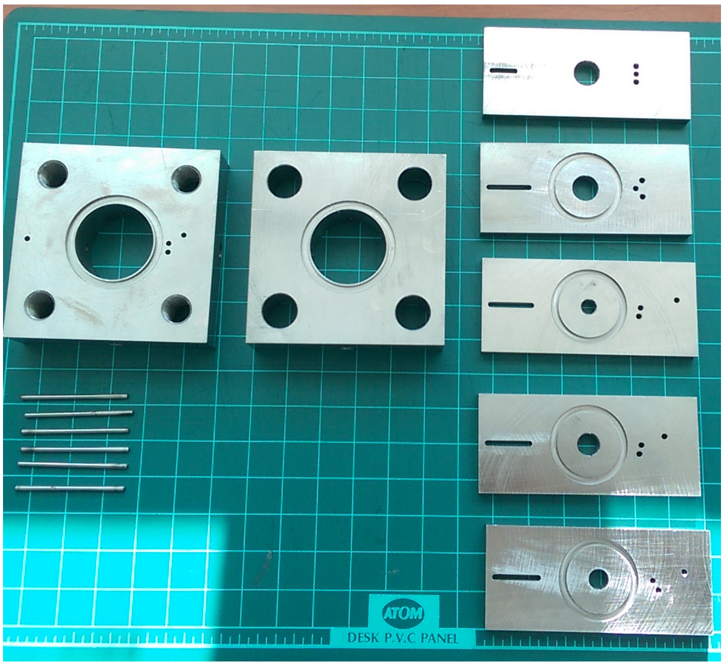
ATOM
DESK P.V.C PANEL

Figure 4.13: Overview of the orifice carrier plates and the single orifice plates

4.7 Pressure gage calibration

In the test setup for the orifice plates are four pressure tappings used. Each pressure tapping will have its own pressure sensor. In the loop are normally two pressure sensor used. One is used to measure the static pressure at the water tank and the other one is used to measure a pressure difference. The pressure difference sensor is normally used for a C_v measurement were only the pressure difference is important. For the orifice test the pressure difference will not suffice. Also this pressure difference sensor has a too limiting range. This one sensor will be replaced by four other sensors. Two pressure sensors have a measuring range of 0-10 kPa and the remaining two have a measureing range of 0 to 4 kPa. The four pressure sensors have not been used previously in this testing facility. Also their history is unknown. The pressure sensors thus have to be calibrated. The calibration is done by comparing the observed values of the sensors with a fifth sensor. The sensor that will be used is the sensor which is already installed in the loop. This sensor has a known history and is relatively accurate compared to the other sensors.

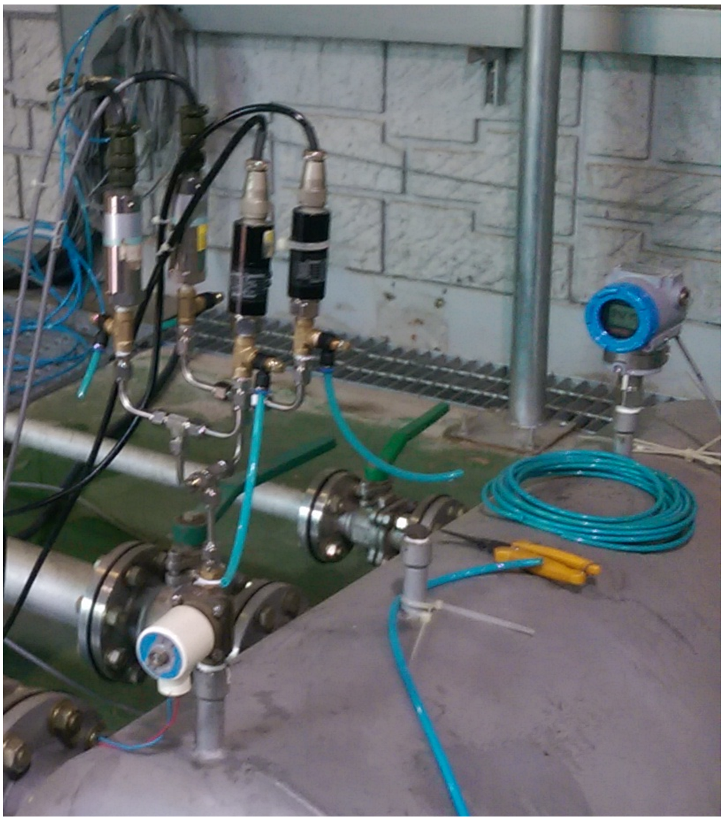

Figure 4.14: Overview of the setup used for the pressure gage calibration

4.7.1 Method

In figure 4.15 a typical scatter plot of a dataset can be seen. In this example the data a pressure sensor p_0 is used. The y-axis represents the pressure measured by the sensor and the x-axis gives the measurement number. A prinicple point for processing the data is the assumption of a normal distribution of the datapoints. The pressure inside the tank is being held at a near to constant pressure. The pressure gages would then also show a constant value in a an ideal situation. The reality is however that there are small fluctuations in the pressure at the tank, the signal going to the processing computer and random noise in the signal. Although the fluctuations and the noise are undesirable their effects can be corrected for. The pressure fluctuation and the noise on the signal are assumed to be random. This implies that when enough datapoints are used, the datapoints will show a gaussian or normal distribution since the average contribution of the noise will converge to a constant value of zero.

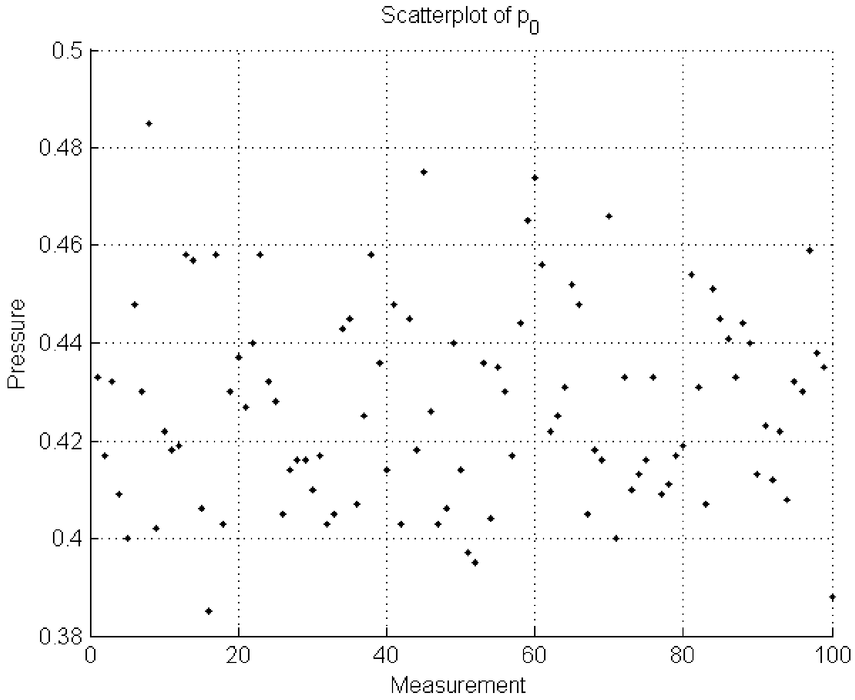

Figure 4.15: Scatterplot of the measurement data of the reference pressure sensor

The use of a normal distribution will allow us to determine the pressure at the tank more precisely. Also it will allow us to compare the pressure to eachother more closely. In figure 4.17 a normal plot of the datapoints in figure 4.15 can be seen. From the normal plot it is easier to see whether the data follows a normal distribution. When the data is normally distributed then all point are on the blue line. The datapoints are overall close the line, but there are some point who deviate. These points are called outliers. With the normal plot the validity of the normal distribution can be investigated. The confidence interval for the fit of the normal distribution is set at 95% or alternatively $\alpha = 0.05$.

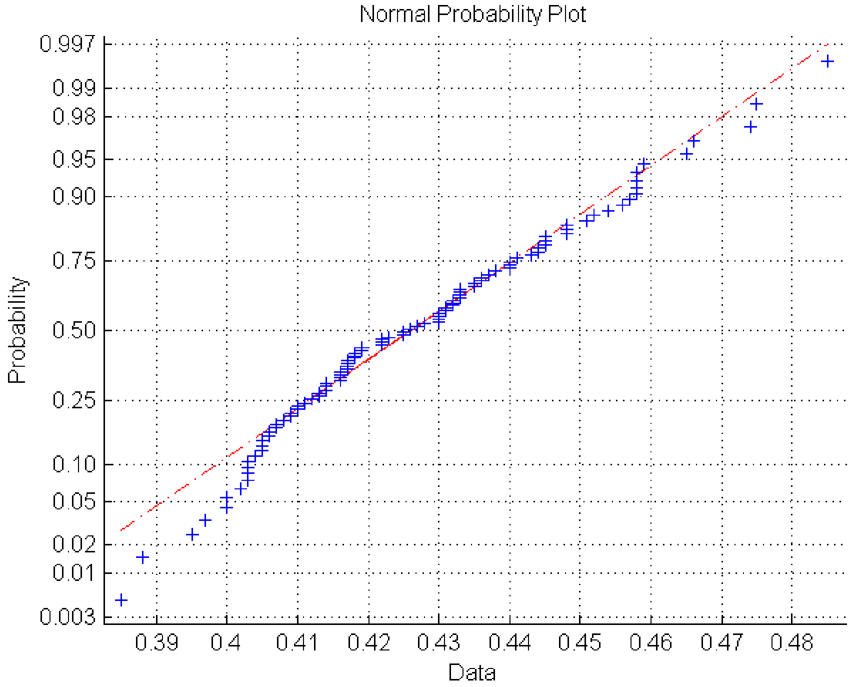

Figure 4.16: Normal plot of the measurement data of the reference pressure sensor

The same process can be done with the data of the other gages. The goal of the process is to determine the difference, if there is between the reference pressure sensor and the other pressure gages. Therefore not the data of the each pressure sensor itself is analysed but rather the difference between the pressure gages. Before the data can be used is has be to be determined that indeed there is a statistical difference between the two sets of data. The same confidence interval of 95% is used here.

After checking that there indeed is a statistical difference between the data of the pressure sensors the pressure difference between the reference sensor p_0 and the other sensors is computed. The difference is then also checked for normal distribution. In figure **??** the normal plot of the different pressure differences is seen.

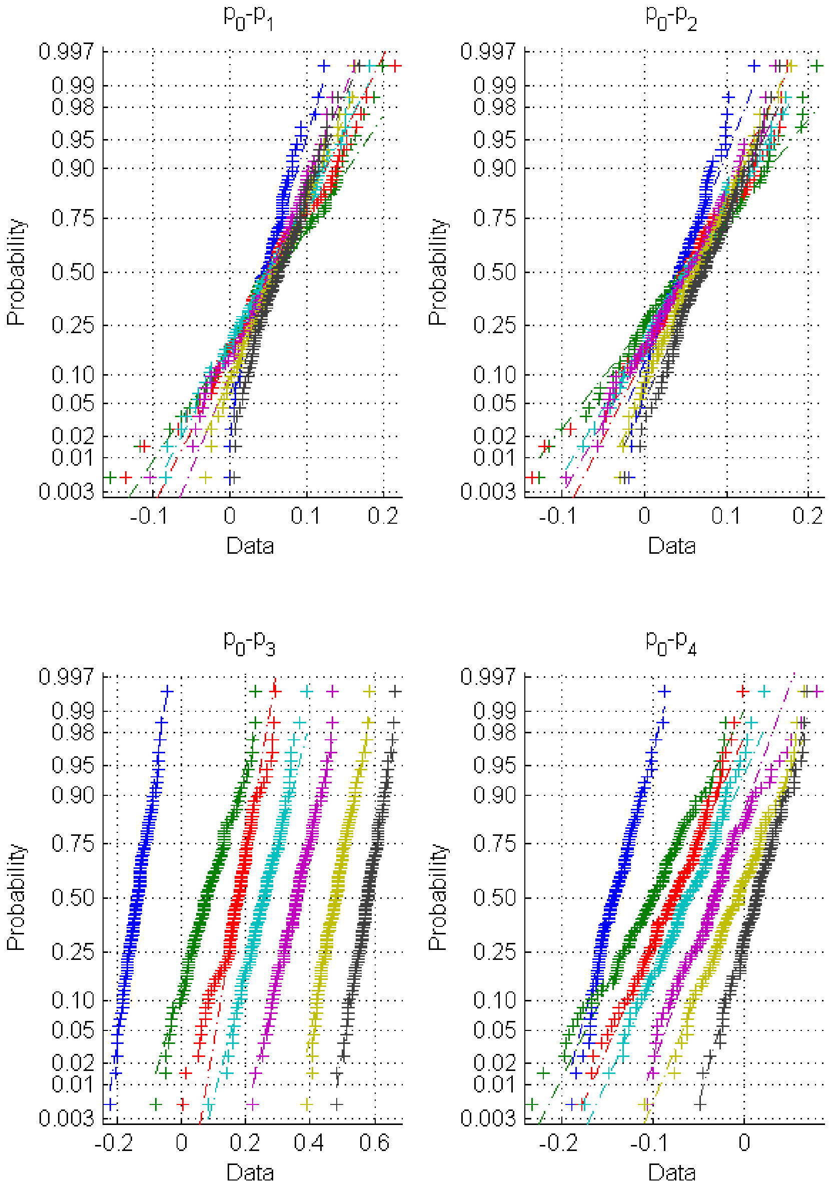

Figure 4.17: Normal plot of the measurement data of the difference pressure with the reference pressure sensor

4.7.2 Outlier Removal

The collection of data from the pressure sensors will contain some incorrect data points. The presence of these datapoint is inevitable and their influence on the results also cannot be neglected. The detection and removal of these incorrect data points, called outliers, can be done in several ways. One method is to manually check all data points an investigate points which are far from the straight line in the normal distribution plot to see whether they can be omitted or not. This is the best but also the most time consuming method, also retracing the reason why point is an outliers is not always straightforward. The shear number of datapoints in the dataset is restricting in using the manual method. The outlier therefore will be identified and removed using Cooks distance method. This is method is that is capable of identifying potential outliers in a regression model. Although the complete dataset is a normal distribution there is an expected regression model to be fitted. This is a line with a zero slope and thus a constant.

$$D_i = \frac{\sum_{j=1}^{n}(\hat{Y}_j - \hat{Y}^2_{j(i)})}{p \cdot MSE} \tag{4.11}$$

In this $\hat{Y}_j$ is the prediction of observation j from the full regression model. $\hat{Y}_{j(i)}$ is the prediction for the same observation, but then with an regression model from which observation i has been omitted. The MSE term stands for the mean square error of the regression model and p is the number of parameters fitted in the regression model. The

The threshold that will be used is given in 4.12. There are many different threshholds being used nowadays. Other threshholds that are begin used as a guideline is $D_i > 1$. The threshhold on basis of the number of observations will be used since it is more conservative and gives usefull resuslts for this application.

$$D_i > 4/n \tag{4.12}$$

An example of outlier removal can be seen in figure 4.18. In red are the outlier that are selected by using Cooks criterium. These outliers will be removed in order to increase the fit of the normal distribution.

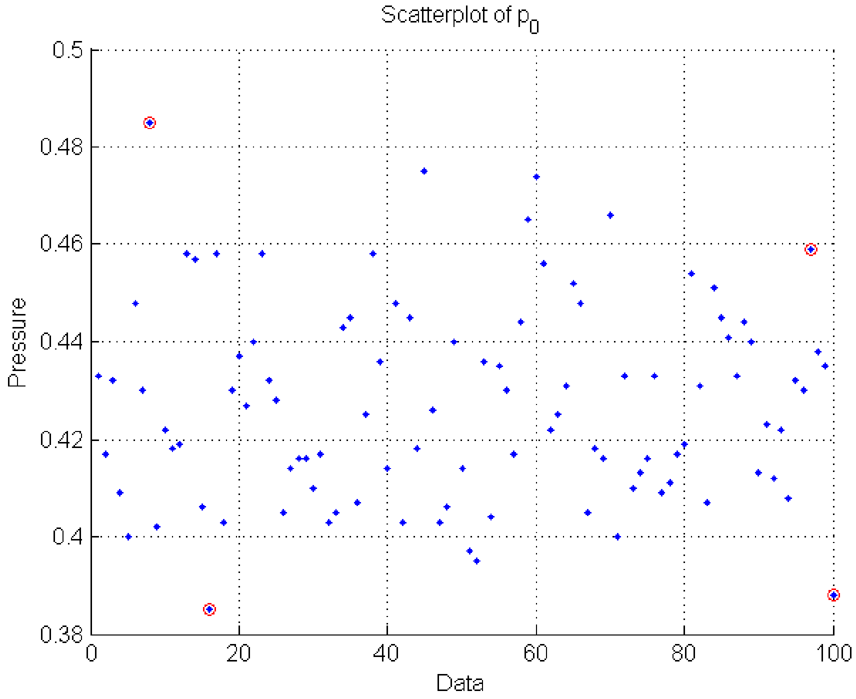

Figure 4.18: Scatterplot of the measurement data of the reference pressure sensor with outlier identified

The method of identifying and removing the outliers will be used on all the data points. From the corrected data the mean and the variance will be computed. The mean and the variance of the pressure difference between the reference pressure sensor p_0 and the other pressure sensors can then be utilized to compute the correctionfactor. The determination of the correctionfactor will be given in section 4.7.3.

4.7.3 Correctionfactor

After the outliers have been removed the correctionfactor for the different pressure gages can be calculated. In figure 4.19 the correction factor for gages 1 until 4 can be seen as a function of the pressure. The points in the graph have been fitted with a polynominal function. The function has been fitted with the aid of the least squared method. The order of the polynominal fit was selected via an interative method by checking the R^2 and the adjusted R^2 values. In many cases a higher order polynominal function gives a better fit, but this does not always hold true. When the adjusted R^2 value is lower than the R^2 value then a higher order polynominal fit does not give a better result. The result is a polynominal function that can be used to corrected the pressures form gages 1 until 4.

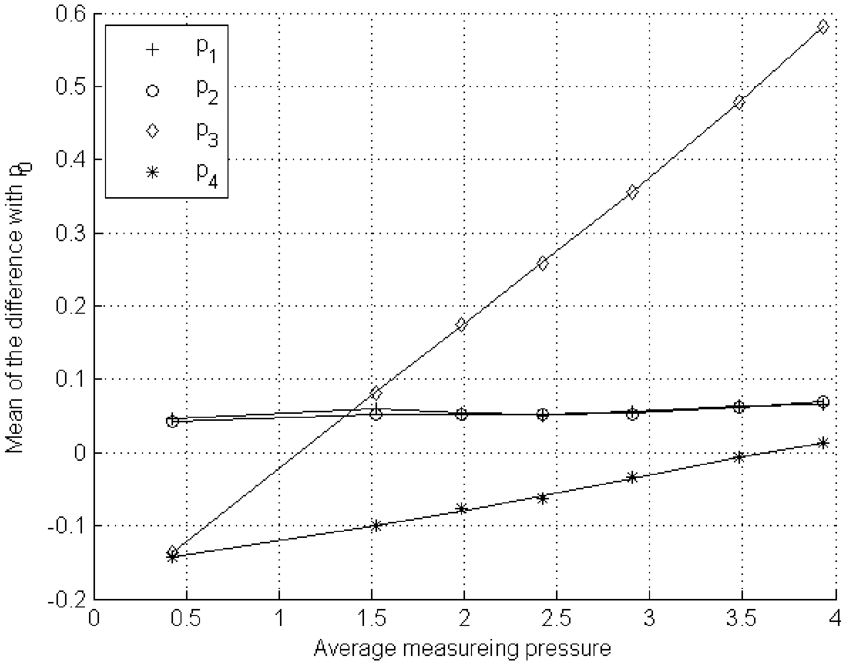

Figure 4.19: Graph of the correction factor for the different pressure gages as a function of the pressure

4.8 Full scale test Data

4.8.1 Single orifice plates

Note that all given pressure are in absolute pressure.

Volume flow rate $[m^3/h]$	Temperature $[°C]$	p_1 $[bar]$	p_2 $[bar]$	p_3 $[bar]$	p_4 $[bar]$
3,89	15,23	4,78	0,86	0,50	0,41
3,59	15,33	3,80	1,64	0,54	0,41
3,25	15,35	2,88	1,86	0,58	0,41
2,94	15,34	2,19	1,71	0,60	0,41
2,80	15,38	2,00	1,63	0,61	0,41

Table 4.19: Data of the 8.2mm orifice

Volume flow rate $[m^3/h]$	Temperature $[°C]$	p_1 $[bar]$	p_2 $[bar]$	p_3 $[bar]$	p_4 $[bar]$
5,86	15,35	4,71	0,93	0,43	0,42
5,39	15,30	3,76	1,66	0,48	0,42
4,85	15,20	2,83	1,86	0,52	0,42
4,33	15,12	2,15	1,69	0,58	0,42
4,11	14,99	1,95	1,60	0,59	0,42

Table 4.20: Data of the 10mm orifice

Volume flow rate $[m^3/h]$	Temperature $[°C]$	p_1 $[bar]$	p_2 $[bar]$	p_3 $[bar]$	p_4 $[bar]$
8,43	14,99	4,63	1,00	0,35	0,44
7,70	15,01	3,70	1,69	0,42	0,43
6,97	15,03	2,78	1,85	0,49	0,43
6,23	15,03	2,08	1,66	0,54	0,42
5,97	15,07	1,89	1,57	0,57	0,42

Table 4.21: Data of the 12.2mm orifice

Volume flow rate $[m^3/h]$	Temperature $[°C]$	p_1 $[bar]$	p_2 $[bar]$	p_3 $[bar]$	p_4 $[bar]$
12,39	14,98	4,51	1,14	0,26	0,47
11,30	14,86	3,60	1,74	0,35	0,46
10,14	14,75	2,68	1,84	0,43	0,45
8,85	14,54	2,02	1,63	0,50	0,44
8,28	14,30	1,83	1,53	0,52	0,44

Table 4.22: Data of the 15mm orifice

4.8.2 Multiple orifice plates

Note that all given pressure are in absolute pressure.

Volume flow rate $[m^3/h]$	Temperature $[°C]$	p_1 $[bar]$	p_2 $[bar]$	p_3 $[bar]$	p_4 $[bar]$
9.90	15.61	4.20	4.20	0.22	0.61
9.01	15.43	3.42	3.48	0.28	0.59
7.97	15.33	2.66	2.66	0.33	0.58
6.87	15.38	2.04	2.04	0.37	0.56
6.48	15.34	1.85	1.86	0.39	0.56

Table 4.23: Data of the orifice configuration 4-5 in normal offset

Volume flow rate $[m^3/h]$	Temperature $[°C]$	p_1 $[bar]$	p_2 $[bar]$	p_3 $[bar]$	p_4 $[bar]$
6.95	16.65	4.33	4.34	0.40	0.55
6.29	16.59	3.55	3.58	0.43	0.55
5.49	16.53	2.76	2.77	0.44	0.54
4.71	16.50	2.12	2.13	0.46	0.54
4.45	16.34	1.94	1.94	0.48	0.53

Table 4.24: Data of the orifice configuration 3-4-5 in normal offset

Volume flow rate $[m^3/h]$	Temperature $[°C]$	p_1 $[bar]$	p_2 $[bar]$	p_3 $[bar]$	p_4 $[bar]$
4.88	16.11	4.37	4.41	0.51	0.54
4.42	16.21	3.62	3.62	0.52	0.54
3.85	16.24	2.81	2.82	0.52	0.53
3.29	16.18	2.17	2.18	0.52	0.53
3.10	16.14	1.99	1.99	0.52	0.53

Table 4.25: Data of the orifice configuration 2-3-4-5 in normal offset

Volume flow rate $[m^3/h]$	Temperature $[°C]$	p_1 $[bar]$	p_2 $[bar]$	p_3 $[bar]$	p_4 $[bar]$
2.67	15.50	4.47	4.53	0.52	0.53
2.39	15.35	3.67	3.68	0.52	0.53
2.10	15.22	2.88	2.88	0.52	0.53
1.78	15.01	2.23	2.23	0.52	0.53
1.67	14.76	2.04	2.04	0.52	0.53

Table 4.26: Data of the orifice configuration 1-2-3-4-5 in normal offset

4.9 Full scale test Results

4.9.1 Single orifice plates

Mass flow rate $[kg/s]$	Reynolds number $[-]$	Density $[kg/m^3]$	Dynamic Visosity $[mPa \cdot s]$	Orifice Coefficient $[C_d]$
1,09	28555,14	1005,06	1,12	0.734
1,00	26432,31	1004,99	1,12	0.748
0,91	23928,79	1004,98	1,12	0.799
0,82	21660,37	1004,99	1,12	0.841
0,78	20620,31	1004,97	1,12	0.850

Table 4.27: Results of the 8.2mm orifice

Mass flow rate $[kg/s]$	Reynolds number $[-]$	Density $[kg/m^3]$	Dynamic Visosity $[mPa \cdot s]$	Orifice Coefficient $[C_d]$
1,64	43154,88	1004,98	1,12	0.703
1,51	39609,71	1005,01	1,12	0.727
1,35	35569,50	1005,07	1,12	0.747
1,21	31711,71	1005,12	1,12	0.776
1,15	30006,68	1005,20	1,12	0.784

Table 4.28: Results of the 10mm orifice

Mass flow rate $[kg/s]$	Reynolds number $[-]$	Density $[kg/m^3]$	Dynamic Visosity $[mPa \cdot s]$	Orifice Coefficient $[C_d]$
2,35	61456,12	1005,21	1,12	0.739
2,15	56216,35	1005,19	1,12	0.750
1,94	50865,84	1005,18	1,12	0.811
1,74	45475,44	1005,18	1,12	0.858
1,66	43609,79	1005,15	1,12	0.882

Table 4.29: Results of the 12.2mm orifice

Mass flow rate $[kg/s]$	Reynolds number $[-]$	Density $[kg/m^3]$	Dynamic Visosity $[mPa \cdot s]$	Orifice Coefficient $[C_d]$
3,46	90316,25	1005,21	1,12	0.728
3,16	82139,92	1005,28	1,12	0.729
2,83	73498,89	1005,35	1,12	0.770
2,47	63800,87	1005,48	1,12	0.821
2,31	59346,34	1005,63	1,12	0.799

Table 4.30: Results of the 15mm orifice

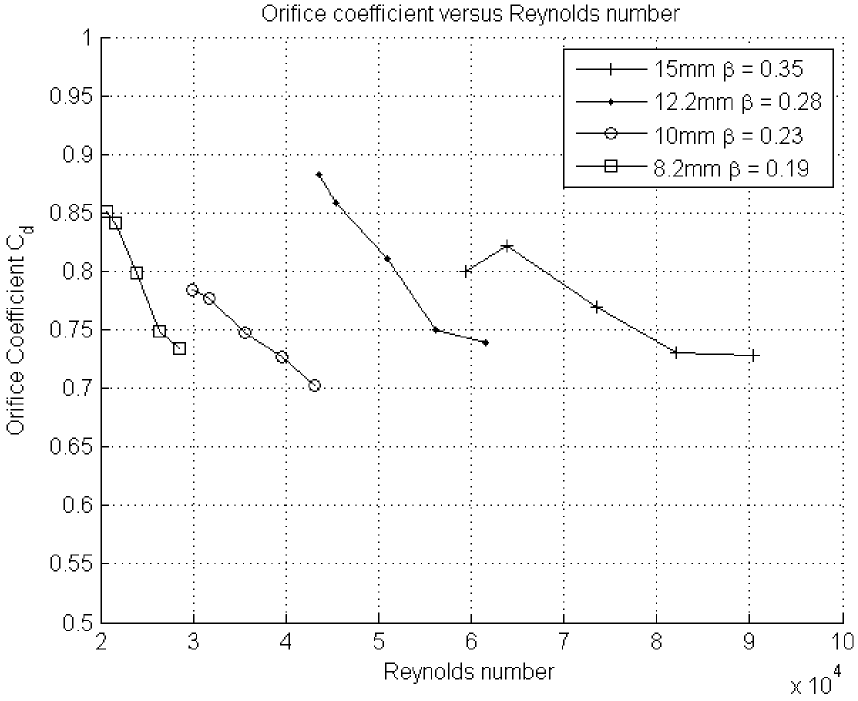

Figure 4.20: Orifice coefficient of the single orifice plates for different Reynolds numbers

4.9.2 Multiple orifice plates

From the measurement report given in section 4.11 we can recalculate the overlap area for the actual situation and correct for the manufacturing incaccuracy and tolerance. The results are given in table 4.31 and in 4.32

Stage	Offset Theoretical $[mm]$	Offset actual $[mm]$	Theoretical Area $[mm^2]$	Actual Area $[mm^2]$
1	$[-]$	$[-]$	176.71	177.23
2	4	3.878	117.80	119.25
3	5.3	5.316	78.53	77.12
4	4.3	4.252	52.35	53.34
5	3.6	3.533	34.90	29.97

Table 4.31: Theoretical and actual dimensions and area's for the normal offset multiple orifice configuration

Stage	Offset Theoretical $[mm]$	Offset actual $[mm]$	Theoretical Area $[mm^2]$	Actual Area $[mm^2]$
1	$[-]$	$[-]$	176.71	177.23
2	4	4.026	117.80	117.49
3	5.3	5.261	78.53	78.26
4	4.3	4.27	52.35	53.14
5	3.6	4.153	34.90	30.85

Table 4.32: Theoretical and actual dimensions and area's for the alternating offset multiple orifice configuration

In table 4.31 and 4.32 the results of the renewed area calculations can be seen. For the first stages the difference between the theorretical and the actual area calculated after the measurements are small in percentage and absolute. For the the final stages the area difference is much more significant, in actual and percentage. Especially the last stage show the necessity for the renewed area calculation after production instead of using the theoretical area. The corrected values for the area will be used for further calculations.

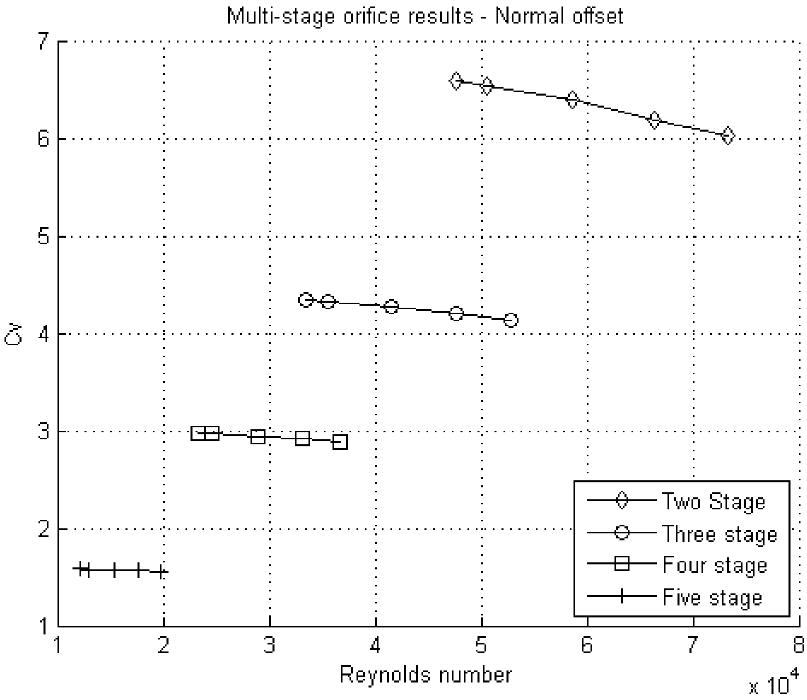

Figure 4.21: Cv results for the multiple orifice configuration with normal offset

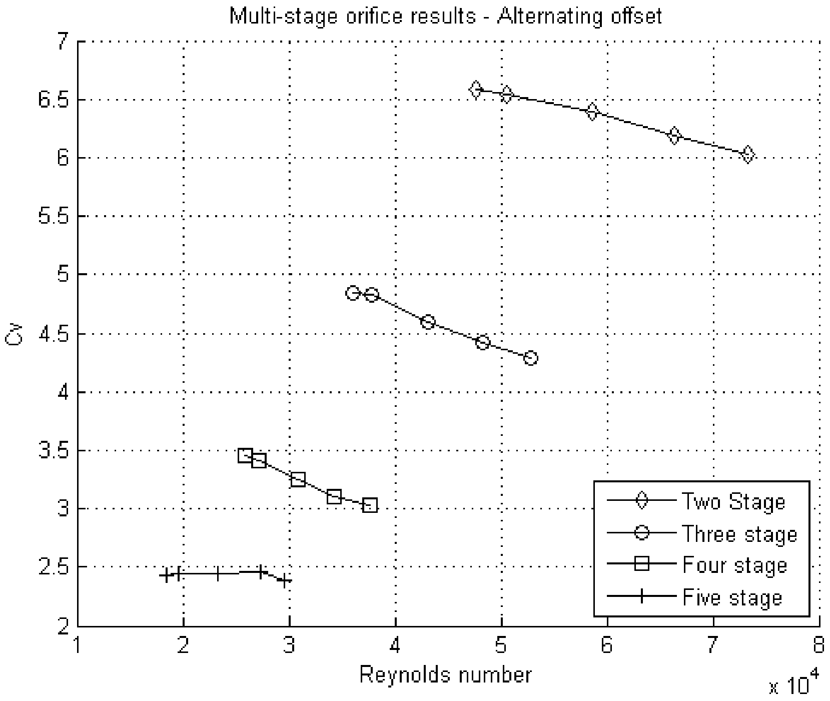

Figure 4.22: Cv results for the multiple orifice configuration with alternating offset

4.10 Comparison between staggered (normal) and alternating offset

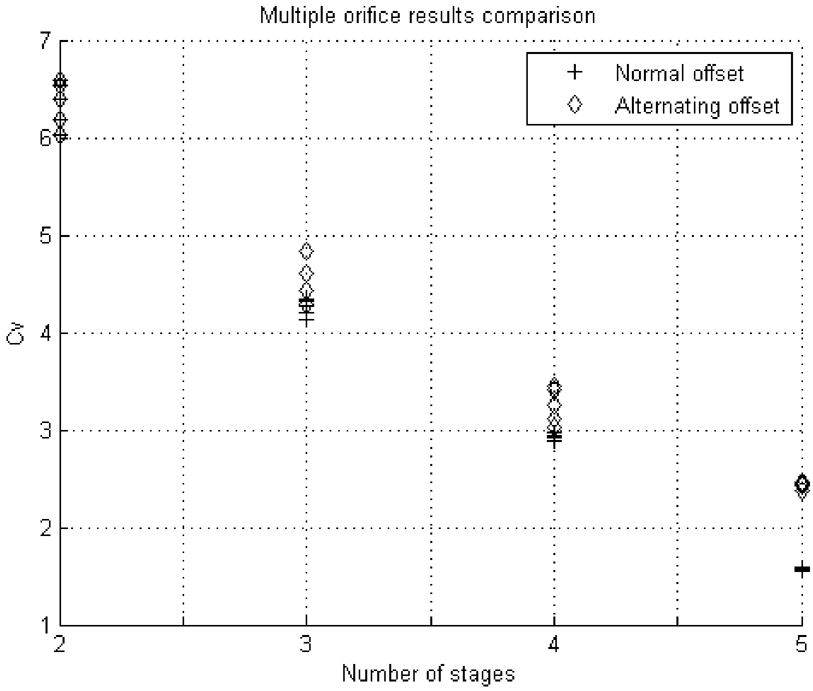

Figure 4.23: Cv results for the multiple orifice configuratiion with staggered and alternating offset

In figure 4.23 the results for the different offsets types can be seen. Multiple configurations have been testen, with different number of stages. The orifice plates are stacked in two different configurations. The first one is the type that is normally present in a control valve trim, this is the staggered configuration. Each plate has a certain offset from the previous one. The total offset measured from the first plate, increases with each plate. The second type is the alternatingoffset. The offset between two plates is the same as in the other configuration, but the total offset is balanced around zero.

The aim of the test was to see wheter there would be a significant difference in the performance between the types of offset. As mentioned before the standard type in a control valve is the staggered offset. The combination of a staggered offset in a circular pattern causes a swirl or vortex in at the oulet of the trim.

From the graph it is clear to see that the measurements for different Reynoldsnumbers for the same type of offset and number of stages are close to eachother. With an increase in the number of stages we can also see that the valve coefficient and inherently also the Orifice coefficient for the normal offset is smaller than with the alternating offset. When only two stages are used there is no difference between the two offset types. This is because the total offset and local offset are the same when only two plates are being used.

4.11 Measurement report orifice plates

In the measurement report the measured values for the most important dimensions are given. The functional dimensions are the diameter of the orifice, the diameter of the positioning holes and the position of the positioning holes measured from the heart of the orifice. In the tables the theoretical dimensions are given as well as the production tolerance. There are different positioning holes for every testing setup.The testing modes are; single concentric mounted, multiple orifice plates with staggered offset (revered to as normal offset) and multiple orifice plates with alternating offset.

All measurement were performed with a Keyence IM Series image dimensioning system. The measureing machine shoots an high resolution photo of the parts and is then able do identify edges and shapes. The dimensions of the object can then be checked by the machine. The resolution of the machine is 0.001mm and more than required for this application.

Orifice Diameter $[mm]$	Beta (β) ratio $[-]$	Measured Diameter $[mm]$	Actual Beta (β) ratio $[-]$
15.00 ±0.2	0.3488	15.022	0.3497
12.20 ±0.2	0.2837	12.125	0.2830
10.00 ±0.2	0.2326	10.263	0.2406
8.20 ±0.2	0.1907	8.148	0.1907

Table 4.33: Measurement report for the diameter of the holes of the orifice plates

Plate number	Theoretical Distance $[mm]$	Actual Distance $[mm]$	Theoretical Diameter $[mm]$	Actual Diameter $[mm]$
1	30 ±0.2	30.089	3 ±0.1	2.933
2	30 ±0.2	30.014	3 ±0.1	2.949
3	30 ±0.2	30.008	3 ±0.1	2.944
4	30 ±0.2	29.985	3 ±0.1	2.941
5	30 ±0.2	30.010	3 ±0.1	2.928

Table 4.34: Measurement report for the location and diameter of the pin holes for concentric mounting

Plate number	Theoretical Distance $[mm]$	Actual Distance $[mm]$	Theoretical Diameter $[mm]$	Actual Diameter $[mm]$
1	34 ±0.2	34.137	3 ±0.1	3.024
2	38 ±0.2	38.015	3 ±0.1	2.930
3	43.3 ±0.2	43.331	3 ±0.1	2.944
4	47.6 ±0.2	47.583	3 ±0.1	3.003
5	51.2 ±0.2	51.116	3 ±0.1	30.82

Table 4.35: Measurement report for the location and diameter of the pin holes for normal offset

Plate number	Theoretical Distance $[mm]$	Actual Distance $[mm]$	Theoretical Diameter $[mm]$	Actual Diameter $[mm]$
1	30 ±0.2	29.973	3 ±0.1	3.089
2	34 ±0.2	33.999	3 ±0.1	2.971
3	28.7 ±0.2	28.738	3 ±0.1	2.930
4	33 ±0.2	33.008	3 ±0.1	3.003
5	29.4 ±0.2	28.855	3 ±0.1	3.005

Table 4.36: Measurement report for the location and diameter of the pin holes for alternating offset

The conclusion of the measurement report is that the main functional dimensions exept for one are within manufactoring tolerance and specification. The only functional dimension which is off is the hole positions on orifice plate number five for an alternating offset. This deviation will be corrected for in the calculations.

4.12 Conclusion and Discussion

The result of the single orifce plates are roughly in line with the estimated values from literature and CFD results. However the difference is significant. In the CFD results the orifice coefficient C_d was fairly constant in the turbulent region. The data from the actual field test does not reflect this behaviour. The orifce coefficient is not constant in the turbulent region and the value has a large deviation range. With reasonable certainty it can be said that the results obtained with the field test are not consistant nor usable. The reason for this is most likely the pressure gages which were being used. Two different observerd phenomena give reason to believe this. Firstly the used correction factor for the pressure gages;for some pressure gages this was very large. A correction of more than 15% for some instances is very undesired, but was necessary. The second reason to suspect the pressure gages is from the obtained data. The data aqcuisition was done with a large number of data points. With a large number of data points from a source at a constant value one would expect a dataset which is normally distributed, this was not the case in all instances. Even after correcting the data by removing the outliers the conformation to normal behaviour was very poorly in some instances.

The results for the multiple orifice plates reflect the previously stated problems even more. The need for accurate results is even larger for the multiple orifce plates test because the mass flowrates are smaller in general and the pressuredrops are larger.

From the results of the CFD calculation and the field test gave vital information on how to classify the multi-stage assembly. From the onset the calculation for the multi-stage trim has been made by seeing it as a series of orifices. The field test and the simulation showed that this is incorrect. The orifice coeffiicients that followed from the simulation and the field test for the intermediate stages were very inconsitent and larger than unity. At first the field data was analysed and faulty measurements were suspected to be a contributing factor to this. After analyzing the CFD results which gave the same overall results it became clear that the method was wrong.

The improved method to look at the multi-stage trim is too see the series of holes as one restriction orifice with an expanding section behind it. When the orifice coefficient is calculated for the complete section, using the smallest area as the vena contracta the obtained coefficients are physical and plausible. The orifice coefficient is about 0.9, which is the value one would expact for an restriction and expanding section.

The measurements on the orifice plates has proven to be very usefull information. The production tolerance have a significant impact on the performance of the multi-stage assembly. The additional information provided by the measurements have significantly improved the quality of the provided data by the oririfce tests.

The fullscale test and the CFD analysis have proven to be very usefull in understanding the mechanisms that are present in the multi-stage trim. The test have shown that the series can be seen a complete orifice or a nozzle with a certain coefficient. The series of stages have a certain value for the liquid pressure recovery factor which can be used to see what number of stages is need to avoid cavitation.

For future reseach i would recommend repreating the test done with the available prototype of the orifice plates and replace the pressure gages with more accurate ones. The Reynolds number at which the data is acquired should also be considered. At the moment the testing setup was the limiting factor in the variation in Reynolds numbers. For the future some research should be done on which Reynolds number region is valid for standard operation and how it can be acquired with the testing facility.

Chapter 5

Full Scale tests

5.1 Testing Setup

In figure 5.1 a schematic layout of the testing setup can be seen. The setup consist of a central water tank which is feeds the two pumps. The pumps feed a buffer tank. On top of the buffertank is a pressure gage installed.The amount of volume flow to the water tank can be adjusted by controlling the bypass valve which feeds a portion of the flowrate from the pump directly back to the main watertank. The buffertank is connected to a header from which three different pipes are connected. The pipes on the header are 1.5", 4" and 6". The different pipes have different flowmeter installed of the electromagnetic type. The upstream and downstream length are used to ensure there is a fully developed flow in the flow meters. Upstream and downstream are ballvalves installed to enable or disable the flow thru a specific flowmeter, depending on the flow. The large header upstream connects the three flowmeters to the measuring section. In the large header also a temperature sensor is installed. The measuring section constist of four different diameter pipes, 1.5", 2.5", 4" and 6". The pipes are mounted with flanges and can be interchanged so 2" and 3" pipes can be installed. In each pipe there are pressure tappings installed. Two tappings are installed 2 times the diameter upstream and two tappings are installed 6 times the diameter downstream. The pressure tappings can be connected via plastic tubing to differential pressure gages. Which of the available pressure gages is being used depends on the flow and the installed valve and characteristic. The main water tank is installed at a height difference of 4 meter with the measuring section downstairs. The height difference gives a constant static pressure of 0.4 bar.

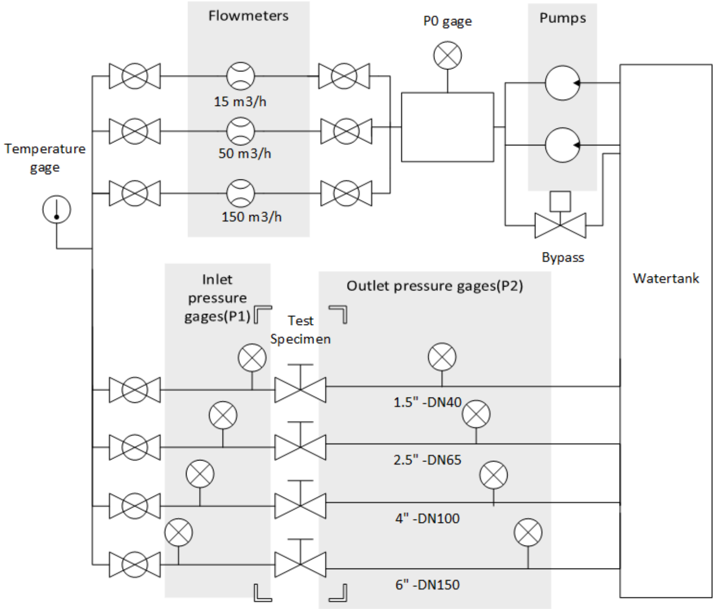
Flowmeters
P0 gage
Pumps
15 m3/h
50 m3/h
150 m3/h
Temperature gage
Bypass
Watertank
Inlet pressure gages(P1)
Test Specimen
Outlet pressure gages(P2)
1.5" -DN40
2.5" -DN65
4" -DN100
6" -DN150

Figure 5.1: Schematic Layout of the flowlab

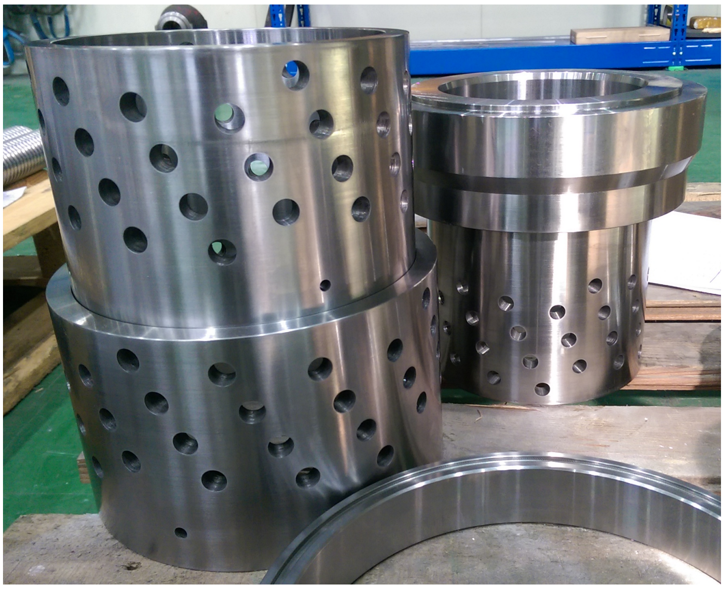

Figure 5.2: Picture of the finished cages after production. Leftbottom - Outercage (3) above it - Middle cage (2) and right the inner cage (1)

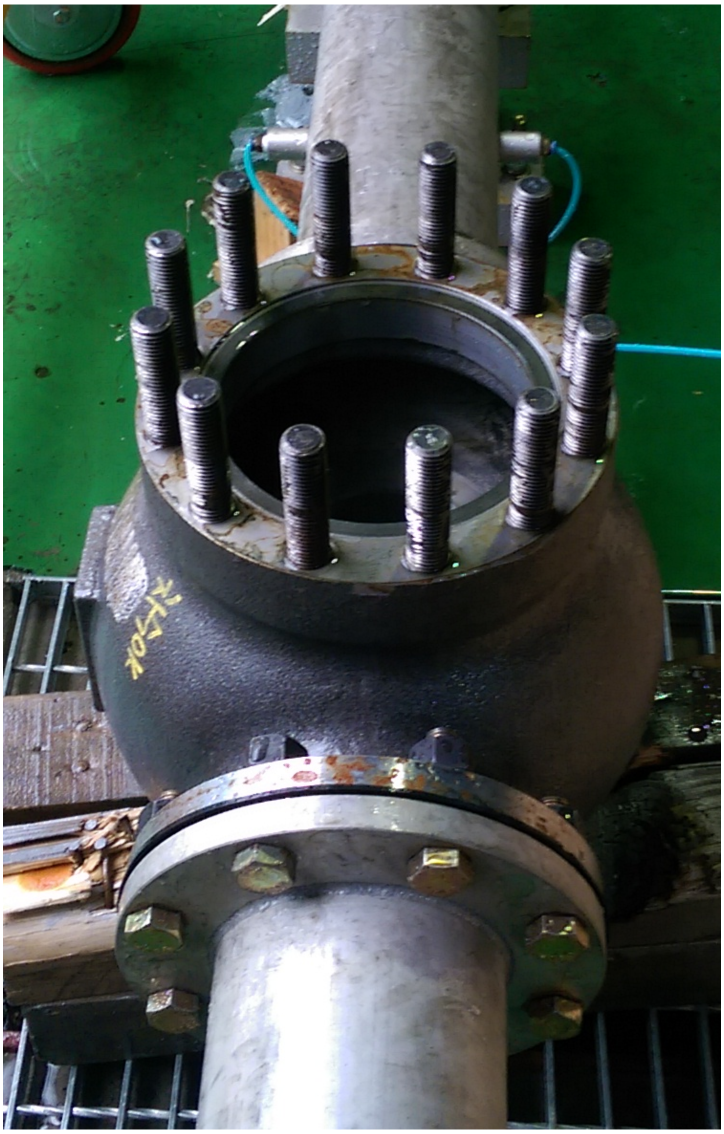

Figure 5.3: Empty valve body installed in the 6” - DN150 piping. Note the presssure tapping at the top of the picture for the upstream pressure gages.

5.1.1 Specifications of the used instrumentation

Type	Make	Model	Range	Precision
Computer program	Labview	7.0	[−]	[−]
Static Pressure gage	Autrol	APT-3200G	-100-1500 kPa	±0.075%
Static Pressure gage	Green Sensor	K2009-2110	0-400 kPa	±1.5%
Staic Pressure gage	Green Sensor	K2009-2110	0-1000 kPa	±1.5%
Differential Pressure gage	Autrol	APT-3100	0-7.5 kPa	±0.075%
Differential Pressure gage	Autrol	APT-3100	0-37.3 kPa	±0.075%
Differential Pressure gage	Autrol	APT-3100	0-186.5 kPa	±0.075%
Differential Pressure gage	Autrol	APT-3100	0-700 kPa	±0.075%
Electromagnetic Flowmeter	Isoil	MS-2500	1.5-15 m^3/h	$\pm 0.25 - 0.5\%$
Electromagnetic Flowmeter	Isoil	MS-2500	5-50 m^3/h	$\pm 0.25 - 0.5\%$
Electromagnetic Flowmeter	Toshiba	LF-620	15-150 m^3/h	$\pm 0.25 - 0.5\%$
Static Temperature gage	Autrol	ATT-2100	-200-650 $°C$	±0.03%

Note that the static pressure gages are gage pressure transmitters. The range of -100 kPa is thus near vacuum conditions. Also the precision is given in a percentage of the total span of the used gage and not of the measured value.

5.2 Calculation Method

The installed pressure gages provides us information of the flowrate, temperature and pressure in the system. Other physical quantities which are usefull for calculation are not directly measured such as density and visosity. The density and visosity of the fluid can be calculated via the thermodynamic state principle. The thermodynamic state principle states that when two properties of a fluid are know, the others can be estimated. For the estimation of the other properties some relations will be introduced in the following sections.

It must be noted that the flow meters used are of the electromagnetci type. This type of flowmeter utilizes the electromagnetic conductivity over a known and calibrated orifice. The result of this is then used to compute the volumeflow, with an estimated density, dependent on the pressure and fluid type. So for the measurement of the volumeflow there is also a relation used, this relation however is unknown since it is processed inside the valve.

5.2.1 Density

The density of the water was calculated with the following formula given in 5.1.

$$\rho = \frac{A}{B^{1+\left(1-\frac{T}{C}\right)^{D}}} \tag{5.1}$$

Symbol	Value
T	[−]
ρ	[−]
A	0.14395
B	0.0112
C	649.727
D	0.05107

Table 5.1: Constants for calculating the density

5.2.2 Dynamic Visosity

The dynamic viscosity is calculated with the formula given in 5.2. The equation used is the so called Vogel equation.

$$\mu = e^{A+\frac{B}{C+T}} \tag{5.2}$$

Symbol	Value
T	[−]
μ	[−]
A	-3.7188
B	578.919
C	-137.546

Table 5.2: Constants for calculating the density

5.3 Testing programme

The testing programme for the valve with trim is seen in table 5.23 and 5.24. Not all combinations are possible. The cages for example cannot be installed without an installed seatring. Also the seatring is a loose component, so testing this in undertype is not possible since it would be carried with the flow. The cages are designed to work in an underflow situation, so testing a combination of cages is not realistic in overflow situations since the area would decrease over the stages. Also it is it not possible to mount each of the cages seperately because the first cages doubles as a mounting carrrier so alway a combination has to be made with the first cage.

With these limitations in mind the testing programme was constructed. The installation of the plug gives more combinations since the stroke of the plug can be altered. The number of different stroke height which are tested are 10 when there is no cage installed and 4 when the cage is installed. When the cage is installed the valve coeffiencent at small values for the stroke becomes so small that it is out of the range of the testing facility. The flow becomes choked very easily because of the small upstream pressure.

The valve coefficient of the body is determined at various flowrates so investigate the dependance of the valve coefficient on the Reynolds number. The tests a various flowrates for the other configurations was omitted because of limited testing time.

Undertype

Body	Seatring	Plug	Cage I	Cage II	Cage III
x					
x		x			
x	x	x	x		
x	x	x	x	x	
x	x	x	x	x	x

Table 5.3: Testing programme for Undertype flow

Overtype

Body	Seatring	Plug	Cage I	Cage II	Cage III
x					
x	x				
x	x	x			
x	x	x	x		

Table 5.4: Testing programme for Overtype flow

5.4 Data

5.4.1 Undertype

Volume flow rate $[m^3/h]$	Inlet pressure $[bar]$	Pressure drop $[kPa]$	Temperature $[°C]$
124.38	0.71	10.01	17.45
101.97	0.62	6.69	17.36
92.70	0.59	5.58	17.32
89.66	0.58	5.17	17.20

Table 5.5: Undertype;Test data of the Body

Opening [%]	Volume flow rate $[m^3/h]$	Inlet pressure $[bar]$	Pressure drop $[kPa]$	Temperature $[°C]$
10	126.41	0.73	12.57	16.81
20	126.44	0.73	12.03	16.85
30	126.33	0.72	11.75	16.87
40	126.31	0.72	11.27	16.92
50	126.30	0.72	11.16	16.93
60	126.41	0.72	10.73	17.00
70	126.44	0.71	10.39	17.02
80	126.39	0.71	10.37	17.06
90	126.43	0.71	10.27	17.10
100	126.41	0.71	10.20	17.13

Table 5.6: Undertype; Test data of the Body with the plug

Opening [%]	Volume flow rate $[m^3/h]$	Inlet pressure $[bar]$	Pressure drop $[kPa]$	Temperature $[°C]$
25	35.40	1.52	98.88	16.02
50	58.77	0.98	48.19	16.10
75	69.02	0.81	31.01	16.22
100	85.70	1.30	32.94	16.29

Table 5.7: Undertype; Test data of the Body with the plug, Seatring and Cage I

Opening [%]	Volume flow rate [m^3/h]	Inlet pressure [bar]	Pressure drop [kPa]	Temperature [$°C$]
25	30.64	1.38	86.15	16.85
50	56.95	1.08	56.98	16.80
75	132.63	1.87	121.21	16.50
100	116.00	1.83	62.45	16.38

Table 5.8: Undertype; Test data of the Body with the plug, Seatring,Cage I and Cage II

Opening [%]	Volume flow rate [m^3/h]	Inlet pressure [bar]	Pressure drop [kPa]	Temperature [$°C$]
25	8.72	2.04	146.62	17.22
50	31.28	1.44	91.21	17.21
75	46.17	1.17	60.04	17.14
100	58.07	0.97	46.60	17.10

Table 5.9: Undertype; Test data of the Body with the plug, Seatring,Cage I,Cage II and Cage III

5.4.2 Overtype

Volume flow rate [m^3/h]	Inlet pressure [bar]	Pressure drop [kPa]	Temperature [$°C$]
100.67	0.61	6.82	15.62
92.30	0.59	5.70	15.65
89.90	0.59	5.42	15.68

Table 5.10: Overtype; Test data of the Body

Volume flow rate [m^3/h]	Inlet pressure [bar]	Pressure drop [kPa]	Temperature [$°C$]
124.89	0.81	20.55	15.88
109.36	0.73	15.98	15.83
97.00	0.67	12.68	15.80
88.24	0.64	10.53	15.77
85.49	0.63	9.81	15.74

Table 5.11: Overtype; Test data of the Body with Seatring

Opening [%]	Volume flow rate [m^3/h]	Inlet pressure [bar]	Pressure drop [kPa]	Temperature [$°C$]
10	111.83	1.91	129.93	16.40
20	123.78	1.13	50.66	16.37
30	124.82	0.93	31.13	16.32
40	125.01	0.85	24.16	16.30
50	125.10	0.83	21.83	16.25
60	125.17	0.82	20.93	16.21
70	125.13	0.82	20.51	16.14
80	125.15	0.81	19.68	16.10
90	125.34	0.81	19.04	16.08
100	125.34	0.80	18.74	16.06

Table 5.12: Overtype; Test data of the Body with the plug

Opening [%]	Volume flow rate [m^3/h]	Inlet pressure [bar]	Pressure drop [kPa]	Temperature [$°C$]
25	37.94	1.50	100.86	16.01
50	106.08	2.25	164.85	16.01
75	120.31	1.60	98.88	15.98
100	123.61	1.36	75.11	15.92

Table 5.13: Overtype; Test data of the Body, with plug, Seatring and Cage I

5.5 Results

5.5.1 Undertype

Cv	Reynolds Number [$-$]	Density [kg/m^3]	Dynamic Visosity [$mPa \cdot s$]
455,24	275241,93	1003,68	1,07
456,45	225987,60	1003,74	1,07
454,73	205176,03	1003,76	1,07
456,69	198365,06	1003,78	1,07

Table 5.14: Undertype; Results of the Body

Opening [%]	Cv	Reynolds Number $[-]$	Density $[kg/m^3]$	Dynamic Visosity $[mPa \cdot s]$
10	413,04	276276,49	1004,08	1,08
20	422,21	276724,13	1004,05	1,08
30	426,90	276629,57	1004,04	1,08
40	435,87	276968,13	1004,01	1,08
50	438,02	276999,65	1004,00	1,08
60	446,94	277623,04	1003,96	1,08
70	454,31	277798,07	1003,95	1,08
80	454,54	277956,07	1003,92	1,08
90	456,87	278355,88	1003,90	1,08
100	458,41	278563,83	1003,88	1,07

Table 5.15: Undertype; Results of the Body with the plug

Opening [%]	Cv	Reynolds Number $[-]$	Density $[kg/m^3]$	Dynamic Visosity $[mPa \cdot s]$
25	41,25	75694,90	1004,57	1,10
50	98,09	126246,28	1004,52	1,10
75	143,62	148830,37	1004,45	1,10
100	173,00	185014,11	1004,40	1,10

Table 5.16: Undertype; Results of the Body with the plug, Seatring and Cage I

Opening [%]	Cv	Reynolds Number $[-]$	Density $[kg/m^3]$	Dynamic Visosity $[mPa \cdot s]$
25	38,24	65978,64	1004,05	1,08
50	87,40	124485,38	1004,08	1,08
75	139,57	287696,57	1004,27	1,09
100	170,07	250921,98	1004,34	1,09

Table 5.17: Undertype; Results of the Body with the plug, Seatring,Cage I and Cage II

Opening [%]	Cv	Reynolds Number $[-]$	Density $[kg/m^3]$	Dynamic Visosity $[mPa \cdot s]$
25	8,35	19251,67	1003,82	1,07
50	37,93	69069,91	1003,83	1,07
75	69,02	101773,79	1003,87	1,07
100	98,54	127939,90	1003,89	1,07

Table 5.18: Undertype; Results of the Body with the plug, Seatring,Cage I,Cage II and Cage III

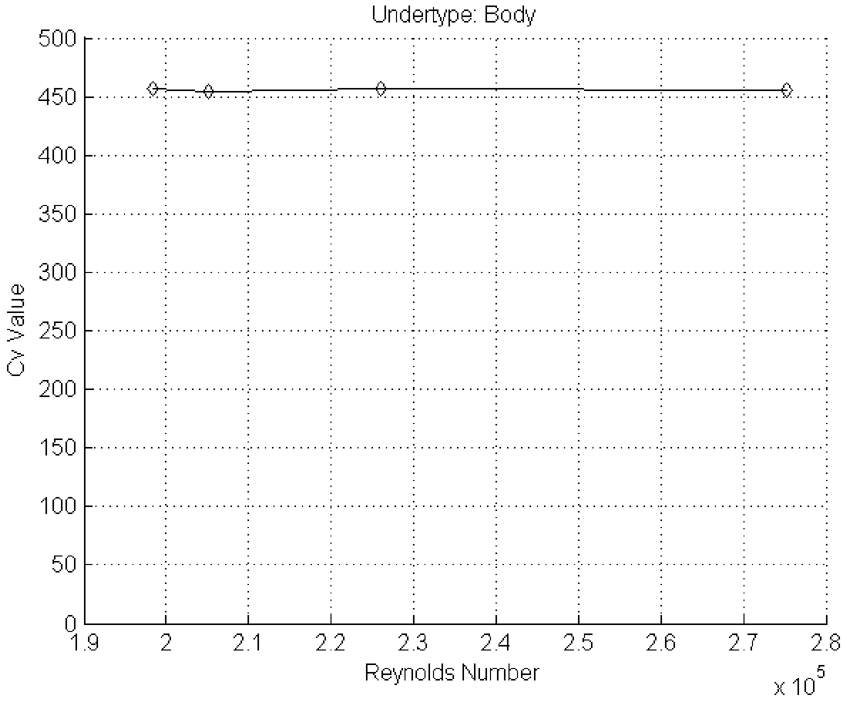

Figure 5.4: Undertype; Cv value of the body for different Reynolds numbers

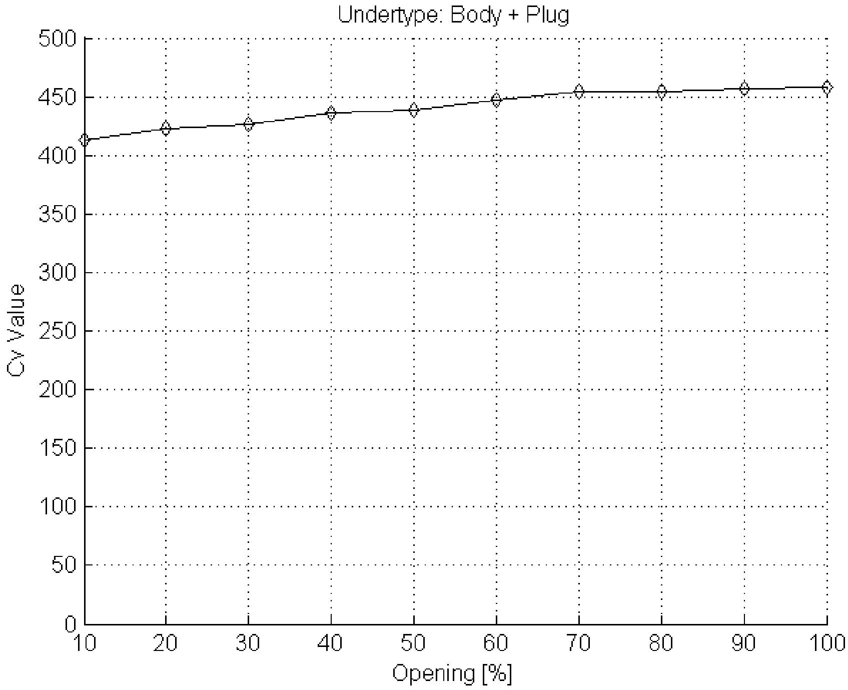

Figure 5.5: Undertype; Cv value of the body with plug installed for different openings

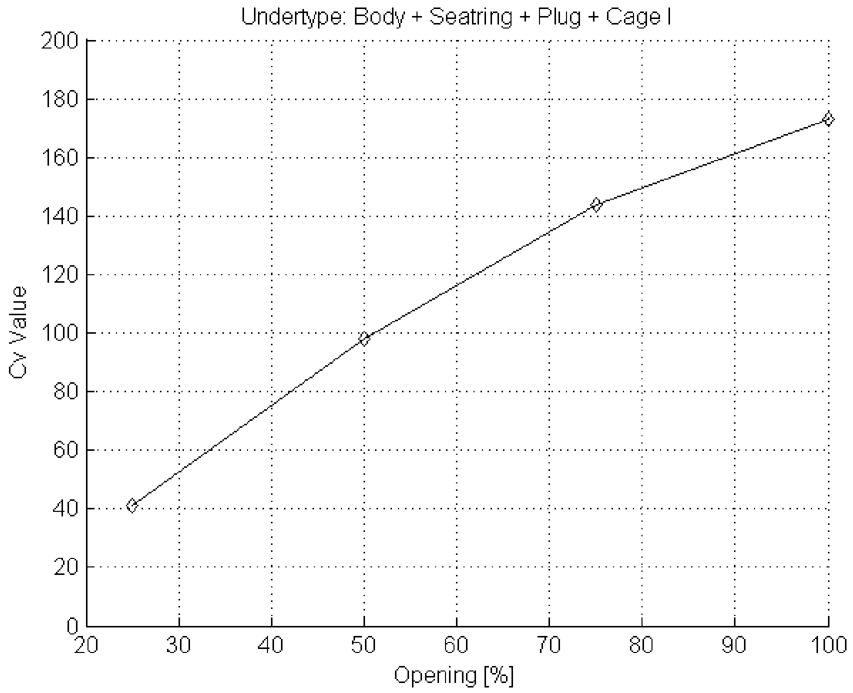

Figure 5.6: Undertype; Cv value of the body with, seatring, plug and cage I installed for different openings

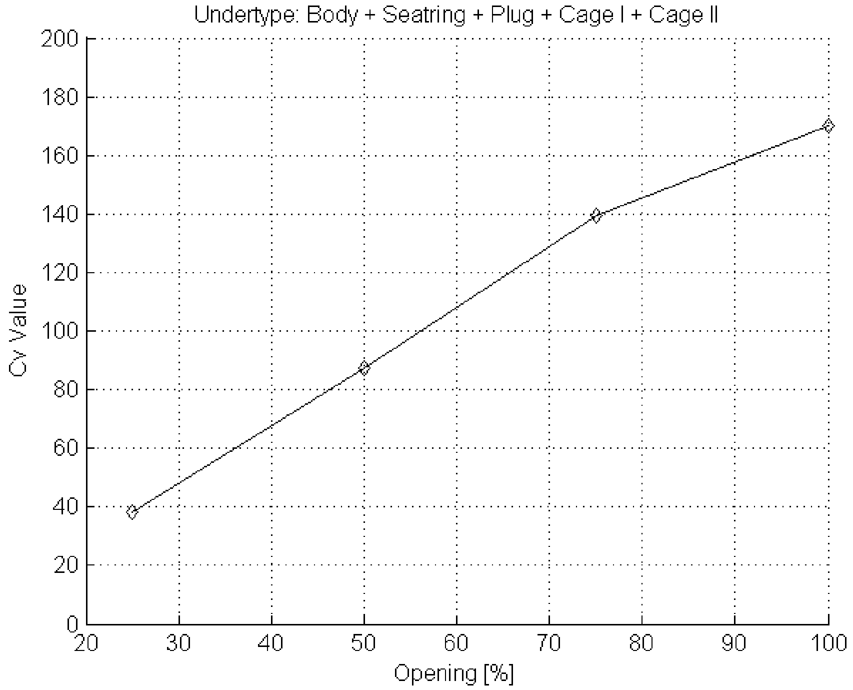

Figure 5.7: Undertype; Cv value of the body with, seatring, plug,Cage I and Cage II installed for different openings

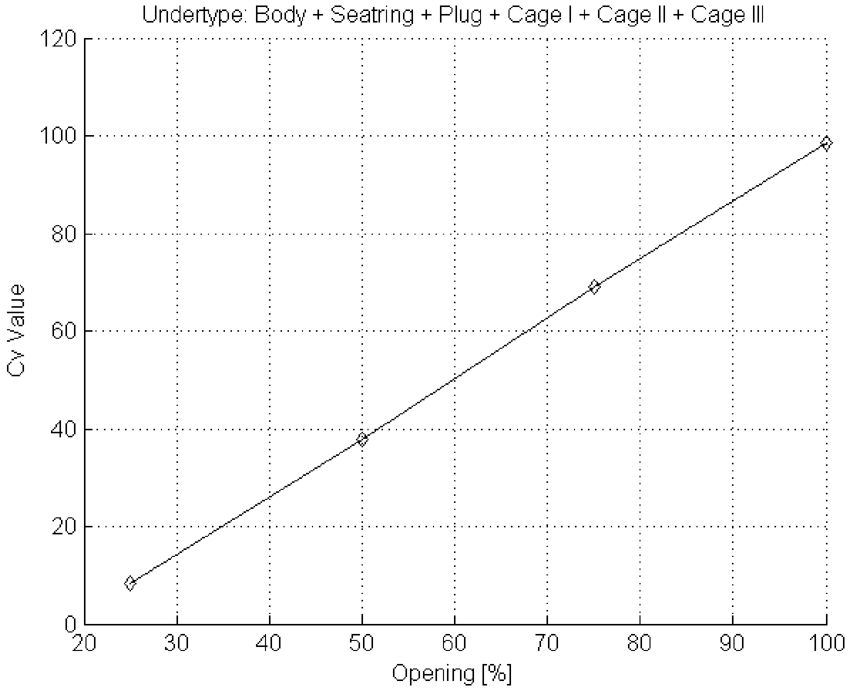

Figure 5.8: Undertype; Cv value of the body with, seatring, plug, Cage I, Cage II and Cage III installed for different openings

5.5.2 Overtype

Cv	Reynolds Number $[-]$	Density $[kg/m^3]$	Dynamic Visosity $[mPa \cdot s]$
446,67	213867,66	1004,81	1,12
447,94	196159,75	1004,80	1,11
447,34	191175,05	1004,78	1,11

Table 5.19: Overtype; Results of the Body

Cv	Reynolds Number $[-]$	Density $[kg/m^3]$	Dynamic Visosity $[mPa \cdot s]$
319,24	266906,06	1004,66	1,11
316,98	233461,23	1004,68	1,11
315,63	206915,83	1004,70	1,11
315,07	188133,00	1004,72	1,11
316,34	182105,31	1004,74	1,11

Table 5.20: Overtype; Results of the Body with Seatring

Opening [%]	Cv	Reynolds Number $[-]$	Density $[kg/m^3]$	Dynamic Visosity $[mPa \cdot s]$
10	113,66	242209,95	1004,33	1,09
20	201,47	267765,39	1004,35	1,09
30	259,21	269721,07	1004,38	1,10
40	294,69	269938,80	1004,40	1,10
50	310,23	269795,93	1004,42	1,10
60	317,03	269666,22	1004,45	1,10
70	320,14	269137,76	1004,49	1,10
80	326,88	268909,81	1004,52	1,10
90	332,85	269137,56	1004,53	1,10
100	335,48	269082,36	1004,55	1,10

Table 5.21: Overtype; Results of the Body with the Seatring and plug

Opening [%]	Cv	Reynolds Number $[-]$	Density $[kg/m^3]$	Dynamic Visosity $[mPa \cdot s]$
25	43,77	81341,82	1004,57	1,10
50	95,74	227437,47	1004,58	1,10
75	140,20	257709,70	1004,59	1,11
100	165,28	264491,36	1004,63	1,11

Table 5.22: Overtype; Results of the Body with the plug, Seatring and Cage I

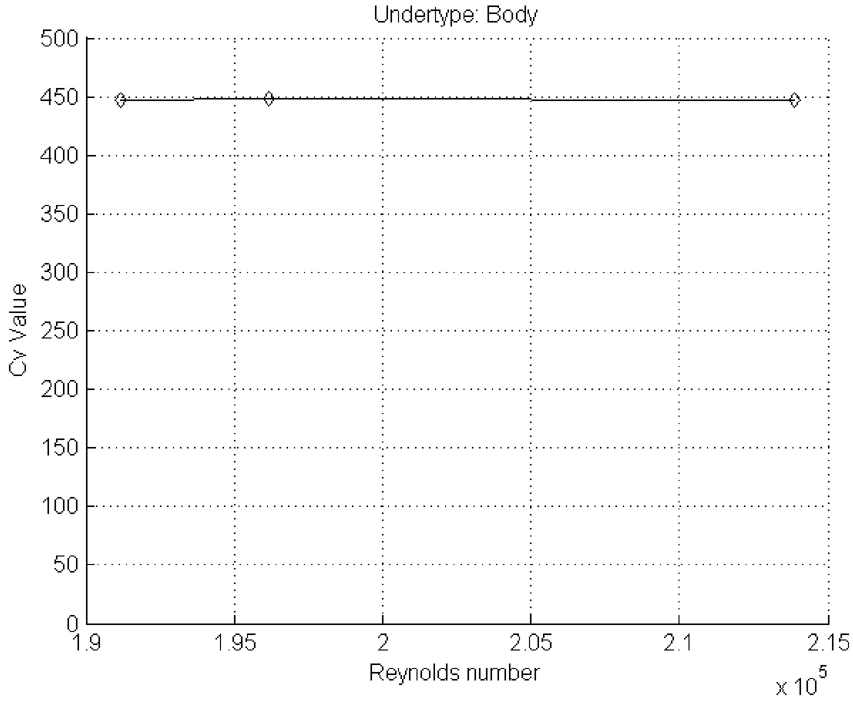

Figure 5.9: Overtype; Cv value of the body for different Reynolds numbers

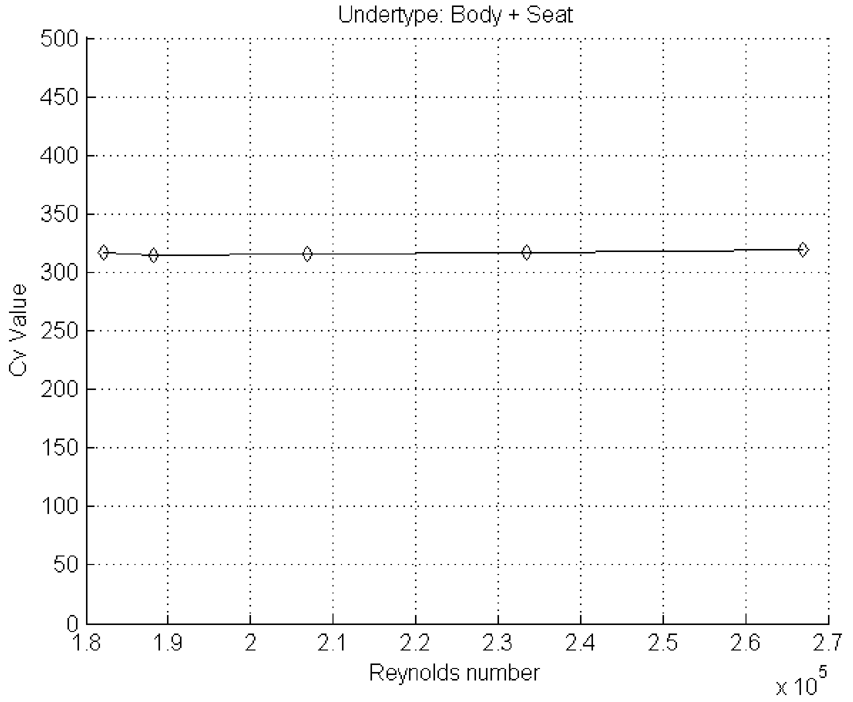

Figure 5.10: Overtype; Cv value of the body with the seatring installed for different Reynolds numbers

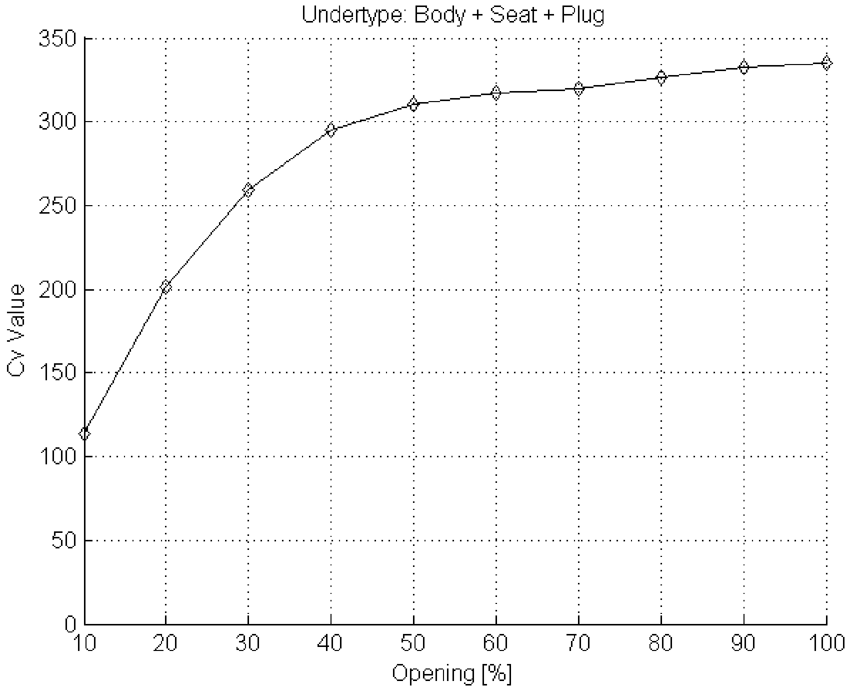

Figure 5.11: Overtype; Cv value of the body with the seatring and plug installed for different openings

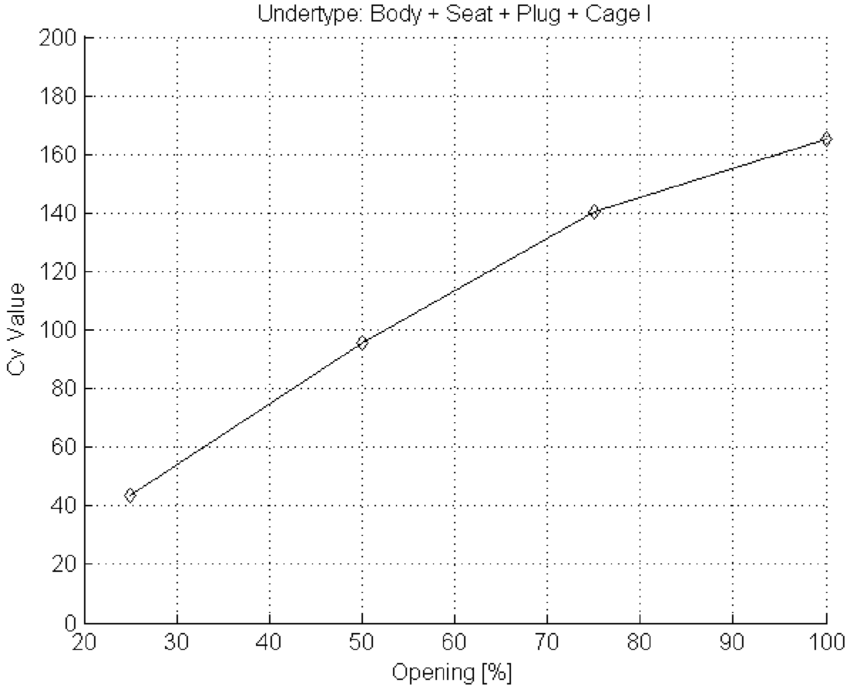

Figure 5.12: Overtype; Cv value of the body with the seatring,plug and Cage I installed for different openings

5.6 Summary Results

Results Undertype

Body	Seatring	Plug	Cage I	Cage II	Cage III	Cv
x						456
x		x				458
x	x	x	x			173
x	x	x	x	x		170
x	x	x	x	x	x	98.5

Table 5.23: Summary testing results for Undertype flow

Results Overtype

Body	Seatring	Plug	Cage I	Cage II	Cage III	Cv
x						447
x	x					316
x	x	x				335
x	x	x	x			165

Table 5.24: Summary testing results for Overtype flow

5.7 Measurement report Concept I

Part	Dimension	Drawing	Actual
Seatring	Inside Diameter	116.0 ±0.1mm	115.95 mm

5.8 Preliminairy conclusions

Component	Cv
Body Overtype	447
Body Undertype	456
Seatring Overtype	446
Cage I Overtype	189
Cage I Undertype	200
Cage I + II Undertype	196
Cage I + II + III Undertype	103

5.9 Orifice coefficients parts

Component	Cv	Area $[mm^2]$	C_d $[-]$
Seatring Overtype	446	10559.2	0.72
Cage I Overtype	189	3987.8	0.81
Cage I Undertype	205	3987.8	0.85

Table 5.25: Orifice coefficient of different parts of the valve

5.10 Orifice coefficients stages

Stage	Ring	Area $[mm^2]$	C_d $[-]$
One stage	1	3988.6	0.85
Two stage	1 & 2	3867.8	0.98
Three Stage	1 & 2 &3	2137.4	0.81

Table 5.26: Undertype; Orifice coefficient of each stage of the multi-stage trim

Stage	Ring	Area $[mm^2]$	C_d $[-]$
One stage	1	3988.6	0.81
Two stage	1 & 2	3867.8	n.a.
Three Stage	1& 2 & 3	2137.4	n.a.

Table 5.27: Overtype; Orifice coefficient of each stage of the multi-stage trim

5.11 Conclusion and Discussion

The results of the full-scale test indicate that the initial assumptions for the orifice coefficient of the final stage was a reasonable one. The estimated orifice coefficient was 0.83 while the measured orifice coefficient was between 0.81 and 0.85. Although more research should be done, the first results look very promising in finding the correct orifice coefficient. The results for the other stages of the multi-stage trim could not all be obtained. The multi-stage trim was designed to work in an overtype flow. Due to various circumstances overtype results for the complete trim could not be obtained. The main reason was a shortage of time available to do the tests. The tests were delayed due to a production time that was longer than anticipated, and the sourcing of parts for the valve assemby which took longer then expected.

The timespan of the tests was also limited becasue due to the coming winter the lab and the facilities had be shut down to prevent frost damage.

The undertype results are complete and available, but since this is not the working direction of the valve,the results are not as usefull as the overtype results. The results that we obtained for the two and three stage are promising.

The orifice coeficient for the two stage is very close to one. This value is very likely not true. The area used to calculate the orifice coeffient of this stage is the theoretical area.The real area is not available because no accurate measurement were done on the trim. The valve trim is a object to perform accurate mesurements on since it is round. The real area is probably smaller, and will propably give a orifice coefficient that is closer to 0.83, what we expect from the other data we obtained from the orifice testing and the CFD simulations. However, this is still a topic of discussion as long as there is no measurement data available.

From the obtained data we also draw some other conclusions. There is a significant difference wheter the valve is used in a undertype or overtype configuration. The undertype configuration has a higher valve coefficient than the overtype. Another effect that is remarkable is the influence of the plug on the C_v. The body has been tested in overtype and undertype configuration, with and without the plug installed. The installation of the plug gave a higher valve coefficient and thus a lower pressure drop. The effect can be explained by the path the fluid has to travel from the inlet to the outlet. With the plug installed the path is more straight and there are less unwanted swirls and wakes in the valve which cause excessive drag.

The valve coeficient values obtained at different Reynolds numbers show that the C_v value of the valve or valve assembly is fairly constant. Some small dependancies on the Reynolds number can be seen in the graphs, but these are negligible.

The valve coefficeint for different positions of the plug has al been tested. The graphs show very different dependancies between the valve coeffient and the opening. When the plug is installed in an empty body the relation between valve coeficient and the openings is that of a quick opening valve. Near constant at high opening percentages and linear near zero. When a single cage is installed with a linear behaviour the relation becomes a mix between linear and quick opening. When more and more stages are installed the relation between the opening and the valve coefficient becomes very near to linear. The valve coefficient is the result of the sum of the resistance of each of the installed components. The cages have a linear characteristic, the body and seatring a constant characteristic and the plug a quick opening one. The resistance of the cages is the dominant contributing factor to the overall resitance and thus becomes the characteristic of the cages the dominant one. This is an important factor to keep in mind when designing the characteristic of a cage, when the cage is less dominant and still a certain behaviour is wanted some corrections will have to be done.

The orifice coeficient of the seatring has also been determined from the collected data. With a know coefficient for the seatring the influence of installing a cage smaller or larger than the current one can be corrected for. However there are limits to the usage. When the installed cages become much smaller or larger the fluid will be restricted agaist either the valve wall or the inside of the cage itself.

Part IV

Conclusion and Discussion

The results of the CFD analysis and the full scale tests have produced large amount of data. This was very usefull for checking the validity of the assumptions made in the design process. The time between the start of the internship and the deadline for the design was relatively short. Beceause of this short time period there was not much time to check all made assumptions so this had to be done later when the trim was already finished.

After reviewing the data I can conclude that the made assumptions for the trim calculation were not correct. The assumption that the trim can be treated as a series of orifices is not correct. This is propably because the distance between the orifices is too small. The standard orifice formula assumes a full pressure recovery between the subsequent orifices, this was clearly not the case.

Because of the invalidity of this assumption much of the work done on the pressuredrop relation/ Area relation and the sigma factor becomen invalid. At least for the multi-stage trim, for a true set of orifices in series this is still valid.

The multi-stage trim should thus not be seen as a series of orifices, but as one orifice with a certain orifice coefficient and a pressure recovery factor. The pressure recovery factor is the important factor to termine the number of stages. The pressure recovery factor of the multi-stage trim converges to one with an increasing number of stages. After calculating the needed C_v from the different load cases, the needed F_L factor can be calculated. With this the appropiate number of stages can be selected. The properties of the stages can be determined by CFD results or actual testing.

The single and multiple orifice assembly was key in the understanding of the multi-stage trim. By testing just a single hole many more iterations could be done. Unfortunately the results can only be used to compare and not in an absolute sence since the inaccuracy of the pressure sensors was high. In an ideal case other sensor would have been used, but these were not available.

The full scale test gave insight in the complete production/assembly and testing process of a control valve. Some results were obtained, but due to lack of time not all desired configurations could have been tested. The results showed that the design assumptions for a linear trim were valid, also the influence of the seperate parts in the valve could be investigated.

Part V

Recommendations

After finishing the test some recommendations can be done for future research;

- Some more reseach could be done with CFD to check the relationship between the beta factor and the pressure recovery coefficient for the multi-stage trim. The single orifice CFD simulations showed a dependancy between the beta factor and the pressure recovery coefficient. A small beta factor gave a small pressure recovery coefficient. Whether this is also true for the multi-stage and to what extend could be investigated. When this relationship is known future multi-stage trims can be designed more easily and more accurate from single hole multi-stage data.

- The testing facility could be altered. In the present configuration there is no controlvalve downstream of the test specimen. This means that there is no way to control the volumeflowrate or pressuredrop and upstream pressure of the test-specimen. The installation of a downstream controlvalve can also be used to checked for chocked flow conditions, to check wheter the flowrate is truely only dependant on the upstream pressure.

- The test of the multi-stage and single orifice can be repeated with more accurate pressure gage to obtain more kwalitiative data. If a chocked flow can be obtained the pressure recovery coefficient for the stage combinations can also be determined.

Part VI

List of Figures

List of Figures

1.1 Drawing of a standard Globe valve 8
1.2 Exploded view of a Cage style Globe Control valve 9

3.1 Pressure drop and sigma value at each stage for Case 1 - Maximum Flow 18
3.2 Pressure drop and sigma value at each stage for Case 3 - Minimal Flow 19
3.3 Different number of starts possible for the hole pattern of the cage. Picture courtesy of KVT Valves LTD. 20
3.4 Hole Pattern of Design I 22

4.1 Drawing of the location of the pressure tappings in the orifice plate carrier. 27
4.2 Velocity plot of the 2D Axi-symmetrical simulations for different orifice sizes 34
4.3 Pressure plot of the 2D Axi-symmetrical simulations for different orifice sizes 35
4.4 Velocity Contours plot from the Axi-symmetrical simulation for the different orifice sizes. 36
4.5 Plot of the orifice coeffients for different Reynolds values . . . 38
4.6 Velocity plot of the 3D simulations for different orifice sizes . 40
4.7 Pressure plot of the 3D simulations for different orifice sizes . 40
4.8 Velocity Contours plot of the different configurations with normal offset 45
4.9 Velocity Contours plot of the different configurations with normal and alternating offset 47
4.10 Pressure Contours plot of the different configurations with normal and alternating offset 47
4.11 Pressure plot of the different configurations with normal and alternating offset 48
4.12 Picture of the orifice carrier plates and one plate installed in the flow-loop 49
4.13 Overview of the orifice carrier plates and the single orifice plates 49
4.14 Overview of the setup used for the pressure gage calibration . 50

4.15 Scatterplot of the measurement data of the reference pressure sensor 51
4.16 Normal plot of the measurement data of the reference pressure sensor 52
4.17 Normal plot of the measurement data of the difference pressure with the reference pressure sensor 53
4.18 Scatterplot of the measurement data of the reference pressure sensor with outlier identified 55
4.19 Graph of the correction factor for the different pressure gages as a function of the pressure 56
4.20 Orifice coefficient of the single orifice plates for different Reynolds numbers 60
4.21 Cv results for the multiple orifice configuration with normal offset 62
4.22 Cv results for the multiple orifice configuration with alternating offset 63
4.23 Cv results for the multiple orifice configuratiion with staggered and alternating offset 64

5.1 Schematic Layout of the flowlab 69
5.2 Picture of the finished cages after production. Leftbottom - Outercage (3) above it - Middle cage (2) and right the inner cage (1) 69
5.3 Empty valve body installed in the 6" - DN150 piping. Note the presssure tapping at the top of the picture for the upstream pressure gages. 70
5.4 Undertype; Cv value of the body for different Reynolds numbers 79
5.5 Undertype; Cv value of the body with plug installed for different openings 79
5.6 Undertype; Cv value of the body with, seatring, plug and cage I installed for different openings 80
5.7 Undertype; Cv value of the body with, seatring, plug,Cage I and Cage II installed for different openings 80
5.8 Undertype; Cv value of the body with, seatring, plug, Cage I, Cage II and Cage III installed for different openings 81
5.9 Overtype; Cv value of the body for different Reynolds numbers 83
5.10 Overtype; Cv value of the body with the seatring installed for different Reynolds numbers 83
5.11 Overtype; Cv value of the body with the seatring and plug installed for different openings 84
5.12 Overtype; Cv value of the body with the seatring,plug and Cage I installed for different openings 84

7.1 Inherent Valve Characteristics 109

7.2 Overview of a Multi-stage Trim - Image courtsey of KVT Valves LTD 111
7.3 Stem and plug interaction for a single stage cage control valve 112
7.4 Layout of the flow area for a two stage trim. A1 is the entrance. A2 is the orifice area and A3 is the exit. 112
7.5 Multi-stage trim - Over and Under the web flows 113
7.6 Pressuredrop over a 10 stage trim for different area ratio values 114
7.7 Pressuredrop per stage of a 10 stage trim 115
7.8 Pressure at each stage of a 5 stage trim with the corresponding sigma values for different values of the area ratio 116

8.1 Correction factor for multiple orifices in series with a constant C_d 131
8.2 Correction factor with incoperated C_d for Concept I 132

Part VII

List of Tables

List of Tables

1.1 Part names of a general Globe Valve 7
1.2 List of used symbols and abbreviations 10

2.1 Design Condtions 12
2.2 Preliminary Calculations 13
2.3 Fluid properties used for the preliminary Calculations 13
2.4 Calculation results for a $F_L = 0.85$ 14
2.5 Calculation results for a $F_L = 0.9$ 14
2.6 Used percentage of stroke for different inherent valve characteristics 15

3.1 Summary of the Design of Concept I 21

4.1 Summary of the testing orifice Design 25
4.2 Configuration and typical values for the single stage orifice configuration 28
4.3 Configuration and typical values for the multiple stage orifice configurations 28
4.4 Configuration and typical values for the multiple stage orifice configurations with alternating offset 28
4.5 Theoretical mass flow for the different orifice sizes with C_d =1 and Δ p = 1 bar. 31
4.6 Boundary Conditions for C_v Analysis 33
4.7 Boundary Conditions for different Reynolds number Analysis 33
4.8 Results of the 2D Axi-symmetrical CV simulation for different orifice sizes 34
4.9 Results of the 2D Axi-symmetrical Orifice simulation for different orifice sizes 37
4.10 C_d values of the 2D Axi-symmetrical Orifice simulation for different orifice sizes 37
4.11 Results of the 3D CV simulation for different orifice sizes . . 41
4.12 Results of the 3D CV simulation for different orifice sizes . . 41
4.13 Pressure recovery coefficient for the 2D and 3D simulations for different orifice sizes 42

4.14 Data of the 3D Multiple orifice simulations with Normal offset 44
4.15 Results of the 3D Multiple orifice simulations with Normal offset 44
4.16 Data of the 3D Multiple orifice simulations with Normal and Alternating offset for configuration 1-2-3-4-5 46
4.17 Results of the 3D Multiple orifice simulations with Normal and Alternating offset for configuration 1-2-3-4-5 46
4.18 Pressure recovery coefficients for normal and alternating offset 48
4.19 Data of the 8.2mm orifice 56
4.20 Data of the 10mm orifice 57
4.21 Data of the 12.2mm orifice 57
4.22 Data of the 15mm orifice 57
4.23 Data of the orifice configuration 4-5 in normal offset 58
4.24 Data of the orifice configuration 3-4-5 in normal offset 58
4.25 Data of the orifice configuration 2-3-4-5 in normal offset . . . 58
4.26 Data of the orifice configuration 1-2-3-4-5 in normal offset . . 58
4.27 Results of the 8.2mm orifice 59
4.28 Results of the 10mm orifice 59
4.29 Results of the 12.2mm orifice 59
4.30 Results of the 15mm orifice 60
4.31 Theoretical and actual dimensions and area's for the normal offset multiple orifice configuration 61
4.32 Theoretical and actual dimensions and area's for the alternating offset multiple orifice configuration 61
4.33 Measurement report for the diameter of the holes of the orifice plates 65
4.34 Measurement report for the location and diameter of the pin holes for concentric mounting 65
4.35 Measurement report for the location and diameter of the pin holes for normal offset 66
4.36 Measurement report for the location and diameter of the pin holes for alternating offset 66

5.1 Constants for calculating the density 72
5.2 Constants for calculating the density 72
5.3 Testing programme for Undertype flow 73
5.4 Testing programme for Overtype flow 73
5.5 Undertype;Test data of the Body 74
5.6 Undertype; Test data of the Body with the plug 74
5.7 Undertype; Test data of the Body with the plug, Seatring and Cage I 74
5.8 Undertype; Test data of the Body with the plug, Seatring,Cage I and Cage II 75

5.9 Undertype; Test data of the Body with the plug, Seatring,Cage I,Cage II and Cage III 75
5.10 Overtype; Test data of the Body 75
5.11 Overtype; Test data of the Body with Seatring 75
5.12 Overtype; Test data of the Body with the plug 76
5.13 Overtype; Test data of the Body, with plug, Seatring and Cage I 76
5.14 Undertype; Results of the Body 76
5.15 Undertype; Results of the Body with the plug 77
5.16 Undertype; Results of the Body with the plug, Seatring and Cage I 77
5.17 Undertype; Results of the Body with the plug, Seatring,Cage I and Cage II 77
5.18 Undertype; Results of the Body with the plug, Seatring,Cage I,Cage II and Cage III 78
5.19 Overtype; Results of the Body 81
5.20 Overtype; Results of the Body with Seatring 82
5.21 Overtype; Results of the Body with the Seatring and plug . . 82
5.22 Overtype; Results of the Body with the plug, Seatring and Cage I 82
5.23 Summary testing results for Undertype flow 85
5.24 Summary testing results for Overtype flow 85
5.25 Orifice coefficient of different parts of the valve 86
5.26 Undertype; Orifice coefficient of each stage of the multi-stage trim 86
5.27 Overtype; Orifice coefficient of each stage of the multi-stage trim 86

6.1 List of symbols used in equations 6.1 and 6.2 102
6.2 List of symbols used in equations 6.6 and 6.7 103
6.3 List of symbols used in equation 6.10 104
6.4 List of symbols used in equations 6.11 6.126.13 and 6.14 . . . 105
6.5 Typical F_L and x_t values for different style valves 106

8.1 C_d coeffiient for the improved correction factor of Concept I . 132

Part VIII

Appendix

Chapter 6

Flow equations for sizing of Control Valves

6.1 Liquid flow service

The valve coefficient for an incompressible fluid is defined as the maximum flow rate thru a valve at a set pressure drop. In the standard definition from ANSI/ISA 75.01.01 [1] it is the maximum volume flow rate in US gallons per minute thru a valve at a pressure drop of 1 psi. In formula form this is given at equation 6.1.

$$C_v = Q\sqrt{\frac{SG}{p_1 - p_2}} \tag{6.1}$$

$$SG = \frac{\rho}{\rho_0} = \frac{\rho}{999.25} \tag{6.2}$$

The term SG stands for the specific gravity and is the density of the fluid relative to water at 60 degrees Fahrenheit or 15.5 degrees Celcius. For most liquid service the density is very close to, or equal to the density of the reference temperature so the term equals unity and cancels. Apart from the

Symbol	Description	Unit
Q	Volume flow rate	US Gallon per minute
p_1	Inlet pressure	psi
p_2	Outlet pressure	psi
SG	Specific gravity	$[-]$
ρ	Density	$kg/m3$

Table 6.1: List of symbols used in equations 6.1 and 6.2

Symbol	Description	Unit
p_v	Vapor pressure	*bar*
F_L	Liquid pressure recovery factor	$[-]$
F_f	Liquid critical pressure ratio factor	$[-]$
p_{vc}	Pressure at the "Vena Contracta"	*bar*
p_c	Absolute thermodynamic critical pressure	*bar*

Table 6.2: List of symbols used in equations 6.6 and 6.7

imperial based valve coefficient, there is also a valve coefficient based on SI units.

$$K_v = Q\sqrt{\frac{SG}{p_1 - p_2}} \tag{6.3}$$

In the SI based valve coefficient the pressure can be given in bar, gage or absolute. The volume flow rate is given in cubic meter per hour. The conversion factors between, K_v and C_v are;

$$K_v = 0.865C_v \tag{6.4}$$

$$C_v = 1.156K_v \tag{6.5}$$

The numerical constant N_1 depends on the units that will be used in the calculations. The value for N_1 will be 0.865 so the pressure can be given in bars, the density in kilograms per cubic meter and the volume flow rate in cubic meter per hour. The definition given above only holds for non-choked flows. When the pressure drop increases over a valve the flow could become choked, making the flow rate thru the valve independent of the pressure drop. Chocked flow conditions occur when the pressure in the valve, at the smallest point, the so called vena contracta drops below the vapor pressure. When the pressure of the fluid is less the vapor pressure for the given temperature is will start to boil. For water this phenomena is called flashing. This essential means that steam is formed form the water inside the valve. The volume of steam is much larger than water. This clogs up the valve and restricts a further increase in flow. The Chocked flow condition that will be used is;

$$[H]p_1 - p_2 = \Delta p \geq F_l^2(p_1 - F_f p_v) \tag{6.6}$$

The liquid pressure recovery factor is the ratio of the pressure drop over the valve at chocked flow conditions and the pressure difference between the inlet pressure and the pressure at the vena contracta. The value of the recovery factor is strongly dependent on the geometry and valve style, often these values are specified by manufacturers.

$$F_L = \sqrt{\frac{p_1 - p_2}{p_1 - p_{vc}}} \tag{6.7}$$

The liquid critical pressure ratio factor is the ratio between the vapor pressure of the fluid at inlet conditions and the apparent pressure at the vena contracta at chocked flow. For vapor pressures which are near to zero this value can be estimated by 0.96. For other conditions the value can be calculated by equation 6.8

$$F_f = 0.96 - 0.28\sqrt{\frac{p_v}{p_c}} \tag{6.8}$$

The absolute thermodynamic critical pressure is a function of the type of fluid and can be found in tables. When chocked flow is present the pressure difference term in the valve coefficient is replaced with the maximum pressure differential possible with chocked flow. The valve coefficient for chocked flow is given in equation 6.9

$$C_v = \frac{Q}{N_1}\sqrt{\frac{\rho/\rho_0}{F_L^2(p_1 - F_f p_v)}} = \frac{Q}{N_1 F_L}\sqrt{\frac{\rho/\rho_0}{(p_1 - F_f p_v)}} \tag{6.9}$$

6.2 Gas flow service

The definition of the valve coeficient is generally used to express the flow rate of water thru a valve with a given pressure drop. Since many valves are also used in steam and other gas services there is also an expression for the Cv value when compressible fluids are used. The definition given here will follow the definition form the ANSI/ISA 75.01.01[1].

$$C_v = \frac{\dot{m}}{N_6 Y \sqrt{x p_1 \rho_1}} \tag{6.10}$$

Symbol	Description	Unit
$\dot{m}$	Mass flow rate	kg/h
N_6	Numerical Constant	$[-]$
Y	Expansion factor	$[-]$
x	Ratio of pressure differential and absolute inlet pressure	$[-]$
ρ_1	Density at inlet	kg/m^3

Table 6.3: List of symbols used in equation 6.10

Symbol	Description	Unit
F_γ	Specific heat ratio factor	[−]
x_t	Pressure differential factor at chocked flow	[−]
γ	Specific heat ratio	[−]

Table 6.4: List of symbols used in equations 6.11 6.126.13 and 6.14

In this equation for the valve coefficient the mass flow rate is used rather than the volume flow rate. This is change is made since the volume of the gas can significantly change when passing thru the valve. Also additional terms have been added to correct for the compressibility effects of the gas like the expansion factor and pressure differential ratio. The factor N6 will have a value of 27.3 when the pressure is measured in bars and the mass flow rate in kilograms per hour. Again for the calculation of the Cv value distinction is made between chocked and non-chocked flow. The chocked flow condition for compressible fluid is slightly different than the one of incompressible fluids. When the flow becomes choked, the expansion factor Y will be equal to 0.667.

$$x = \frac{p_1 - p_2}{p_1} \tag{6.11}$$

$$Y = 1 - \frac{x}{3F_\gamma x_t} \tag{6.12}$$

$$F_\gamma = \frac{\gamma_{gas}}{\gamma_{air}} = \frac{\frac{C_{p_{gas}}}{C_{p_{gas}}}}{\frac{C_{p_{air}}}{C_{p_{air}}}} = \frac{\gamma_{gas}}{1.4} \tag{6.13}$$

When the chocked flow condition is used for the maximum pressure drop the valve coeffient can be obtained for a chocked gas flow. The result is seen in equation 6.14

$$C_v = \frac{\dot{m}}{N_6 0.667\sqrt{F_\gamma x_t p_1 \rho_1}} \tag{6.14}$$

The expansion factor is a function of the shape of the flow path, the ratio between the seat and inlet area, the pressure differential ratio and the specific heat. The pressure differential factor at chocked flow is a value that is typically determined by the geometry and will have to be measured in full-scale test. Although guidelines for the value are given for each body style by ANSI/ISA 75.01.01 [1] Typical values per body style are given in table 6.5

Body Style	F_l	x_t
Globe	0.9	0.72
Butterfly	0.62	0.35
Ball Valve	0.74	0.42
Globe with Cage style Trim	0.9	0.68

Table 6.5: Typical F_L and x_t values for different style valves

Chapter 7

Valve Design and Design considerations

7.1 Cavitaition factor sigma σ

When a valve operates at liquid service and high pressure and pressure changes there is an imminent chance of cavitation. Cavitation occurs when due to a large change in pressure small void in the fluid form. When these void travels to another area of high pressure they will implode and can generate an intense shockwave. This shockwave, although being small can still cause significant damage and erosion to a surface.

In a valve the highest velocity will be in the vena contracta. This is the place where the free stream flow area is the smallest. Consequently the pressure in the valve is also at its lowest point at this location.This is usually near the seating area. When pressure of the fluid becomes less than the vapor pressure for this given temperature the fluid will start to boil and become a gas. Further on in the valve the flow passage will become narrower again, since it already passed the largest area the vena contracta. When the pressure recovers again the small vapor bubbles will collapse. The collapsing of the bubbles is called cavitation. The severity and presence of cavitation can be expressed in terms of the actual pressure drop versus the maximum pressure drop possible, to that of the vapor pressure. This ratio is called sigma [2].

$$\sigma = \frac{p_1 - p_v}{p_1 - p_2} \tag{7.1}$$

When sigma reaches a value of one, flashing will occur. The outlet pressure p_2 will then be equal to the vapor pressure and bubbles will form and keep growing.The liquid is fully transformed into a gas. If the value is larger than one the bubbles will collapse after forming. Different severity regions for cavitation can be expressed in terms of sigma. For general purposes the guidelines are given in equation 7.2.

$$\begin{array}{rc} \sigma \geq 2: & \text{No cavitation} \\ 1.7 \leq \sigma \leq 2: & \text{Some cavitation might occur} \\ 1. \leq \sigma \leq 1.7: & \text{Onset of cavitation} \\ 1 \leq \sigma \leq 1.5: & \text{Severe cavitation} \\ \sigma \leq 1: & \text{Flashing} \end{array} \tag{7.2}$$

These basic guidelines give a rough estimate of when cavitation might occur and the severity. However these guidelines are conservative, specially designed anti-cavitation trims are able to operate at sigma value near to one (1.002). Cavitation will not start at an exact value of one.

Cavitation will start when the pressure of the fluid drops below the vapor pressure. Although the overall pressure in the valve is well above the vapor pressure cavitation can still occur. The start of cavitation is strongly associated with region of large pressure drops, in a control valve this are the areas where the boundary layer separates from the wall. The pressure in the wake will drop significantly and provoke the generation of small vapor bubbles. These bubbles can only form easily if there is a nuclei to assist the formation. Without this a pure fluid could experiences pressure below the vapor pressure and remain an liquid. In practice this will not be the case since there is always debris in the pipelines or small amounts of trapped gas. The separation of the boundary layer in a control valve is very likely. When the fluid passes thru the valve is has to make a kinds of sharp turns and undergo several area changes. Also the overall pressure drops are significant. The result of cavitation can be very different. This depends on the severity of the cavitation.

The ISA defines multiple cavitation regions; incipient cavitation, constant cavitation, incipient damage, chocking cavitation and maximal vibration cavitation. The results of the cavitation can be excessive noise, vibration, performance loss and ultimately physical damage can range from the look of a frosted glass to a cinder like structure.

The damaging mechanism itself is a debated subject. Two dominant theories exist which seem to be valid each in their own situation. One theory is the formation of a high velocity jet. When the vapor bubble collapses asymmetrically a small high velocity jet will form. This jet impinges on the surface and erodes it. Another theory suggest the formation of shock waves. The rapid movement of the vapor-liquid interface establishes a shockwave. The compressive loading on the wall will make the material fail due to fatigue or plastic deformation. Both damaging mechanisms do dictate that the collapsing bubble, whether it forms a jet or a shockwave needs to be near to the wall to cause damage. Another important aspect is the chocked flow cavitation. This is the cavitation that might occur when the flow true a valve is completely chocked. The sigma expression for this is given in equation 7.3.

$$\sigma_c = \frac{p_1 - p_v}{F_L^2(p_1 - F_f p_v)} \tag{7.3}$$

7.2 Inherent Valve Characteristics

The inherent valve characteristics are is the relation between the opening of the plug and the flow thru the valve. The inherent characteristics are and geometrical property determined by the shape of the plug, seat, and if applicable the hole pattern in the cage of a control valve. The type of relation between the opening and the flow can be divided into three different categories; Quick opening, linear and equal percentage.

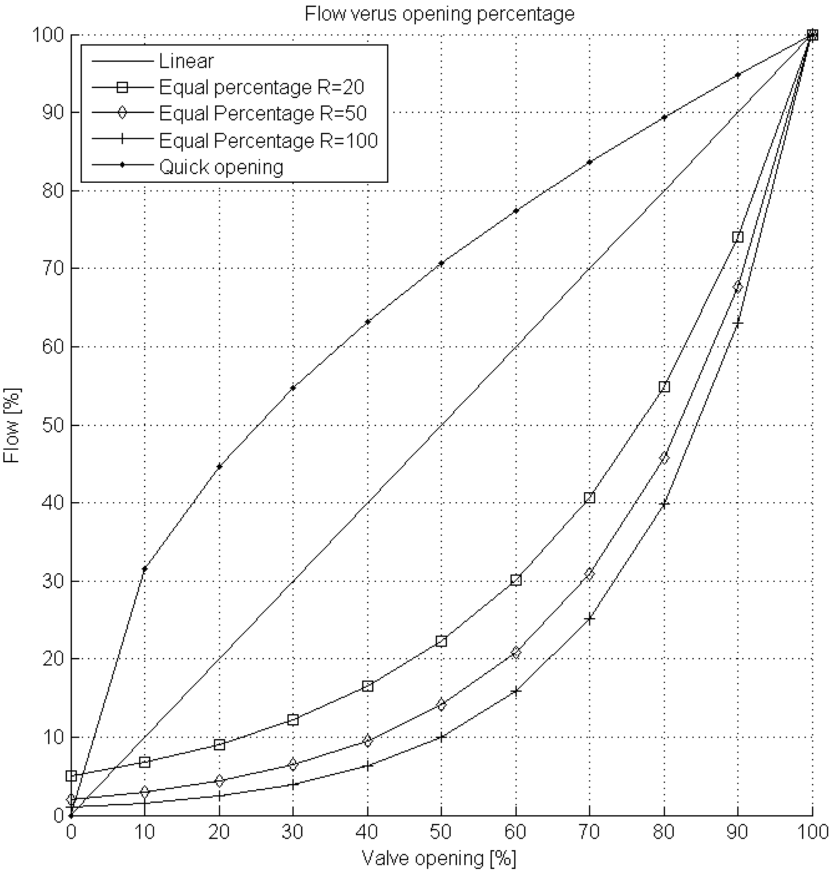

Figure 7.1: Inherent Valve Characteristics

7.2.1 Quick opening

The quick opening has a relation between the valve opening and the volume flow which might look like a square root. This type of characteristic has the largest increase in flow opening in the beginning of the stroke. The relationship between the percentage of flow and the percentage of opening is given in equation 7.4.

$$\text{flow }\% = \sqrt{\frac{\text{opening }\%}{100}} \tag{7.4}$$

7.2.2 Linear

The linear type of characteristic has a plug or a plug and cage combination that ensures a directly proportional relation between the opening and the flow. The linear combination has a constant increase. The formula for the linear relation is given in equation 7.5.

$$\text{flow }\% = \frac{\text{opening }\%}{100} \tag{7.5}$$

The opening of a linear valve which is needed for certain performance can be calculated by equation 7.6

$$\text{opening }\% = \frac{C_{v_{required}}}{C_{v_{maximum}}} 100\% \tag{7.6}$$

7.2.3 Equal percentage

The equal percentage type also has set relation between the opening and the flow. The equal percentage type has a set increase in flow in percents for a given increase in stroke. The increase in percent stays the same with each increase in opening, but the increase in flow is not the same with each opening increment. The formula for the equal percentage is given in equation 7.7

$$\text{flow }\% = R^{\frac{opening\%}{100}-1} \tag{7.7}$$

The ratio R is the Rangeability of the valve. Defined as the ratio between the maximum and the minimal controllable Cv. The opening of an equal percentage can be calculated with equation 7.8.

$$
\begin{gathered}
\frac{C_{v_{required}}}{C_{v_{maximum}}} = R^{\frac{\text{opening }\%}{100}-1} = R^{\frac{\text{opening }\%}{100}} R^{-}1 \\
\frac{C_{v_{required}}}{C_{v_{maximum}}} R = R^{\frac{\text{opening }\%}{100}} \\
\frac{\text{opening }\%}{100} = \frac{\log \frac{C_{v_{required}}}{C_{v_{maximum}}} R}{\log R}
\end{gathered}
\tag{7.8}
$$

7.3 Multi-stage trim

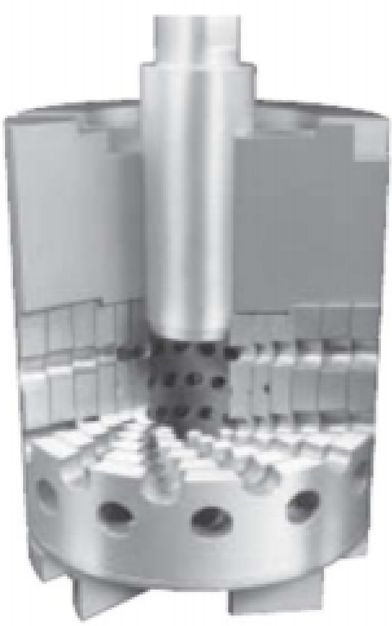

Figure 7.2: Overview of a Multi-stage Trim - Image courtsey of KVT Valves LTD

The multi-stage trim consist of several cylinder which are placed inside each other. In each ring are sets of openings which could be circles or other geometrical forms. The openings in each cylinder is lined up with the next one but staggered to some amount. When the fluid passes thru the holes the flow area alters in size first becoming smaller and the larger again. The pressure is relieved gradually over the length of the flow path.

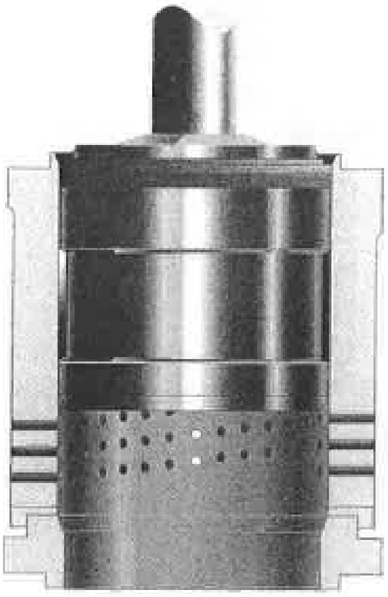

Figure 7.3: Stem and plug interaction for a single stage cage control valve

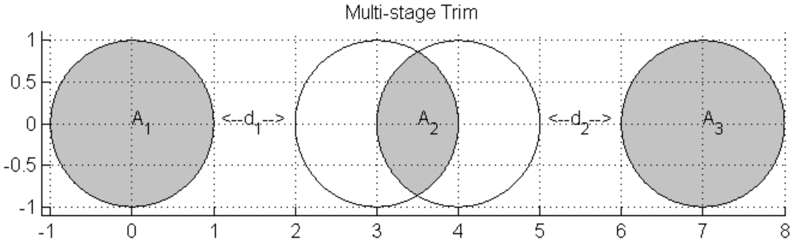

Figure 7.4: Layout of the flow area for a two stage trim. A1 is the entrance. A2 is the orifice area and A3 is the exit.

Figure 7.4 shows a visual representation of the flow area and the relationship between them when the fluid travels from one ring to another. The figure shows a two ring, or two stage assembly. The flow area changes from A1 to A2 and finally A3. Since A1 is the smallest area, the majority of the pressure drop will be accounted for by this restriction. In general will the number of ring determine the amount of steps in the pressure drop from the inlet pressure to the desired outlet pressure. The amount of stages is n when the number of ring is n.

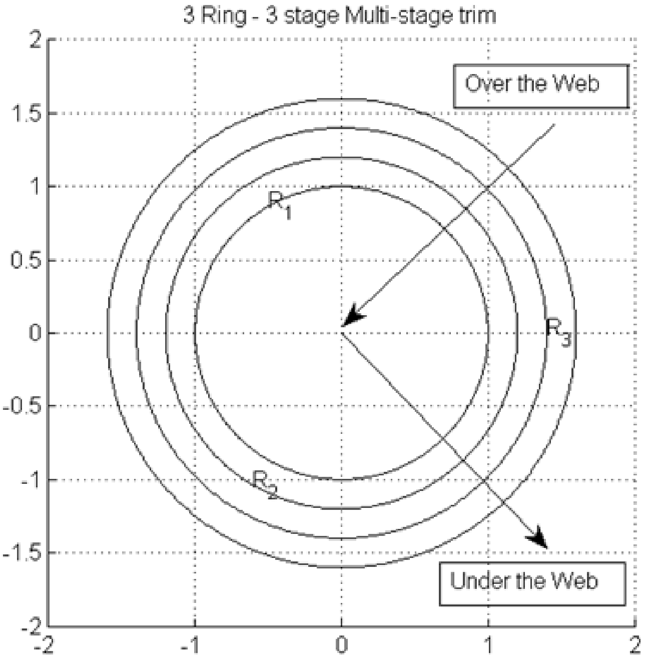

Figure 7.5: Multi-stage trim - Over and Under the web flows

The direction of the flow can be either inwards or outwards seen from the ring-assembly. The more common name used is Over-type and Under-type, or Over-the-Web and Under-the-Web. The over the web and type refer to the flow going first up to the cage, travelling from the outside to the inside. The under-the-web and type refer to the fluid coming from underneath the plug and travelling from the inside to the outside. For the sizes of the holes there are some general considerations. The change is area from one orifice to the next is about 1.5 times. The area directly after an orifice is 1.5 times larger than the orifice. But other values are also used.

7.4 Number of stages and the pressure drop relation

The number of stages that is needed for in order to complete the pressure drop from the inlet pressure to the desired outlet pressure in a design variable. The number of stages which could be used should however be minimized in order to reduce cost, complexity and unwanted pressure drop due to resistance in the channels. Leading in determining the number of step in the pressure drop is the sigma number. The sigma number expresses

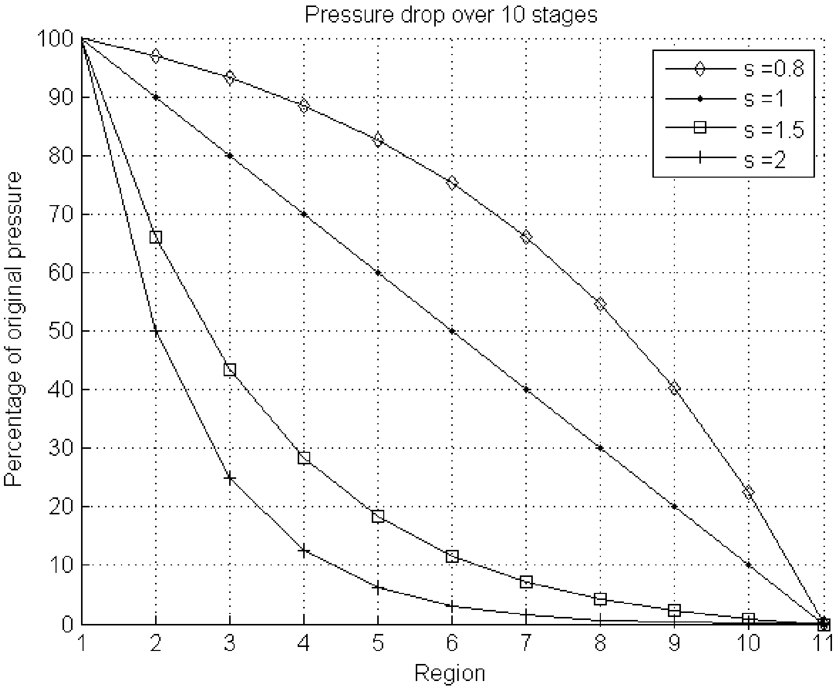

Figure 7.6: Pressuredrop over a 10 stage trim for different area ratio values

the likelihood that cavitation will take place inside the valve. The relation between the sigma number and the pressure drop per stage will discussed further. The pressure can be reduced in several ways, linear, progressive and regressive. The different forms of pressure drop can be seen in a graphical representation in figure 7.6

The value of s determines the ratio between the previous pressure drop and the next one. When the value of s is equal to unity it means that all pressure drop steps are the same. When the value is larger than one is means that the pressure drop is decreased at each step towards the final exit pressure. The inverse correlation holds for the values smaller than one. In the example a pressure drop is seen for 10 stage trim. The pressure given as a percentage of the difference between the inlet and outlet pressure. The number of steps used in this example is arbitrary.

The graph above shows the pressure drop as a function of the region The result is plotted for different values of s. From the graphs it is clear that a value of 1 gives a linear connection between the region inside the trim and the pressure there, the pressure drop at each stage is also constant. The values of s smaller than unity shows in increase in pressure drop per stage. The larger than unity values shown an decreasing pressure drop per stage. Although all three methods give the same end result and are equally

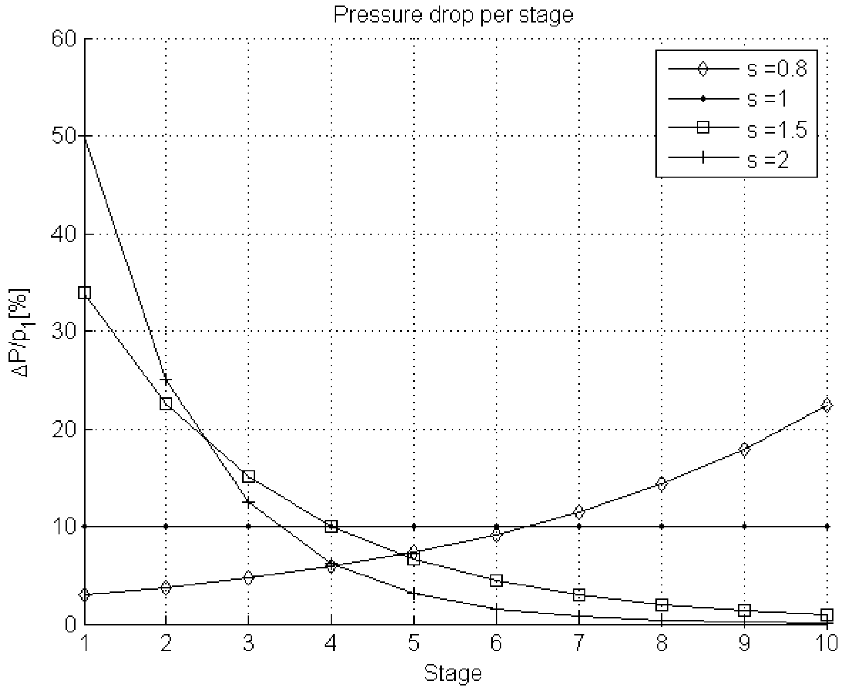

Figure 7.7: Pressuredrop per stage of a 10 stage trim

in terms of manufacturing complexity, the digressive method is favored.

When a fluid travels from one area to the next and the passage area for the fluid is decreased then according to Bernoullis law the velocity will increase. With the increase in velocity the pressure will be reduced. When the fluid then enters another area which is larger again the pressure recovers. Even when the size of the area is the same as the first one there will still be a loss in pressure due to friction and unrecoverable pressure losses.

Suppose we have a fluid flow which experiences a pressure decrease going from point one to point two. In this process from going from the pressure at one to the pressure of point two the pressure drop overshoots and locally a lower pressure than pressure two will occur. This overshoot happens at the vena contracta and is linked to the pressure drop and the pressure recovery factor. When the pressure drop increases the overshoot is also increases, thus the local pressure will become lower. The pressure recovery factor is the ratio between the recoverable and the unrecoverable pressruedrop. This ratio is always the same and can be used to predict the overshoot in pressuredrop. In general we can say, when the pressedrop get largers, the overshoot also becomes larger. This is especially significant when the pressure of the fluid is already near the vapor pressure. Any additional overshoot can then be a cause for cavitation. The value of s can be modified to accommodate for a small as possible cavitation risk and thus a large sigma number.

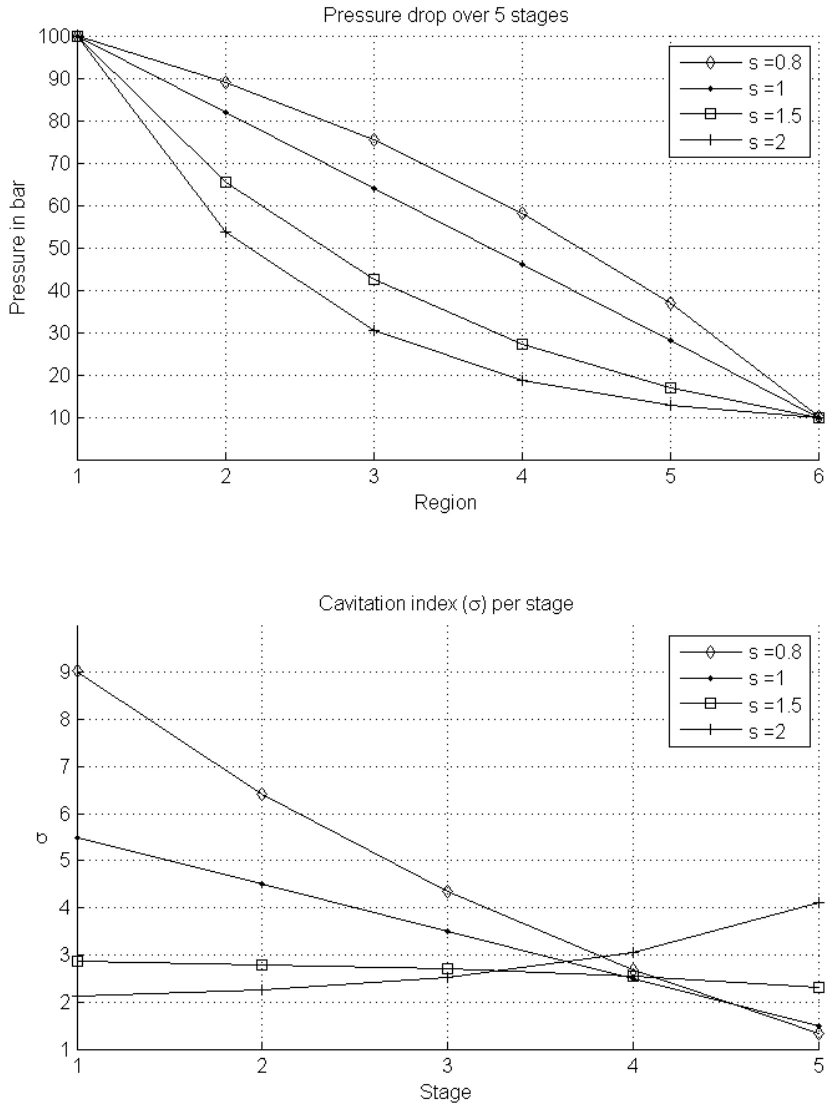

Figure 7.8: Pressure at each stage of a 5 stage trim with the corresponding sigma values for different values of the area ratio

The graph above shows the pressure drop for water is 100 degrees Celsius from 100 bar to 10 bar. The curves have been made for multiple values of s. The lower graph shows the cavitation number as a function of the value of s and the stage. The cavitation index should be as higher than one to avoid severe cavitation and higher than two to be completely free of cavitation. The between a sigma number of 1 and 2 multiple regions are defined such as the incipient cavitation region, incipient damage region. The graphs shows that a clear favoring for the degressive pressure drop per stage. The progressive pressure drop line with an s value smaller than one has an high sigma number in the beginning but the final stages are problematic. The same applies for the linear pressure drop with s equal to unity. The sigma number is large in the beginning and there is no risk of cavitation and further downstream the initial safety fades away as the sigma number becomes increasingly smaller. The minimal number of stages is thus dependent on the sigma number, the value of s can be tweaked to increase the protection again cavitation. A value for s which is larger than unity gives the best protection against cavitation. Finally we can write the relation between the pressure drop per stage and the total pressure drop in a formula form is given by equation 7.9

$$\Delta p_{total} = \sum_{1}^{n} \Delta p_n = \Delta p_1 + \Delta p_2 + \Delta p_3 + ...\Delta p_n \tag{7.9}$$

The relation between the different pressure steps is given by equation 7.10.

$$\begin{gathered} \Delta p_1 = s\Delta p_2 \\ \Delta p_2 = s\Delta p_3 \\ ...... \\ \Delta p_n - 1 = s\Delta p_n \end{gathered} \tag{7.10}$$

From equation 7.10 we can determine the smallest pressure step. This is given by relation 7.11.

$$\Delta p_{min} = \frac{\Delta p_{total}}{1 + s + s^2 + ...s^{n-1}} \tag{7.11}$$

The pressure drop at each stage can now be determined with equation 7.12.

$$\Delta p_n = \Delta p_{min} s^{n_{total}-n} \tag{7.12}$$

Subsequently we can determine the pressure at each stage as inlet pressure minus the sum of de previous pressure drops. The relation is given in equation 7.13

$$p_{n+1} = p_1 - \sum_{1}^{n} \Delta p_n \tag{7.13}$$

7.5 C_v value and resistance coefficient K

The valve coefficient of any given valve can be seen as an expression for the amount of resistance the valve adds to a section of piping. The definition of C_v states that is the maximum amount of water that can pass true a valve with a set pressure loss of 1 psi, of 1 bar for K_v. For piping the resistance factor K is used, this is expressed used to express the loss of head in meters water column over a section of pipe. The relation between the loss in meters of head is chosen because the performance of a pump is usually expressed in this unit. When one know the amount of head a pump delivers one can then easily calculate the need pipe diameter when the total length is known. The equation for the loss in head is given by;

$$H = K\frac{V^2}{2g} \tag{7.14}$$

Using $\Delta p = \rho g H$;

$$\Delta p = K\frac{1}{2}\rho V^2 \tag{7.15}$$

Using the definition for C_v form the ANSI/ISA [1] and equation 6.1.

$$C_v = \frac{Q}{N_1}\sqrt{\frac{SG}{p_1 - p_2}} \tag{7.16}$$

Substituting 7.15 into equation 6.1 and some rewriting gives the relationship given by Crane et al [7].

$$C_v = 29.9\frac{d^2}{\sqrt{K}}(\text{Imperial}) \tag{7.17}$$

$$C_v = \left(\frac{d}{4.654 \cdot K}\right)^2 \tag{7.18}$$

$$C_v = 0.04634\frac{d^2}{\sqrt{K}} \tag{7.19}$$

Other relations are;

$$K_v = 0.04007\frac{d^2}{\sqrt{K}} \tag{7.20}$$

$$K = 2.148 \cdot 10^{-}3\frac{d^4}{C_v^2} \tag{7.21}$$

$$K = 1.604 \cdot 10^{-}3\frac{d^4}{K_v^2} \tag{7.22}$$

When a different diameters and sections of pipe are linked together the total head loss can be calculated as function of a reference diameter, the same can be done for a valve. The relation between the individual pipe lengths and diameters and the equivalent diameter will be given in the following section.

7.6 K and C_v values in series

The equivalent resistance coefficient can be determined when the section of pipe and/or valves are placed in series and parallel. For this the analogy with an electrical system is easy to make, instead of expressing the resistance in Ohm, we use the resistance coefficient and instead of a drop in voltage we can expect an pressure drop. The amount of volume flow thru a valve can be compared with the amount of amperes in an electrical circuit. The total head loss coefficient will then be for pieces op pipe in series.

$$K_{total} = \sum_{n}^{1} K_1 + K_2 + ...K_n \tag{7.23}$$

Parallel;

$$\frac{1}{K_{total}} = \sum_{n}^{1} \frac{1}{K_n} = \frac{1}{K_1} + \frac{1}{K_2} + ...\frac{1}{K_n} \tag{7.24}$$

Note the similarities with the law of Kirchhoff in the electrical domain. The same can be done for the valve coefficient, using the relation found earlier.

Series;

$$\frac{1}{C_{v_{total}}} = \sum_{n}^{1} \frac{1}{C_{v_n}} = \frac{1}{C_{v_1}} + \frac{1}{C_{v_2}} + ...\frac{1}{C_{v_n}} \tag{7.25}$$

Parallel;

$$C_{v_{total}} = \sum_{n}^{1} = C_{v_1} + C_{v_2} + ...C_{v_n} \tag{7.26}$$

The relation for the value coefficient are the inverse of the ones with the head loss coefficient due to the relation between K and C_v to the power -2. The total or equivalent C_v can not only be used for calculation when a number of valves are mounted together but also for valve elements such as, body, seat, cage, trim and plug. The different parts of the valve can be designed separately with its own C_v rating and then a total C_v for the combination can be calculated. When the same valve body can be equipped with several different trims or plugs this is very useful to estimate the valve coefficient.

$$C_{v_{total}} = \sum_{n}^{1} = C_{v_{Seat}} + C_{v_{Plug}} + C_{v_{Cage}} + C_{v_{Body}} + ... \tag{7.27}$$

Chapter 8

Orifice Theory

8.1 Derrivation of the orifice equation

An orifice is a device which is used for controlling the amount of flow, or measuring the amount of flow. The orifice itself consist of a small hole perpendicular to the flow direction, which can have various shapes, the most widely used is a circle. The orifice uses Bernoullis principle which states that there is a direct relationship between the pressure differential and the velocity of the fluid. When the velocity increases the pressure drops and vice versa. Starting from Bernoullis equation for an incompressible, in viscid and laminar flow. The effects of gravity and change in height have been omitted. The subscripts indicate the properties at two different points in a flow.

Starting from Bernoullis equation 8.1 for an incompressible, in viscid and laminar flow. The effects of gravity and change in height have been omitted. The subscripts indicate the properties at two different points in a flow.

$$p_1 + \rho_1 \frac{1}{2} V_1^2 = p_2 + \rho_2 \frac{1}{2} V_2^2 \tag{8.1}$$

We can rewrite equation 8.1 in terms of the pressure differential between the two points.

$$p_1 - p_2 = \rho_2 \frac{1}{2} V_2^2 - \rho_1 \frac{1}{2} V_1^2 \tag{8.2}$$

Using the continuity equation 8.3 we can derrive a relation between the volume flow and the area

$$\begin{gathered} Q = A_1 V_1 = A_2 V_2 \\ V_1 = \frac{Q}{A_1} \\ V_2 = \frac{Q}{V_2} \\ p_1 - p_2 = \frac{1}{2} \rho \left(\frac{Q}{A_2} \right)^2 - \frac{1}{2} \rho \left(\frac{Q}{A_1} \right)^2 \end{gathered} \tag{8.3}$$

When we solve equation 8.3 we can obtain a relation between the volume flow and the pressure, density and area.

$$\begin{aligned} p_1 - p_2 &= \tfrac{1}{2}\rho \left[\left(\tfrac{Q}{A_2}\right)^2 - \tfrac{1}{2}\left(\tfrac{Q}{A_1}\right)^2 \right] \\ 2(p_1 - p_2)/\rho &= \left[\left(\tfrac{Q}{A_2}\right)^2 - \left(\tfrac{Q}{A_1}\right)^2 \right] \\ 2(p_1 - p_2)/\rho &= \left[\left(\tfrac{Q}{A_2}\right)^2 - \left(\tfrac{A_2}{A_1}\right)\left(\tfrac{Q}{A_1}\right)^2 \right] \\ &= \left(\tfrac{Q}{A_2}\right)^2 \left[1 - \left(\tfrac{A_2}{A_1}\right)^2 \right] \\ \left(\tfrac{Q}{A_2}\right)^2 &= \tfrac{2(p_1 - p_2)/\rho}{\left[1 - \left(\frac{A_2}{A_1}\right)^2\right]} \\ Q &= A_2 \sqrt{\tfrac{2(p_1 - p_2)/\rho}{\left[1 - \left(\frac{A_2}{A_1}\right)^2\right]}} \end{aligned} \tag{8.4}$$

In the found relation at 8.4 we can replace the ratio of the areas with the contraction coefficient β.

$$\beta = \frac{A_2}{A_1} = \frac{0.25 \cdot \pi d_2^2}{0.25 \cdot \pi d_1^2} = \frac{d_2^2}{d_1^2} \tag{8.5}$$

The last missing element is the discharge coefficient. The found relation is based on the bernoulli equations, this yields that the flow is assumed to be incompressible and inviscid. In reality will such flow not exist. The discharge coefficient relates the actual mass flow with the theoretical mass flow.

$$C_d = \frac{\dot{m}_{actual}}{\dot{m}_{theoretical}} \tag{8.6}$$

Combining equations 8.4, 8.5 and 8.6 gives us the final relation between the orifice size, pressure, density and volume flow.

$$Q = A_2 \frac{C_d}{\sqrt{1 - \beta^4}} \sqrt{\frac{2(p_1 - p_2)}{\rho}} \tag{8.7}$$

8.1.1 Orifice Theory for compressible flows

The equation can be further expanded when compressible flows are considered. It makes more sense now to alter the equation to a mass flow since the density and thus the volume flow can vary largely over the orifice, but the mass flow will remain constant. The additional term is one to correct for the compressibility effects. This equation only holds for a non-chocked, compressible, in viscid, horizontal flow.

$$\dot{m} = A_2 Y \frac{C_d}{\sqrt{1-\beta^4}} \sqrt{2(p_1 - p_2)} \tag{8.8}$$

8.2 Derivation of the relation between C_d and C_v

The performance of valves is generally specified in a valve coefficient rather than specific flow conditions. In order to make the calculation for the valve easier and applicable to more situations it is useful to determine the orifice sizes also in terms of the valve coefficient. In this part a derivation is given for the relation between the orifice size and the valve coefficient Cv.

8.2.1 Compressible flow

Chocked flow

The chocked flow condition for a valve and a orifice is given by ANSI/ISA 75.01.01 [1].

$$\frac{p_1 - p_2}{p_1} \geq F_\gamma x_t \tag{8.9}$$

$$Y = 0.667 \tag{8.10}$$

$$N_6 = 27.3 \tag{8.11}$$

The valve coefficient is given by equation 6.14

$$C_v = \frac{\dot{m}}{N_6 0.667 \sqrt{F_\gamma x_t p_1 \rho_1}} \tag{8.12}$$

We can rewrite equation 6.14 to;

$$\dot{m} = C_v Y N_6 \sqrt{F_\gamma x_t p_1 \rho_1} \tag{8.13}$$

Form the ANSI/ISA Standard [1] we can also obtain a relation for the flow thru an orifice.

$$C_d = \frac{\dot{m}}{Y N_6 \left(\frac{d}{4.654}\right)^2 \sqrt{F_\gamma x_t p_1 \rho_1}} \tag{8.14}$$

$$\dot{m} = C_d Y N_6 \left(\frac{d}{4.654}\right)^2 \sqrt{F_\gamma x_t p_1 \rho_1} \tag{8.15}$$

The similarity between equations 6.14 and 8.15 is easily seen. The relation between the valve coefficient and the orifice coefficient can now be obtained by combining the two equations.

$$C_v Y N_6 \sqrt{F_\gamma x_t p_1 \rho_1} = C_d Y N_6 \left(\frac{d}{4.654}\right)^2 \sqrt{F_\gamma x_t p_1 \rho_1} \tag{8.16}$$

$$C_v = C_d \left(\frac{d}{4.654}\right)^2 \tag{8.17}$$

Non-Chocked flow

Following the method as used earlier, we can do the same for a non-chocked flow. Also for this derrivation the fomulas from ANSI/ISA 75.01.01 [1] are used.

$$\frac{p_1 - p_2}{p_1} \leq F_\gamma x_t \tag{8.18}$$

$$Y = \left(1 - \frac{\frac{p_1 - p_2}{p_1}}{3F_\gamma x_t}\right) \tag{8.19}$$

$$N_6 = 27.3 \tag{8.20}$$

The valve coefficient is given by equation 6.10.

$$C_v = \frac{\dot{m}}{N_6 Y \sqrt{x p_1 \rho_1}} \tag{8.21}$$

$$\dot{m} = C_v Y N_6 \sqrt{(p_1 - p_2)\rho_1} \tag{8.22}$$

The orifice coefficient for a Non-chocked gas flow is given by equation 8.24

$$C_d = \frac{\dot{m}}{Y N_6 \left(\frac{d}{4.654}\right)^2 \sqrt{(p_1 - p_2)\rho_1}} \tag{8.23}$$

$$\dot{m} = C_d Y N_6 \left(\frac{d}{4.654}\right)^2 \sqrt{(p_1 - p_2)\rho_1} \tag{8.24}$$

Combining equations 6.10 and 8.24 yields;

$$C_v Y N_6 \sqrt{(p_1 - p_2)\rho_1} = C_d Y N_6 \left(\frac{d}{4.654}\right)^2 \sqrt{(p_1 - p_2)\rho_1} \tag{8.25}$$

$$C_v = C_d \left(\frac{d}{4.654}\right)^2 \tag{8.26}$$

8.2.2 Incompressible flow

Chocked flow

The derrivation for the liquid flow regime is very similair to the gas flow. Once again the starting point are the ANSI/ISA 75.01.01 equations [1].

The Chocked flow condition is given by equation 6.6.

$$p_1 - p_2 = \Delta p \geq F_l^2(p_1 - F_f p_v) \tag{8.27}$$

$$N_1 = 0.865 \tag{8.28}$$

The valve coefficient for a liquid chocked flow is given by 6.9

$$C_v = \frac{Q}{N_1}\sqrt{\frac{\rho/\rho_0}{F_L^2(p_1 - F_f p_v)}} \tag{8.29}$$

$$C_v = \frac{Q}{N_1 F_L}\sqrt{\frac{\rho/\rho_0}{(p_1 - F_f p_v)}} \tag{8.30}$$

$$Q = C_v N_1 F_L \sqrt{\frac{(p_1 - F_f p_v)}{\rho/\rho_0}} \tag{8.31}$$

The orifice coefficient is;

$$C_d = \frac{Q}{Y N_1 \left(\frac{d}{4.654}\right)^2}\sqrt{\frac{\rho/\rho_0}{(p_1 - F_f p_v)}} \tag{8.32}$$

$$Q = C_d Y N_1 \left(\frac{d}{4.654}\right)^2 \sqrt{\frac{(p_1 - F_f p_v)}{\rho/\rho_0}} \tag{8.33}$$

Combining yields;

$$C_v N_1 F_L \sqrt{\frac{(p_1 - F_f p_v)}{\rho/\rho_0}} = C_d Y N_1 \left(\frac{d}{4.654}\right)^2 \sqrt{\frac{(p_1 - F_f p_v)}{\rho/\rho_0}} \tag{8.34}$$

$$C_v = C_d \left(\frac{d}{4.654}\right)^2 \tag{8.35}$$

Non-Chocked flow

The last flow regime is the non-chocked liquid service flow. Following the same procedure and using [1] we can obtain;

$$p_1 - p_2 = \Delta p \leq F_l^2(p_1 - F_f p_v) \tag{8.36}$$
$$N_1 = 0.865 \tag{8.37}$$

The valve coefficient is given by equation 6.1

$$C_v = \frac{Q}{N_1}\sqrt{\frac{SG}{p_1 - p_2}} \tag{8.38}$$
$$Q = C_v N_1 \sqrt{\frac{p_1 - p_2}{SG}} \tag{8.39}$$

For the orifice;

$$C_d = \frac{Q}{N_1 \left(\frac{d}{4.654}\right)^2}\sqrt{\frac{SG}{p_1 - p_2}} \tag{8.40}$$
$$Q = C_d N_1 \left(\frac{d}{4.654}\right)^2 \sqrt{\frac{p_1 - p_2}{SG}} \tag{8.41}$$

Combining again these two expressions;

$$C_v N_1 \sqrt{\frac{p_1 - p_2}{SG}} = C_d N_1 \left(\frac{d}{4.654}\right)^2 \sqrt{\frac{p_1 - p_2}{SG}} \tag{8.42}$$
$$C_v = C_d \left(\frac{d}{4.654}\right)^2 \tag{8.43}$$

The derivation shows that the correlation between the Cv value and the orifice is only dependent on the diameter of the orifice and the discharge coefficient of the nozzle. In the regular orifice equation there is also a term *beta* which is the contraction coefficient. The term $\sqrt{1 - \beta^4}$ is near to unity so it is omitted fom these equations. Important to note is that the orifice coefficient is dependent on the fluid. The factor 4.654 is used for the conversion from the diameter in mm to an area in inches together with a factor of 38 from the conversion from US units to metric.

$$d = 1inch$$
$$\left(\frac{25.4}{4.654}\right)^2 \approx 29.8 \approx 38 \cdot 0.25 \cdot \pi 1^2$$

8.2.3 Alternative derrivation

An alternate derivation comes from the combination of the sizing equation for valves from ISA 75.01.01[1] and the relief valve sizing equation form API 520 [4].

$$A = \frac{Q}{C_d K_w K_c K_v} \sqrt{\frac{\frac{\rho}{\rho_0}}{p_1 - p_2}} \tag{8.44}$$

The additional terms are a correction factor for a backpressure correction K_w, a correction for the viscosity K_v when the Reynolds number is smaller than 10^5, and finally K_c for the installation of a rupture disk. The rupture disk is not applicable at a regular orifice, so this term will be omitted and set to unity. For the derrivation the other two term will also be omitted and set to unity, although they do matter. The correction will be done by using a Reynolds number(visosity) and fluid dependent discharge coefficient in stead of using the seperate terms.

The reduced formula is;

$$A = \frac{Q}{C_d} \sqrt{\frac{\frac{\rho}{\rho_0}}{p_1 - p_2}} \tag{8.45}$$

When we compare the relation found with the valve coefficient for non chocked, liquid flow, we can see the resemblance.

$$Q = N_1 C_v \sqrt{\frac{\frac{\rho}{\rho_0}}{p_1 - p_2}} \tag{8.46}$$

Combining these two formula's gives;

$$38AC_d = Cv = \frac{Q}{N_1} \sqrt{\frac{\frac{\rho}{\rho_0}}{p_1 - p_2}} \text{for liquids} \tag{8.47}$$

$$27.66AC_d = Cv\text{for gasses} \tag{8.48}$$

The numerical constant of 38 is due to the conversion between different US units; A constant of 27.66 is used for compressible fluids. The difference lies is in the increase discharge coefficient when changing from a liquid to a gas. The increase in Cd is roughly between 1.37 and 1.38. Alternatively we can formulate it like this;

$$38A\frac{C_{d_{liquid}}}{1.37} = C_v\text{for gasses} \tag{8.49}$$

8.3 Orifice in series and parallel

When multiple orifices are placed in series of parallel the equivalent orifice size can be calculated. This is very useful since the complete trim can now be treated as one large single orifice without the need to determine the size and number of holes in each stage. The more detailed calculations about the number of holes and the size per stage can be done from this equivalent area.

NOTE; After the tests were performed it became clear that the multiple orifice assumption is not valid for a controlvalve trim. This is only valid for orifices placed in series with enough intermediate distance for the pressure to recover.

8.3.1 Series

The connection between the series orifices and the equivalent size is given by;

$$\left(\frac{1}{C_{d_eq}A_{eq}}\right)^2 = \left(\frac{1}{C_{d_1}A_1}\right)^2 + \left(\frac{1}{C_{d_2}A_2}\right)^2 + ... \left(\frac{1}{C_{d_n}A_n}\right)^2 \tag{8.50}$$

$$\left(\frac{1}{C_{d_eq}A_{eq}}\right)^2 = \sum_1^n \left(\frac{1}{C_{d_n}A_n}\right)^2 \tag{8.51}$$

The discharge coefficient Cd is assumed to be equal for each orifice or stage in the multi-stage trim. The contraction coefficient term$(1/\sqrt{1-\beta^4})$ in this derrivation is omitted since it is assumed to be close to unity. The equivalent area is then only dependent on the difference in area. The ratio between the areas of the orifices has already been determined when the number of stages and the pressure drop per stage was determined. The ratio between each consecutive orifice area is s. We can now rewrite the equation;

$$\left(\frac{1}{C_{d_eq}A_{eq}}\right)^2 = \left(\frac{1}{C_dA_1}\right)^2 + \left(\frac{1}{C_dA_2}\right)^2 + ... \left(\frac{1}{C_dA_n}\right)^2 \tag{8.52}$$

$$\left(\frac{1}{C_{d_eq}A_{eq}}\right)^2 = \sum_1^n \left(\frac{1}{C_dA_n}\right)^2 \tag{8.53}$$

The relation between the areas is;

$$\begin{aligned} A_2 &= A_1\sqrt{s} \\ A_3 &= A_2\sqrt{s} \\ &..... \\ A_n &= A_{n-1}\sqrt{s} \end{aligned} \tag{8.54}$$

This is because of the exponential relation between orifice area and pressure drop.

$$
\begin{aligned}
Q &= A \cdot C\sqrt{\frac{2\Delta P}{\rho}} \\
C &= \frac{C_d}{\sqrt{1-\beta^4}}
\end{aligned}
$$

If we decrease the pressure drop with a factor s we need to increase the area with a factor of square root s since the volume or mass flow thru both orifices must be same due to the law of mass conservation.

$$
\begin{aligned}
&Q_1 = A_1 \cdot C\sqrt{\frac{2\Delta P_1}{\rho}} \\
&Q_2 = A_2 \cdot C\sqrt{\frac{2\Delta P_2}{\rho}} \\
&Q_1 = Q_2 \\
&A_2 = A_1\sqrt{s} \\
&A_1 \cdot C\sqrt{\frac{2\Delta P_1}{\rho}} = A_1 \cdot \sqrt{s} \cdot C\sqrt{\frac{2\Delta P_1 \frac{1}{s}}{\rho}}
\end{aligned}
$$

We can now use the found relation between the areas in the formula for the equivalent area;

$$
\begin{aligned}
\left(\frac{1}{C_{d_{eq}} A_{eq}}\right)^2 &= \left(\frac{1}{C_d A_1}\right)^2 + \left(\frac{1}{C_d\sqrt{s}A_1}\right)^2 \\
C_{d_{eq}} A_{eq} &= \left[\left(\frac{1}{C_d A_1}\right)^2 + \left(\frac{1}{C_d\sqrt{s}A_1}\right)^2\right]^{0.5} \\
= \left[\frac{1}{C_d^2 A_1^2}\frac{1}{sC_d^2 A_1^2}\right]^{0.5} \\
= \left[\frac{C_d^2 A_1^2 + sC_d^2 A_1^2}{C_d^4 A_1^4 s}\right]^{0.5}
\end{aligned}
$$

$$
C_d A_{eq} = \left[\frac{1+s}{C_d^2 A_1^2 s}\right]^{-0.5} = C_d A_1\sqrt{\frac{s}{s+1}} \tag{8.55}
$$

Now if we add another stage;

$$\left(\frac{1}{C_{d_{eq}}A_{eq}}\right)^2 = \left(\frac{1}{C_dA_1\sqrt{\frac{s}{s+1}}}\right)^2 + \left(\frac{1}{C_dA_1s}\right)^2$$
$$= \left[\frac{C_d^2A_1^2\frac{s}{s+1} + C_d^2A_1^2s^2}{C_d^4A_1^4\frac{s^3}{s+1}}\right]^{-0.5}$$
$$= \left[\frac{C_d^2A_1^2\left(\frac{s}{s+1} + s^2\right)}{C_d^4A_1^4\frac{s^3}{s+1}}\right]^{-0.5}$$
$$= C_dA_1\sqrt{\frac{s^2}{s^2+s+1}}$$

Now for a four stage orifice in series we can also derrive the equivalent area in a similair fashion;

$$\left(\frac{1}{C_{d_{eq}}A_{eq}}\right)^2 = \left(\frac{1}{C_dA_1\sqrt{\frac{s^2}{s^2+s+1}}}\right)^2 + \left(\frac{1}{C_dA_1s^{1.5}}\right)^2$$
$$= \left[\frac{C_d^2A_1^2\frac{s^2}{s^2+s+1} + C_d^2A_1^2s^3}{C_d^4A_1^4\frac{s^5}{s^2+s+1}}\right]^{-0.5}$$
$$= \left[\frac{C_d^2A_1^2\left(\frac{s^2}{s^2+s+1} + s^3\right)}{C_d^4A_1^4\frac{s^5}{s^2+s+1}}\right]^{-0.5}$$

$$C_dA_{eq} = C_dA_1\sqrt{\frac{s^3}{(s^2+1)(s+1)}} \tag{8.56}$$
$$C_dA_{eq} = C_dA_1\sqrt{\frac{s^3}{s^3+s^2+s+1}} \tag{8.57}$$

And so on; from this we can create a general rule;

$$C_dA_{eq} = C_dA_1\sqrt{\frac{s^{n-1}}{\sum_1^n s^{n-1}}} \tag{8.58}$$

We can now introduce a correction factor c, the definition of c is given in equation 8.59

$$c = \sqrt{\frac{s^{n-1}}{\sum_1^n s^{n-1}}} \tag{8.59}$$

The correction factor versus the number of stages for different pressure ratios, and thus area ratios are plotted in figure 8.1.

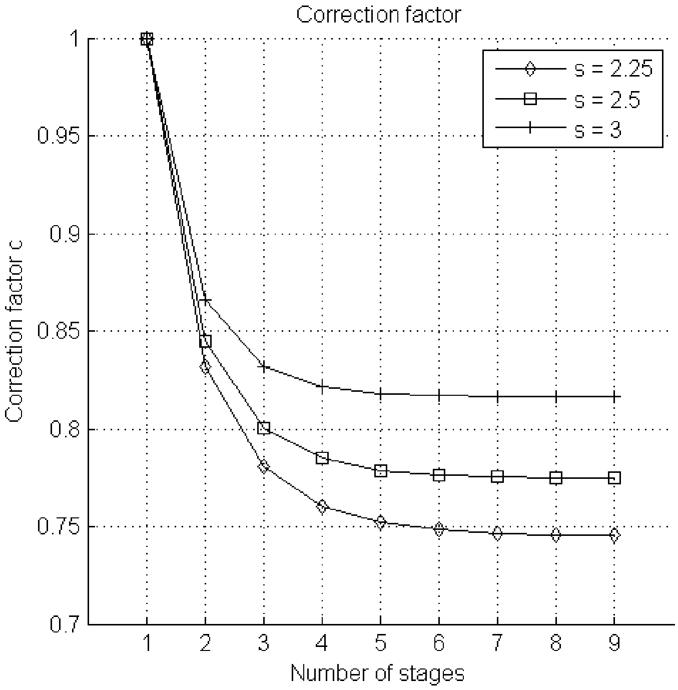

Figure 8.1: Correction factor for multiple orifices in series with a constant C_d

8.3.2 Improved correction factor Concept I

The correction factor above applies when the discharge coefficient is constant for all stages. The multi-stage trim however does not have a constant discharge coefficient. There are two different situations present. The last step in the pressure drop is when the fluid leaves the trim and flows into the valve body. This last step can be seen as a pipe-type orifice. The second situation is present between the stages. Between the stages is sharp edge type orifice. De orifice coefficient is in general dependent on the contraction factor, the Reynolds number and the diameter . The orifice coefficients used are empirically determined factors; These however are still general values. The coefficient can be tweaked by using test data. For the calculations of concept I we will assume the following data given in table 8.1

With this data in improved estimation of the correction coefficient can be made. There is also one other improvement. The initial method only corrected the area from one pressure step to the next, this was allowed since the Cd was constant. With a varying Cd the product of the area timed

Stage	C_d Coefficient
1	0.83
2	0.62
3	0.62
4	0.62
5	0.62
6	0.62
7	0.62
8	0.62
9	0.62

Table 8.1: C_d coeffiient for the improved correction factor of Concept I

Cd will be corrected per pressure step. This gives the following correction curve; note that the value of Cd is already incorporated in this correction factor.

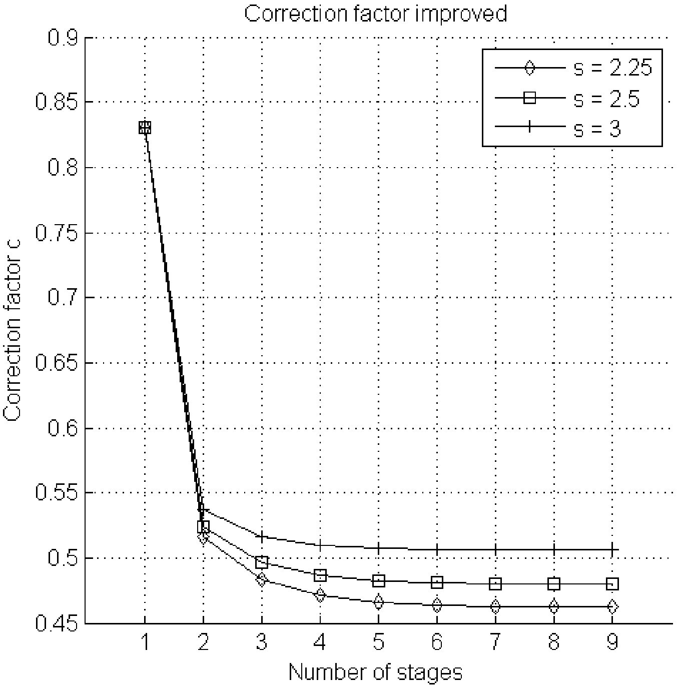

Figure 8.2: Correction factor with incoperated C_d for Concept I

8.3.3 Parallel

The equivalent diameter for orifice parallel is much simpler than the when orifice are in series. The equivalent area of multiple is the sum of the individual areas. Also there is the contraction coefficient term in this derrivation is since it is assumed to be close to unity.

$$C_{d_{eq}} A_{eq} = C_{d_1} A_1 + C_{d_2} A_2 + ... + C_{d_n} A_n \tag{8.60}$$

$$C_{d_{eq}} A_{eq} = \sum_{1}^{n} C_{d_n} A_n \tag{8.61}$$

The area of the individual areas is the same for each hole, so the total equivalent area is the area of one hole or orifice times the total number of holes. This will enable us to calculate the area of individual hole when the total number of holes in known.

$$C_{d_{eq}} A_{eq} = N_{holes} \sqrt{\frac{s^{n-1}}{\sum_{1}^{n} s^{n-1}}} C_d A_1 \tag{8.62}$$

Note again that equation 8.62 is only valid when each stage has the same orifice coeffiient. When the orifice coefficient differs each stage the regular equation for orifice in series 8.51 will have to be evaluated in order to find the equivalent.

8.4 Derrivation of the pressure ratio

NOTE: This section is purely for background information. The pressure ratio was not used in the results because the measurements from the pressure gages were too unreliable.

The relation between the pressure difference over the orifice plate and the non-recoverable pressure loss given by ISO 5167-2 [6] is derived in this chapter. The regions surrounding an orifice can be split in two different areas. The area upstream, where we assume that no friction losses take place. The second area is downstream of the orifice where we do assume that friction losses take place. The computation in area one can be done with the law of Bernoulli assuming an in viscid, incompressible flow. The second area will be evaluated via the law of momentum conservation. The incoming flow has velocity v_1, pressure p_1 and density ρ. The pressure at the intermittent region is then;

$$p_1 + \frac{1}{2}\rho u_1^2 = p_2 + \frac{1}{2}\rho u_2^2 \tag{8.63}$$

$$p_1 - p_2 = \frac{1}{2}\rho u_2^2 - \frac{1}{2}\rho u_1^2 \tag{8.64}$$

For the pressure at the end we utilize the impulse law;

$$p_2 + \rho u_1 u_2 = p_3 + \rho u_3 u_3 \tag{8.65}$$

$$p_3 - p_2 = \rho u_1 u_2 - \rho u_3 u_3 \tag{8.66}$$

Using the law of mass conservation

$$Q_1 = A_1 u_1 \qquad Q_3 = A_3 u_3$$

$$Q_1 = Q_3 \qquad A_1 = A_3$$

$$u_1 = u_3 \tag{8.67}$$

With these given relationships the ratio between the total pressure loss between 1 and 3 and the static pressure difference between 1 and 2.

$$\frac{\Delta \omega}{\Delta p} = \frac{p_3 - p_1}{p_1 - p_2} \tag{8.68}$$

$$\begin{aligned}
&= \frac{(p_3 - p_2) + (p_2 - p_1)}{(p_2 - p_1)} \\
&= \frac{(\rho u_1 u_2 - \rho u_1 u_1) - (\frac{1}{2}\rho u_2^2 - \frac{1}{2}\rho u_1^2)}{\frac{1}{2}\rho u_2^2 - \frac{1}{2}\rho u_1^2} \\
&= \frac{\rho u_1 u_2 - \frac{\rho}{2} u_2^2 + \frac{\rho}{2} u_1^2}{\frac{1}{2}\rho u_2^2 - \frac{1}{2}\rho u_1^2} \\
&= \frac{2 u_1 u_2 - u_2^2 + u_1^2}{u_2^2 - u_1^2} \\
&= \frac{(u_2 - u_1)(u_1 - u_2)}{(u_1 - u_2)(u_1 + u_2)} \\
&= \frac{u_2 - u_1}{u_2 + u_1}
\end{aligned}$$

$$\frac{\Delta \omega}{\Delta p} = \frac{1 - \frac{u_1}{u_2}}{1 + \frac{u_1}{u_2}} \tag{8.69}$$

Using the continuity equation to formulat the area ratio

$$\frac{u_1}{u_2} = \frac{A_2}{A_1} = \beta^2 \tag{8.70}$$

We can now use this relation to expres the pressure ratio as a function of the contraction coefficient

$$\frac{\Delta\omega}{\Delta p} = \frac{1-\beta^2}{1+\beta^2} \tag{8.71}$$

The relation found above only holds for an ideal orifice. In reality there the vena contracta will be smaller and at a different location than the geometrical one. We can correct for this with ϕ. The derrivation of ϕ will be done next. Firstly we will correct the found β with ϕ by equating them. The new relation for the pressure ratio is now;

$$\frac{\Delta\omega}{\Delta p} = \frac{1-\phi\beta^2}{1+\phi\beta^2} \tag{8.72}$$

The mass flow thru an orifice with $A_d = \beta^2 A$ according to ISO 5167-2 [6] is;

$$\dot{m} = C_d \cdot \frac{1}{\sqrt{1-\beta^4}} A\beta^2 \sqrt{\frac{2\Delta p}{\rho}} \tag{8.73}$$

The mass flow thru the corrected nozzle $\phi\beta$ then becomes;

$$\dot{m} = \frac{1}{\sqrt{1-\phi^2\beta^4}} A\phi\beta^2 \sqrt{\frac{2\Delta p}{\rho}} \tag{8.74}$$

Equating the two equations and solving for ϕ

$$\begin{aligned}
C_d \cdot \frac{1}{\sqrt{1-\beta^4}} A\beta^2 \sqrt{\frac{2\Delta p}{\rho}} &= \frac{1}{\sqrt{1-\phi^2\beta^4}} A\phi\beta^2 \sqrt{\frac{2\Delta p}{\rho}} \\
\frac{C_d}{\sqrt{1-\beta^4}} &= \frac{\phi}{\sqrt{1-\phi^2\beta^4}} \\
C_d\sqrt{1-\phi^2\beta^4} &= \phi\sqrt{1-\beta^4} \\
C_d^2(1-\phi^2\beta^4) &= \phi^2(1-\beta^2) \\
\phi^2(1-\beta^4-C_d^2\beta^4) &= C_d \\
\phi &= \sqrt{\frac{C_d}{(1-\beta^4-C_d^2\beta^4)}}
\end{aligned}$$

$$\phi = \frac{C_d}{\sqrt{1-\beta^4(1-C_d^2)}} \tag{8.75}$$

The pressure ratio now finally becomes;

$$\frac{\Delta\omega}{\Delta p} = \frac{\sqrt{1-\beta^4(1-C_d^2)} - C_d\beta^2}{\sqrt{1-\beta^4(1-C_D^2)} + C_d\beta^2} \tag{8.76}$$

Bibliography

[1] American National Standard, *ANSI/ISA-75.01.01 (IEC 60534-2-1 Mod)2007:Flow equations for Sizing Control Valves.* Research Triangle Park, North Carolina, First Edition, 2007.

[2] American National Standard, *ISA-RP75.23-1995:Considerations for evaluating Control Valve Cavitation.* Research Triangle Park, North Carolina, First Edition, 1995.

[3] American National Standard, *ANSI/ISA-S75.02-1996:Control Valve Capacity Test Procedures.* Research Triangle Park, North Carolina, First Edition, 1996.

[4] American Petroleum Institute, *API 520:Selection and installation of Pressure-Relieving Devices in Refineries.* Washington D.C,Columbia, Seventh Edition, 2000.

[5] International Standard Organization, *BS EN ISO 5167-1:Measurement of fluid flow by means of pressure differential devices; Part 1. Orifice plates, nozzles and Venturi tubes inserted in circular cross sections conduits running full.* Brussels, Third Edition, 1997

[6] International Standard Organization, *EN ISO 5167-2:Measurement of fluid flow by means of pressure differential devices in circular cross-section conduits running full-Part 2: Orifice plates.* Brussels, Third Edition, 2003.

[7] Crane et al, *Technical Paper No. 410m:Flow of fluid through valves, fittings and pipe.* New York,New York, Fourth Edition, 1982.

[8] Spirax-Sarco, *The Steam and Condensate Loop.* Gloucestershire, First Edition, 2007.

[9] Linkping University:Department of Management and Engineering, *Formula book for Hydraulics and Pneumatics.* Linkping, First Edition,2008.

[10] Gerd Urner, *Pressure loss of orifice plates according to ISO 5167-1*,Dresden, First Edition,1996.

Ⓢ01 ▽▽

REV.	DESCRIPTION	DATE	DGN	CHK	APP
0	1ST ISSUE	14.10.08	S.H.K	J.T.K	J.S.W

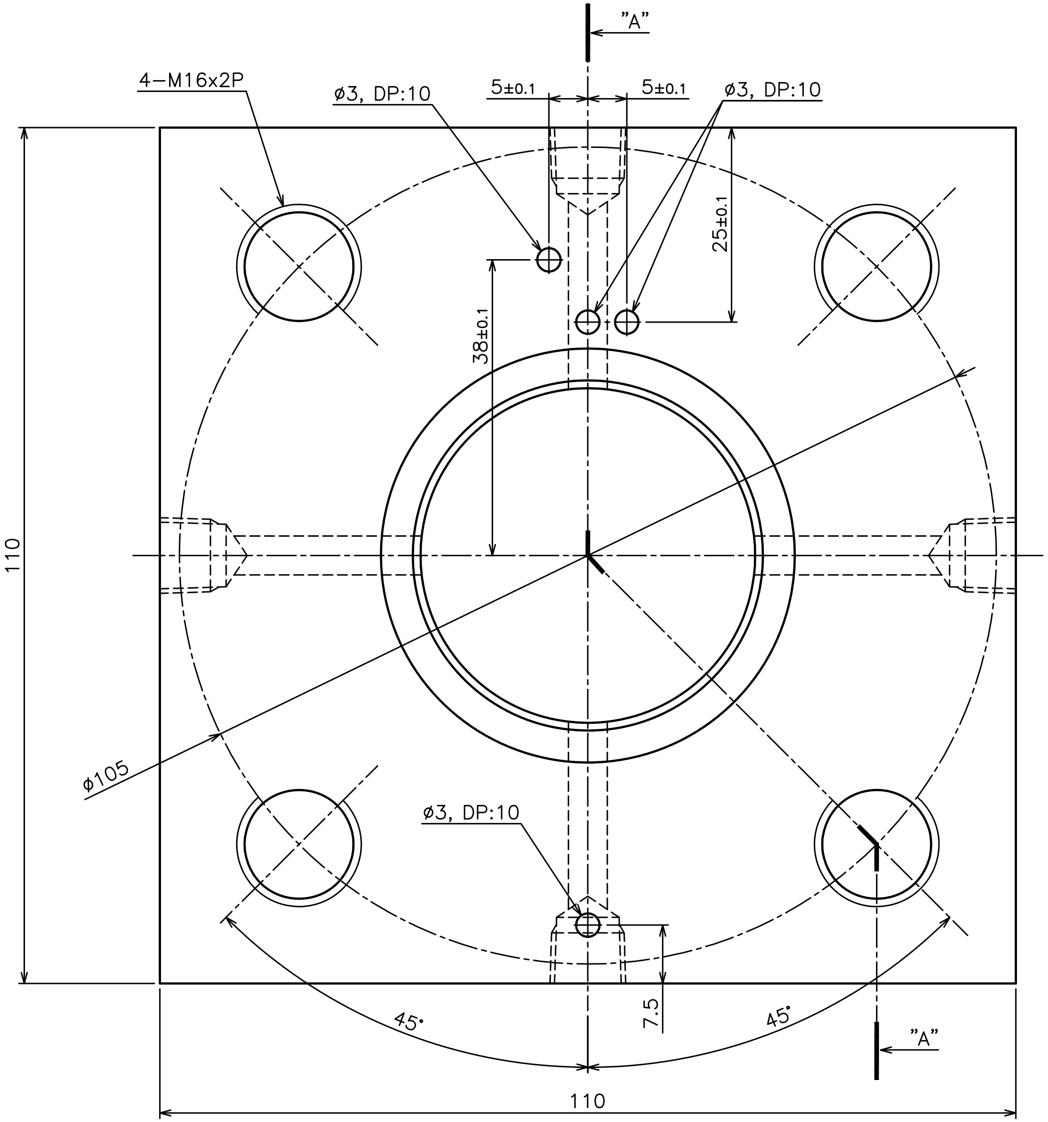
4-M16x2P
ø3, DP:10
"A"
5±0.1
5±0.1
ø3, DP:10
25±0.1
38±0.1
110
ø105
ø3, DP:10
7.5
45°
45°
"A"
110

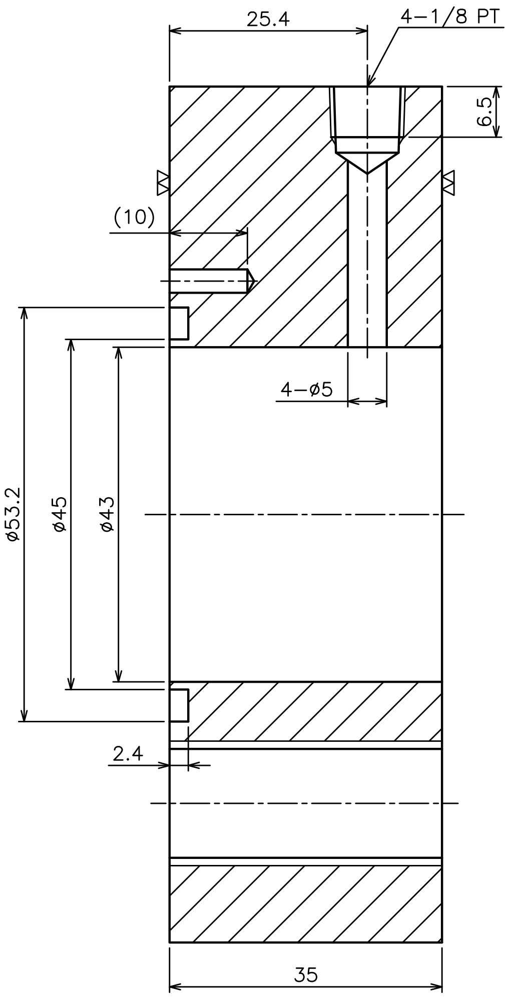
25.4
4-1/8 PT
6.5
(10)
ø53.2
ø45
ø43
4-ø5
2.4
35

SECTION "A-A"

NOTE

1. 날카로운 모서리 및
   지시없는 모서리 C0.3, R0.2 이내 가공
2. 기입외 모따기 C:1

MATERIAL	Q'TY	UNIT	SCALE		GENERAL MACHINING TOLERANCE	1-6	6-30	30-120	120-315	315-1000	ROUGHNESS MAX.	▽▽▽▽	▽▽▽	▽▽	▽	∼
		mm	N/A			±0.1	±0.2	±0.3	±0.5	±0.8		0.4S	1.6S	12.5S	50S	–

TITLE	FLANGE-INLET 1.5" PIPE WITH ORIFICE TEST		
DWG NO	RND-141008-001	REV	0

KVT Fluid Flow & Valve Specialist
KEY VALVE TECHNOLOGIES LTD.

A4 (297x210mm)

REV.	DESCRIPTION	DATE	DGN	CHK	APP
0	1ST ISSUE	14.10.08	S.H.K	J.T.K	J.S.W

(S02) ▽▽

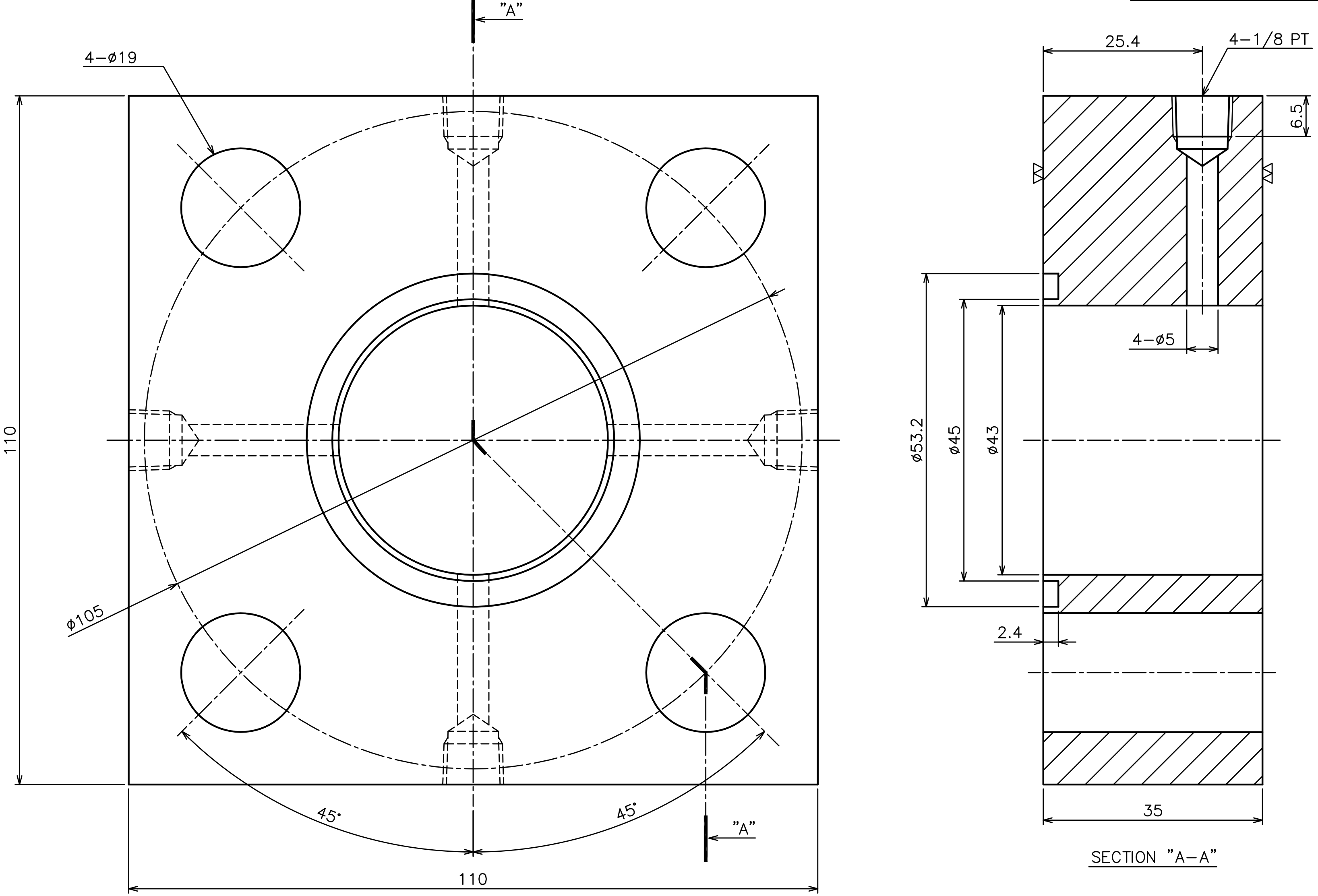
"A"
4-ø19
110
ø105
45°
45°
110
"A"
25.4
4-1/8 PT
6.5
4-ø5
ø53.2
ø45
ø43
2.4
35

SECTION "A-A"

NOTE

1. 날카로운 모서리 및
   지시없는 모서리 C0.3, R0.2 이내 가공
2. 기입외 모따기 C:1

MATERIAL	Q'TY	UNIT	SCALE		GENERAL MACHINING TOLERANCE	1-6	6-30	30-120	120-315	315-1000	ROUGHNESS MAX.	▽▽▽▽	▽▽▽	▽▽	▽	∾
		mm	N/A			±0.1	±0.2	±0.3	±0.5	±0.8		0.4S	1.6S	12.5S	50S	–

TITLE	FLANGE-OUTLET 1.5" PIPE WITH ORIFICE TEST		
DWG NO	RND-141008-002	REV	0

Fluid Flow & Valve Specialist
KEY VALVE TECHNOLOGIES LTD.

REV.	DESCRIPTION	DATE	DGN	CHK	APP
0	1ST ISSUE	14.10.08	S.H.K	J.T.K	J.S.W

(S03) ▽▽

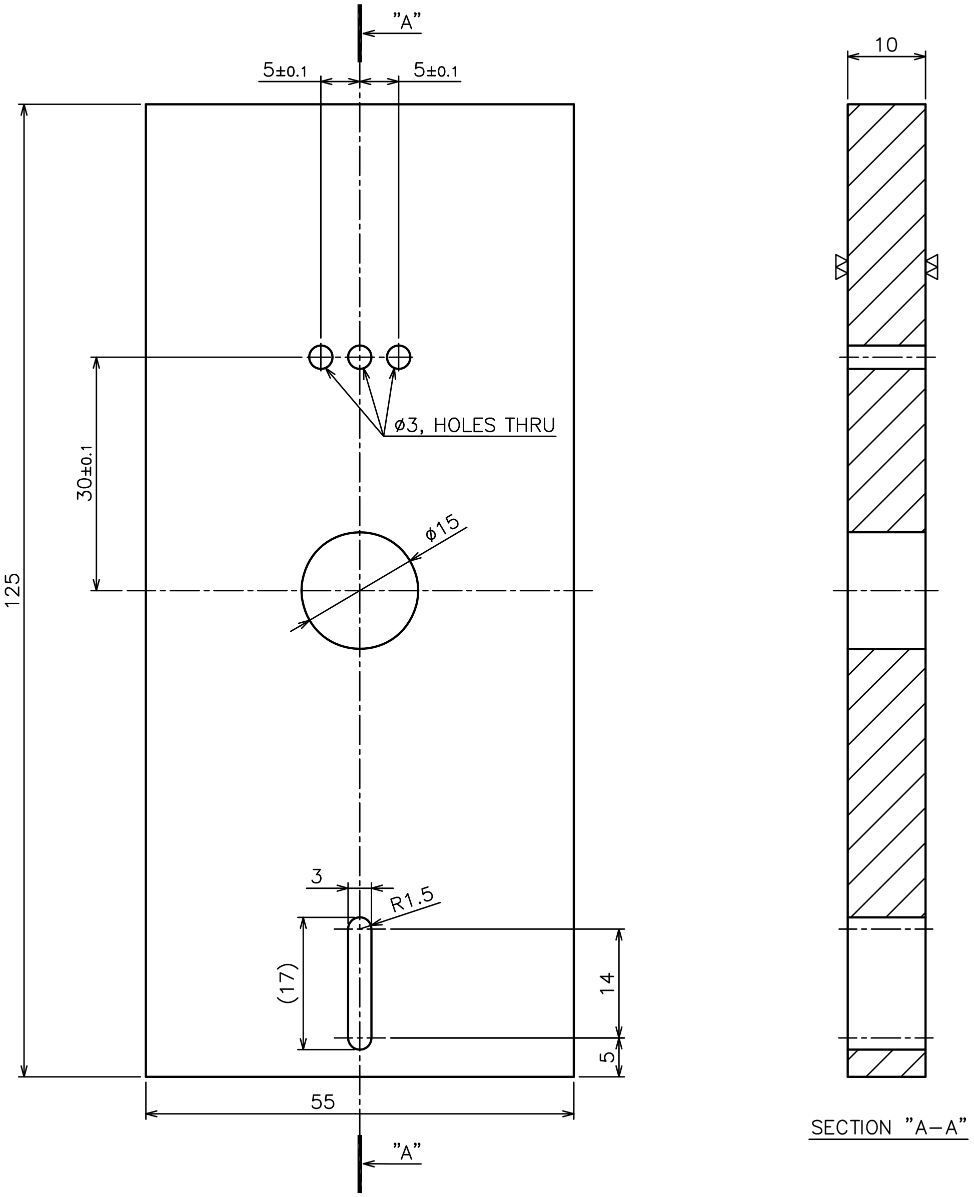
"A"
5±0.1
5±0.1
10
125
30±0.1
ø3, HOLES THRU
ø15
3
R1.5
(17)
14
5
55
"A"
SECTION "A-A"

NOTE

1. 날카로운 모서리 및
   지시없는 모서리 C0.3, R0.2 이내 가공
2. 기입외 모따기 C:1

TITLE	ORIFICE PLATE-1 1.5" PIPE WITH ORIFICE TEST		
DWG NO	RND-141008-003	REV	0

Fluid Flow & Valve Specialist
KEY VALVE TECHNOLOGIES LTD.

MATERIAL	Q'TY	UNIT	SCALE		GENERAL MACHINING TOLERANCE	1-6	6-30	30-120	120-315	315-1000	ROUGHNESS MAX.	▽▽▽▽	▽▽▽	▽▽	▽	∼
		mm	N/A			±0.1	±0.2	±0.3	±0.5	±0.8		0.4S	1.6S	12.5S	50S	-

S04 ▽▽

REV.	DESCRIPTION	DATE	DGN	CHK	APP
0	1ST ISSUE	14.10.08	S.H.K	J.T.K	J.S.W

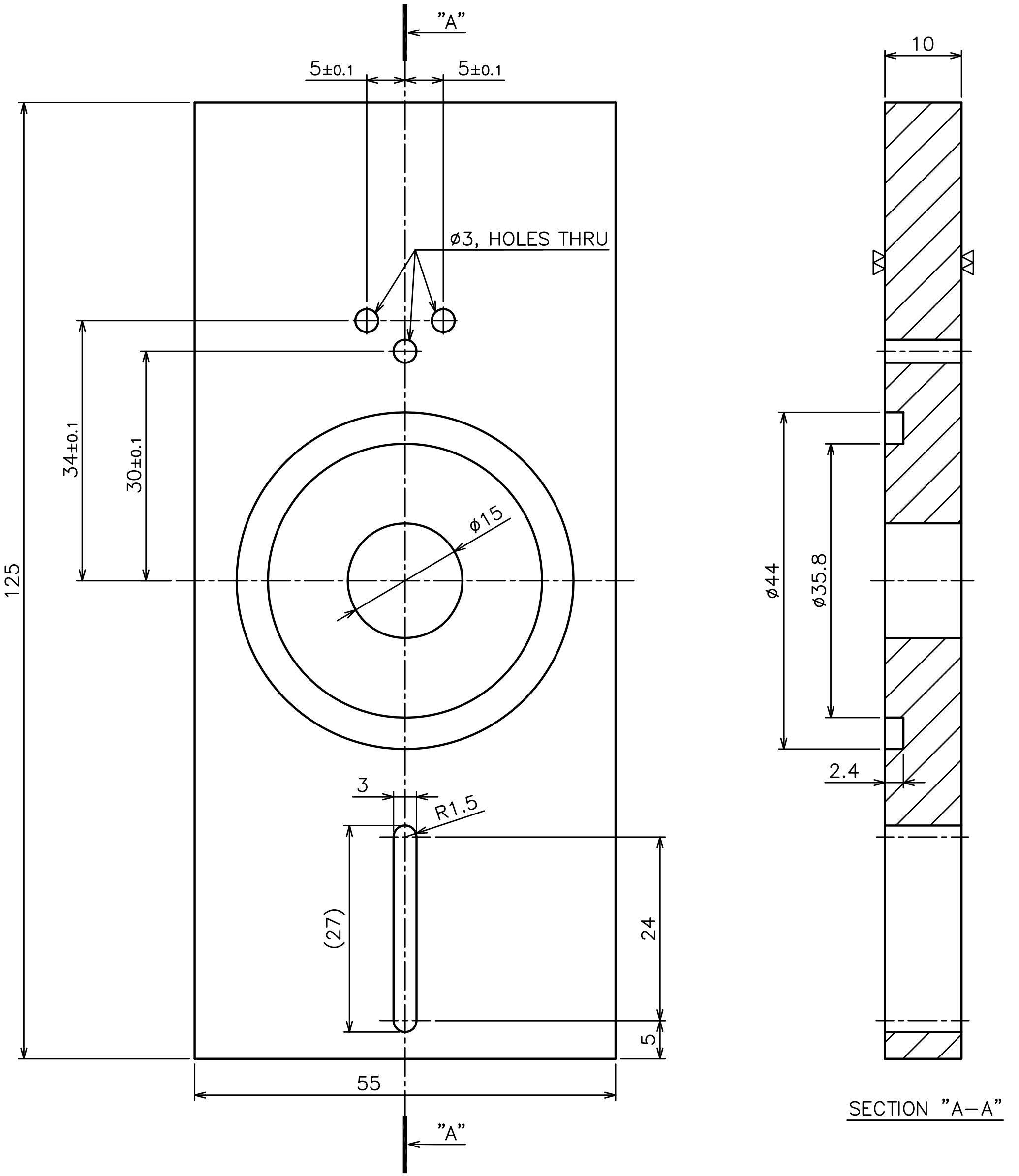
"A"
5±0.1
5±0.1
ø3, HOLES THRU
34±0.1
30±0.1
125
ø15
3
R1.5
(27)
24
5
55
"A"
10
ø44
ø35.8
2.4

SECTION "A-A"

NOTE

1. 날카로운 모서리 및
   지시없는 모서리 C0.3, R0.2 이내 가공

2. 기입외 모따기 C:1

TITLE	ORIFICE PLATE−2 1.5" PIPE WITH ORIFICE TEST	
DWG NO	RND−141008−004	REV 0

MATERIAL	Q'TY	UNIT	SCALE		GENERAL MACHINING TOLERANCE	1−6	6−30	30−120	120−315	315−1000	ROUGHNESS MAX.	▽▽▽▽	▽▽▽	▽▽	▽	∼
		mm	N/A			±0.1	±0.2	±0.3	±0.5	±0.8		0.4S	1.6S	12.5S	50S	−

KVT Fluid Flow & Valve Specialist
KEY VALVE TECHNOLOGIES LTD.

A4 (297x210mm)

REV.	DESCRIPTION	DATE	DGN	CHK	APP
0	1ST ISSUE	14.10.08	S.H.K	J.T.K	J.S.W

S05 ▽▽

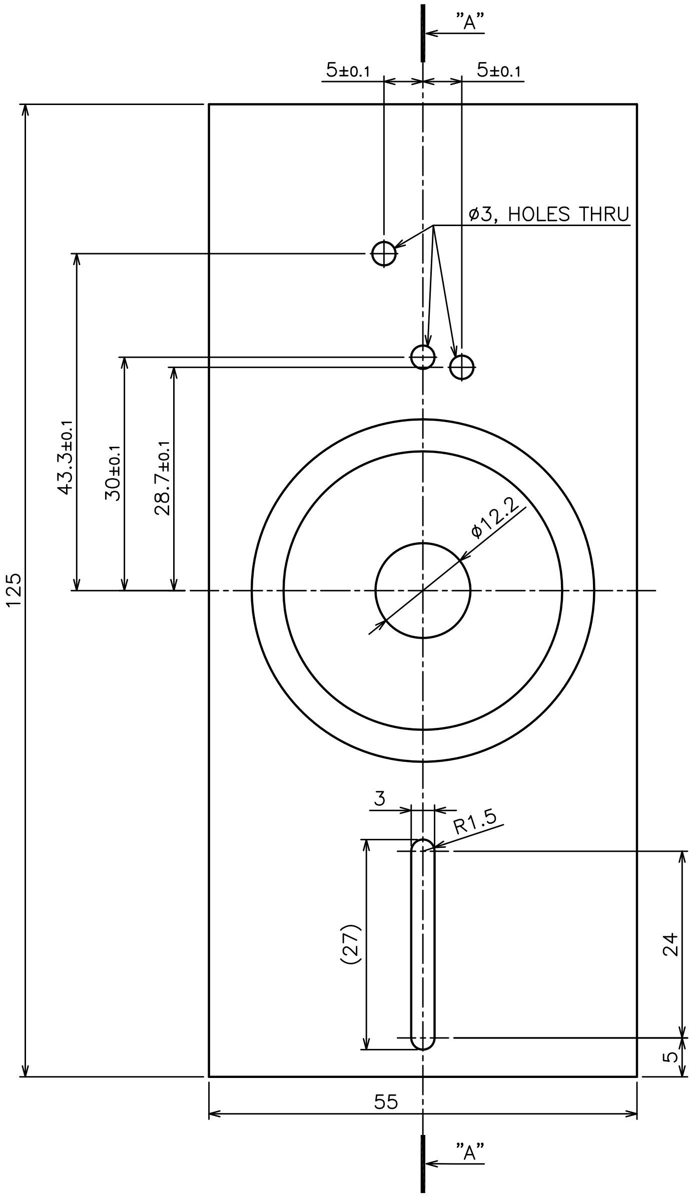
"A"
5±0.1
5±0.1
ø3, HOLES THRU
43.3±0.1
30±0.1
28.7±0.1
125
ø12.2
3
R1.5
(27)
24
5
55
"A"

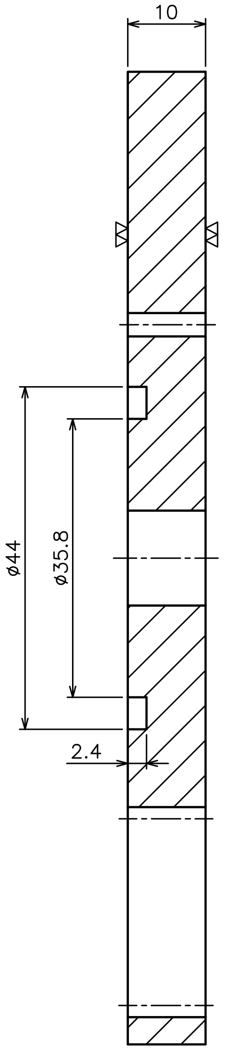
10
ø44
ø35.8
2.4

SECTION "A-A"

NOTE

1. 날카로운 모서리 및
   지시없는 모서리 C0.3, R0.2 이내 가공
2. 기입외 모따기 C:1

TITLE	ORIFICE PLATE-3 1.5" PIPE WITH ORIFICE TEST		
DWG NO	RND-141008-005	REV	0

Fluid Flow & Valve Specialist
KEY VALVE TECHNOLOGIES LTD.

MATERIAL	Q'TY	UNIT	SCALE	GENERAL MACHINING TOLERANCE	1-6	6-30	30-120	120-315	315-1000	ROUGHNESS MAX.	▽▽▽▽	▽▽▽	▽▽	▽	∼
		mm	N/A		±0.1	±0.2	±0.3	±0.5	±0.8		0.4S	1.6S	12.5S	50S	-

A4 (297x210mm)

REV.	DESCRIPTION	DATE	DGN	CHK	APP
0	1ST ISSUE	14.10.08	S.H.K	J.T.K	J.S.W

S06 ▽▽

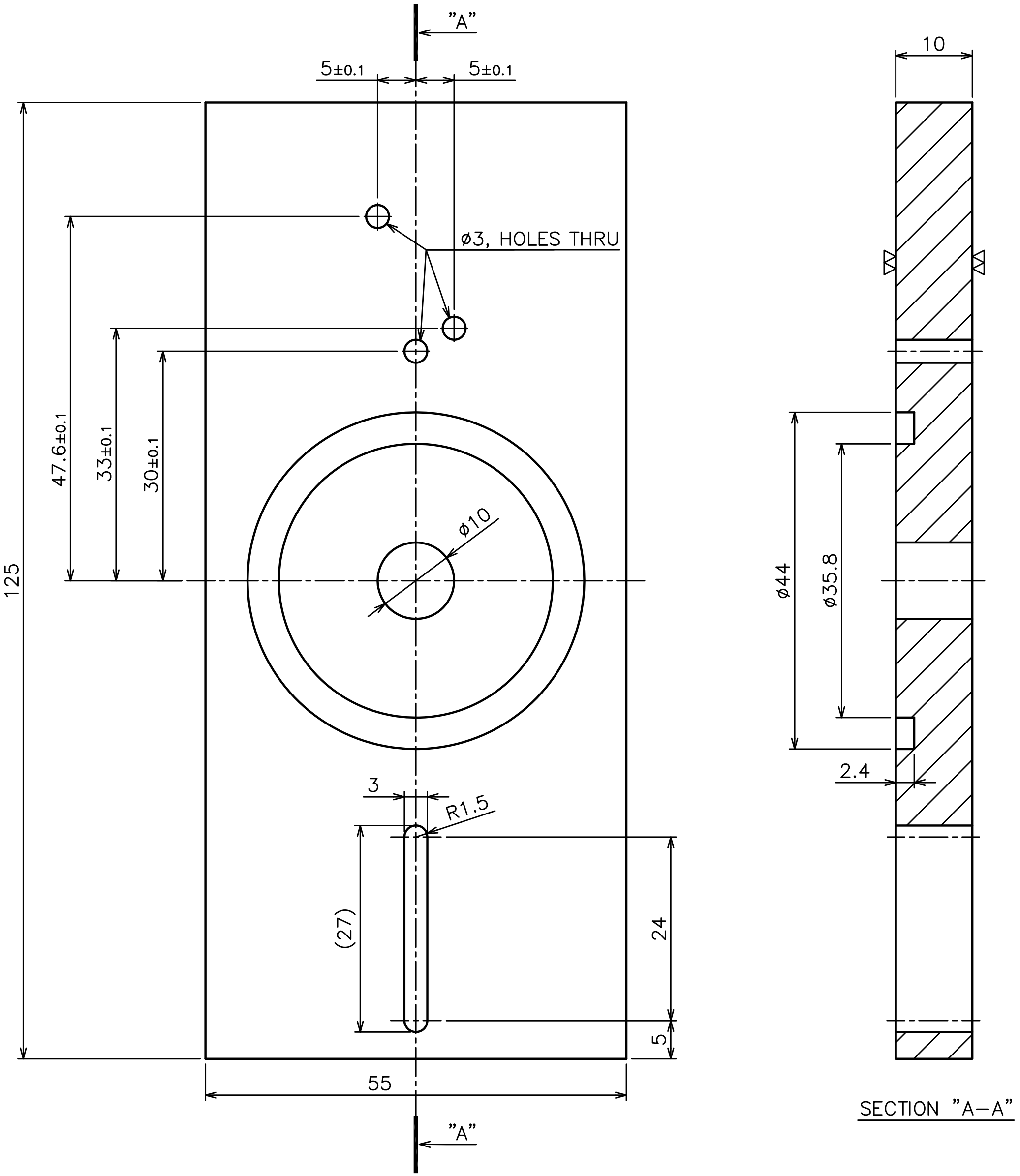

"A"
5±0.1
5±0.1
ø3, HOLES THRU
47.6±0.1
33±0.1
30±0.1
125
ø10
3
R1.5
(27)
24
5
55
"A"
10
ø44
ø35.8
2.4

SECTION "A-A"

NOTE

1. 날카로운 모서리 및
   지시없는 모서리 C0.3, R0.2 이내 가공
2. 기입외 모따기 C:1

TITLE	ORIFICE PLATE-4 1.5" PIPE WITH ORIFICE TEST		
DWG NO	RND-141008-006	REV	0

MATERIAL	Q'TY	UNIT	SCALE		GENERAL MACHINING TOLERANCE	1-6	6-30	30-120	120-315	315-1000	ROUGHNESS MAX.	▽▽▽▽	▽▽▽	▽▽	▽	∼
		mm	N/A			±0.1	±0.2	±0.3	±0.5	±0.8		0.4S	1.6S	12.5S	50S	-

Fluid Flow & Valve Specialist
KEY VALVE TECHNOLOGIES LTD.

A4 (297x210mm)

REV.	DESCRIPTION	DATE	DGN	CHK	APP
0	1ST ISSUE	14.10.08	S.H.K	J.T.K	J.S.W

(S07) ▽▽

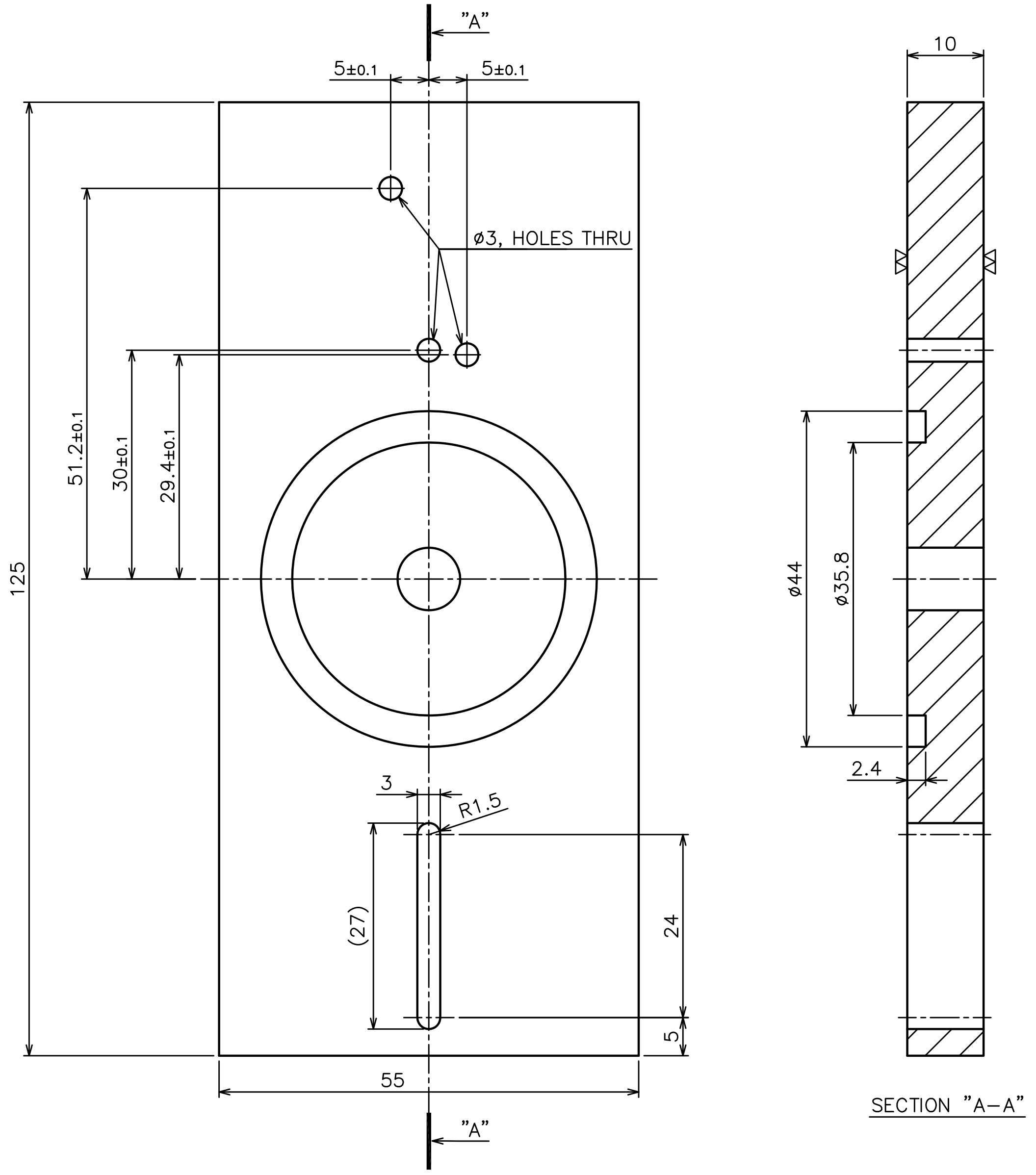
"A"
5±0.1
5±0.1
ø3, HOLES THRU
51.2±0.1
30±0.1
29.4±0.1
125
3
R1.5
(27)
24
5
55
"A"
10
ø44
ø35.8
2.4

SECTION "A-A"

NOTE

1. 날카로운 모서리 및
지시없는 모서리 C0.3, R0.2 이내 가공
2. 기입외 모따기 C:1

TITLE	ORIFICE PLATE-5 1.5" PIPE WITH ORIFICE TEST		
DWG NO	RND-141008-007	REV	0

Fluid Flow & Valve Specialist
KEY VALVE TECHNOLOGIES LTD.

MATERIAL	Q'TY	UNIT	SCALE		GENERAL MACHINING TOLERANCE	1-6	6-30	30-120	120-315	315-1000	ROUGHNESS MAX.	▽▽▽▽	▽▽▽	▽▽	▽	∼
		mm	N/A			±0.1	±0.2	±0.3	±0.5	±0.8		0.4S	1.6S	12.5S	50S	-

A4 (297x210mm)

(112-1) ▽▽ (▽▽▽)

REV.	DESCRIPTION	DATE	DGN	CHK	APP
0	1ST ISSUE	13.07.11	S.H.K	J.S.W	J.S.W

PLANAR FIGURE

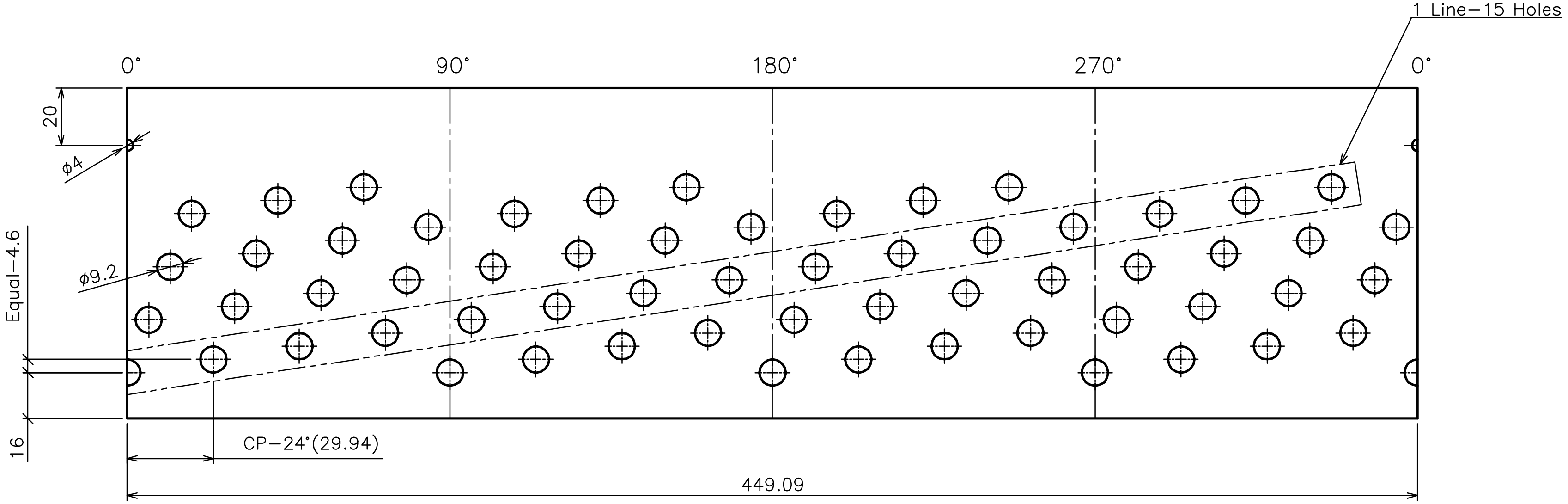
1 Line−15 Holes
0°
90°
180°
270°
0°
20
φ4
Equal−4.6
φ9.2
16
CP−24°(29.94)
449.09

1st Out Dia

FOR : 6" VALVE WITH (120A) TRIM HEST−II/ 3 Cylinder

CAGE−1

DWG NO	−	REV	0

Fluid Flow & Valve Specialist
KEY VALVE TECHNOLOGIES LTD.

MATERIAL	Q'TY	UNIT	SCALE		GENERAL MACHINING TOLERANCE	1−6	6−30	30−120	120−315	315−1000	ROUGHNESS MAX.	▽▽▽▽	▽▽▽	▽▽	▽	∼
		mm	N/A			±0.1	±0.2	±0.3	±0.5	±0.8		0.4S	1.6S	12.5S	50S	−

REV.	DESCRIPTION	DATE	DGN	CHK	APP
0	1ST ISSUE	13.07.11	S.H.K	J.S.W	J.S.W

(112-2) ▽▽ (▽▽▽)

PLANAR FIGURE

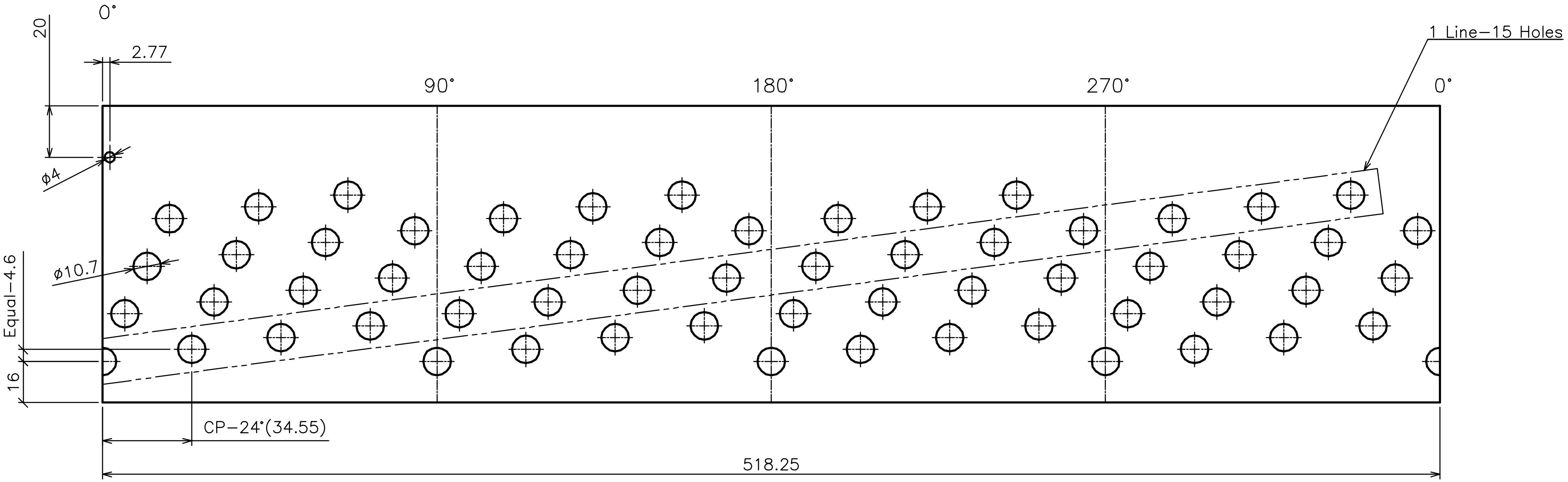
0°
20
2.77
90°
180°
270°
0°
1 Line-15 Holes
φ4
φ10.7
Equal-4.6
16
CP-24°(34.55)
518.25

2nd Out Dia

FOR : 6" VALVE WITH (120A) TRIM HEST-II/ 3 Cylinder

CAGE-2

DWG NO	–	REV	0

MATERIAL	Q'TY	UNIT	SCALE		GENERAL MACHINING TOLERANCE	1-6	6-30	30-120	120-315	315-1000	ROUGHNESS MAX.	▽▽▽▽	▽▽▽	▽▽	▽	∼
		mm	N/A			±0.1	±0.2	±0.3	±0.5	±0.8		0.4S	1.6S	12.5S	50S	–

Fluid Flow & Valve Specialist
KEY VALVE TECHNOLOGIES LTD.

(112-3) ▽▽ (▽▽▽)

REV.	DESCRIPTION	DATE	DGN	CHK	APP
0	1ST ISSUE	13.07.11	S.H.K	J.S.W	J.S.W

PLANAR FIGURE

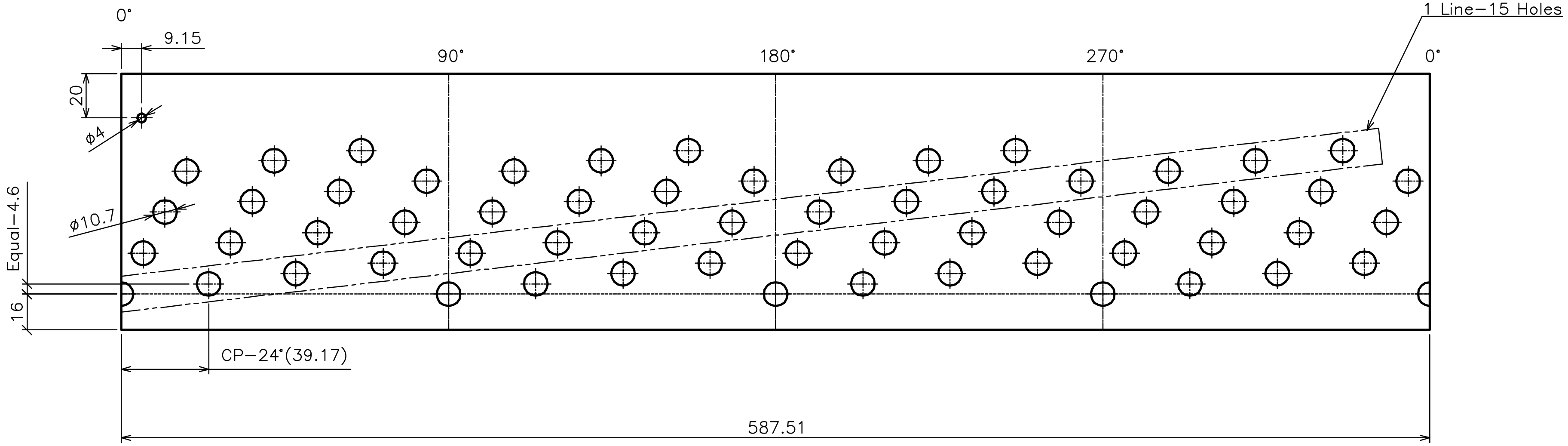
0°
9.15
20
ϕ4
90°
180°
270°
0°
1 Line-15 Holes
ϕ10.7
Equal-4.6
16
CP-24°(39.17)
587.51

3rd Out Dia

NOTE

1. +0.2 −0.2

FOR : 6" VALVE WITH (120A) TRIM HEST-II/ 3 Cylinder

CAGE-3

DWG NO	-	REV	0

Fluid Flow & Valve Specialist
KEY VALVE TECHNOLOGIES LTD.

MATERIAL	Q'TY	UNIT	SCALE	GENERAL MACHINING TOLERANCE	1-6	6-30	30-120	120-315	315-1000	ROUGHNESS MAX.	▽▽▽▽	▽▽▽	▽▽	▽	∼
		mm	N/A		±0.1	±0.2	±0.3	±0.5	±0.8		0.4S	1.6S	12.5S	50S	-

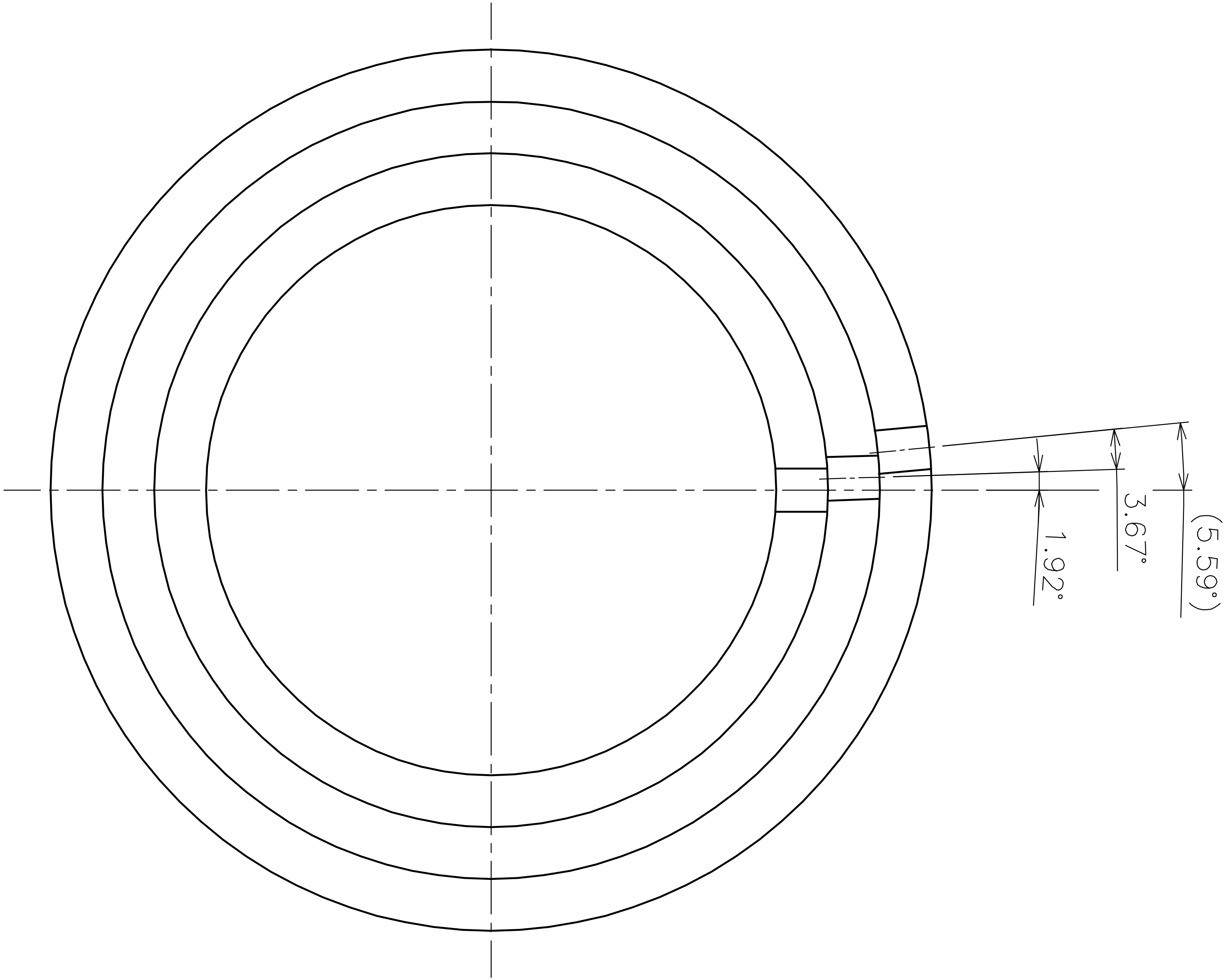
1.92°
3.67°
(5.59°)